AD-754 847

Electromagnetic Pulse Sounding for Geological Surveying with Application in Rock Mechanics and Rapid Excavation Program

Ohio State University

prepared for
Bureau of Mines
Advanced Research Projects Agency

SEPTEMBER 1972

Distributed By:

NTIS
National Technical Information Service
U. S. DEPARTMENT OF COMMERCE

ELECTROMAGNETIC PULSE SOUNDING FOR GEOLOGICAL SURVEYING WITH APPLICATION IN ROCK MECHANICS AND RAPID EXCAVATION PROGRAM

L. Peters, Jr. and D.L. Moffatt

The Ohio State University

ElectroScience Laboratory

Department of Electrical Engineering
Columbus, Ohio 43212

Final Report 3190-2
September 1972

Contract Number: H0210042
Principal Investigator: D. L. Moffatt
614-422-5749
Contract Officer: Alan Granruth
303-233-3611 - Ext. 8871
Effective Date of Contract: 24 February 1971
Contract Expiration Date: 23 February 1972
Amount of Contract: $33,306

Sponsored by
Advanced Research Projects Agency
ARPA Order No. 1579, Amend. 2
Program Code 1F10

U. S. Dept. of Interior
Bureau of Mines
Advanced Research Projects Agency

NOTICES

When Government drawings, specifications, or other data are used for any purpose other than in connection with a definitely related Government procurement operation, the United States Government thereby incurs no responsibility nor any obligation whatsoever, and the fact that the Government may have formulated, furnsihed, or in any way supplied the said drawings, specifications, or other data, is not to be regarded by implication or otherwise as in any manner licensing the holder or any other person or corporation, or conveying any rights or permission to manufacture, use, or sell any patented invention that may in any way be related thereto.

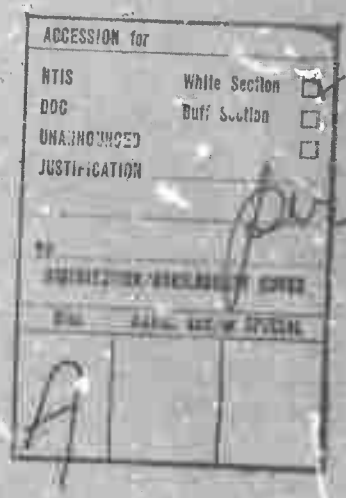

DOCUMENT CONTROL DATA - R&D

(Security classification of title, body of abstract and indexing annotation must be entered when the overall report is classified.)

1. ORIGINATING ACTIVITY *(Corporate author)*
The Ohio State University ElectroScience Laboratory, Department of Electrical Engineering, Columbus OH

2a. REPORT SECURITY CLASSIFICATION
Unclassified

2b. GROUP

3. REPORT TITLE
ELECTROMAGNETIC PULSE SOUNDING FOR GEOLOGICAL SURVEYING WITH APPLICATION IN ROCK MECHANICS AND RAPID EXCAVATION PROGRAM

4. DESCRIPTIVE NOTES *(Type of report and inclusive dates)*
Final Report - 24 February 1971 to 23 February 1972

5. AUTHOR(S) *(Last name, first name, initial)*
Moffatt, David L. and Peters, L., Jr.

6. REPORT DATE
September 1972

7a. TOTAL NO. OF PAGES
~~108~~ 115

7b. NO. OF REFS
15

8a. CONTRACT OR GRANT NO.
Contract H0210042

b. PROJECT NO.

c. TASK

d.

9a. ORIGINATOR'S REPORT NUMBER(S)
ElectroScience Laboratory 3190-2

9b. OTHER REPORT NO(S) *(Any other numbers that may be assigned this report)*

10. AVAILABILITY/LIMITATION NOTICES

11. SUPPLEMENTARY NOTES

12. SPONSORING MILITARY ACTIVITY
U.S. Dept. of Interior, Bureau of Mines
Advanced Research Projects Agency
Denver, Colorado 80225

13. ABSTRACT

Progress toward the development of an electromagnetic pulse sounding probe for the detection and delineation of geological anomalies, primarily in a hard rock medium, is reported. This report covers research performed on Contract H0210042 during the period 24 February 1971 to 23 February 1972. Analytical studies on design data for the probe and on the scattering by planar and spherical contrasts are summarized. Successful measurements made using a "first generation" version of the probe on conducting and dielectric cylindrical targets in a lossy overburden and on specific anomalies in a limestone medium are reported.

DD FORM 1 JAN 64 1473

14. KEY WORDS	LINK A		LINK B		LINK C	
	ROLE	WT	ROLE	WT	ROLE	WT
Electromagnetic Probe Pulse Geological Hard rock Tunneling						

INSTRUCTIONS

1. ORIGINATING ACTIVITY: Enter the name and address of the contractor, subcontractor, grantee, Department of Defense activity or other organization *(corporate author)* issuing the report.

2*a*. REPORT SECURITY CLASSIFICATION: Enter the overall security classification of the report. Indicate whether "Restricted Data" is included. Marking is to be in accordance with appropriate security regulations.

2*b*. GROUP: Automatic downgrading is specified in DoD Directive 5200.10 and Armed Forces Industrial Manual. Enter the group number. Also, when applicable, show that optional markings have been used for Group 3 and Group 4 as authorized.

3. REPORT TITLE: Enter the complete report title in all capital letters. Titles in all cases should be unclassified. If a meaningful title cannot be selected without classification, show title classification in all capitals in parenthesis immediately following the title.

4. DESCRIPTIVE NOTES: If appropriate, enter the type of report, e.g., interim, progress, summary, annual, or final. Give the inclusive dates when a specific reporting period is covered.

5. AUTHOR(S): Enter the name(s) of author(s) as shown on or in the report. Enter last name, first name, middle initial. If military, show rank and branch of service. The name of the principal author is an absolute minimum requirement.

6. REPORT DATE: Enter the date of the report as day, month, year, or month, year. If more than one date appears on the report, use date of publication.

7*a*. TOTAL NUMBER OF PAGES: The total page count should follow normal pagination procedures, i.e., enter the number of pages containing information.

7*b*. NUMBER OF REFERENCES: Enter the total number of references cited in the report.

8*a*. CONTRACT OR GRANT NUMBER: If appropriate, enter the applicable number of the contract or grant under which the report was written.

8*b*, 8*c*, & 8*d*. PROJECT NUMBER: Enter the appropriate military department identification, such as project number, subproject number, system numbers, task number, etc.

9*a*. ORIGINATOR'S REPORT NUMBER(S): Enter the official report number by which the document will be identified and controlled by the originating activity. This number must be unique to this report.

9*b*. OTHER REPORT NUMBER(S): If the report has been assigned any other report numbers *(either by the originator or by the sponsor)*, also enter this number(s).

10. AVAILABILITY/LIMITATION NOTICES: Enter any limitations on further dissemination of the report, other than those imposed by security classification, using standard statements such as:

(1) "Qualified requesters may obtain copies of this report from DDC."

(2) "Foreign announcement and dissemination of this report by DDC is not authorized."

(3) "U. S. Government agencies may obtain copies of this report directly from DDC. Other qualified DDC users shall request through _____."

(4) "U. S. military agencies may obtain copies of this report directly from DDC. Other qualified users shall request through _____."

(5) "All distribution of this report is controlled. Qualified DDC users shall request through _____."

If the report has been furnished to the Office of Technical Services, Department of Commerce, for sale to the public, indicate this fact and enter the price, if known.

11. SUPPLEMENTARY NOTES: Use for additional explanatory notes.

12. SPONSORING MILITARY ACTIVITY: Enter the name of the departmental project office or laboratory sponsoring *(paying for)* the research and development. Include address.

13. ABSTRACT: Enter an abstract giving a brief and factual summary of the document indicative of the report, even though it may also appear elsewhere in the body of the technical report. If additional space is required, a continuation sheet shall be attached.

It is highly desirable that the abstract of classified reports be unclassified. Each paragraph of the abstract shall end with an indication of the military security classification of the information in the paragraph, represented as *(TS)*, *(S)*, *(C)*, or *(U)*.

There is no limitation on the length of the abstract. However, the suggested length is from 150 to 225 words.

14. KEY WORDS: Key words are technically meaningful terms or short phrases that characterize a report and may be used as index entries for cataloging the report. Key words must be selected so that no security classification is required. Identifiers, such as equipment model designation, trade name, military project code name, geographic location, may be used as key words but will be followed by an indication of technical context. The assignment of links, rules, and weights is optional.

ELECTROMAGNETIC PULSE SOUNDING FOR GEOLOGICAL SURVEYING WITH APPLICATION IN ROCK MECHANICS AND RAPID EXCAVATION PROGRAM

Final Report 3190-2

ElectroScience Laboratory
The Ohio State University

This research was supported by the Advanced Research Projects Agency of the Department of Defense and was monitored by Bureau of Mines under Contract No. H0210042

ic

ABSTRACT

Progress toward the development of an electromagnetic pulse sounding probe for the detection and delineation of geological anomalies, primarily in a hard rock medium, is reported. This report covers research performed on Contract H0210042 during the period 24 February 1971 to 23 February 1972. Analytical studies on design data for the probe and on the scattering by planar and spherical contrasts are summarized. Successful measurements made using a "first generation" version of the probe on conducting and dielectric cylindrical targets in a lossy overburden and on specific anomalies in a limestone medium are reported.

TABLE OF CONTENTS

I. TECHNICAL REPORT SUMMARY

A unique electromagnetic pulse sounding probe for the detection, diagnosis and identification of geological and man-made anomalies within the earth is being developed. The immediate application of the probe is as a hazard detection device in advance of hard rock rapid tunneling operations. Numerous other applications in geophysical exploration, geophysical prospecting and as a monitor device in mining or drilling operations can be envisioned. In each application the basic pulse sounding technique is the same but the probe structure and interrogating pulse would be adjusted to fit the parameters of the problem. The goals of the program during this contract period are to design and build a probe structure which effectively couples electromagnetic energy into a ground or rock medium, is insensitive to surface obstructions (for example equipment near the tunnel working face) and with this probe measure the scattering characteristics of selected targets and anomalies in ground and rock media.

Our effort during this contract period has been separated into two parts. First, analytical studies were conducted to secure design data for the probe and to obtain the scattering characteristics of planar and spherical contrasts as idealized models of geological anomalies. At the same time, the necessary equipment, instrumentation and interfacing to initiate an experimental measurememt program were assembled and tested. The second part of our effort, the measurement program, was viewed as the most essential portion of the contract. Our reasoning was that the feasibility of the pulse sounding technique must be demonstrated first, in a real world environment, using admittedly less than optimum probe designs and processing methods. Once this was done, analytical and experimental studies to optimize the performance of the pulse sounding probe could be pursued on later contracts with the secure knowledge that the goals are attainable. For this reason, once a "first generation" version of the probe could be constructed, the contract funds and personnel were concentrated on the measurement effort. Consequently, the computer programs developed to provide probe design and scattering data have not been fully exploited as yet.

The electromagnetic pulse sounding system currently in use employs a source which produces a periodic train of video-type pulses. The pulses are coupled into the ground or rock medium by the transmit arm of a broadband probe consisting of a pair of orthogonally oriented balun-fed dipoles stretched over the surface of the medium. The probe can be operated either in a direct mode where only one dipole is used or in an orthogonal mode where one dipole serves as a source and the other as a receiver. In the orthogonal mode, the probe does not respond to the air-medium interface and pulsed energy has been successfully coupled into the medium over the broad spectrum of the pulse. On a ground medium, the probe is extremely insensitive to surface obstructions (a vehicle driven between probe elements was

not detected). On a rock medium, some sensitivity to large surface obstructions is noted, but a change in the shape of the dipole arms should obviate this problem. In operation, a pulse is launched on one dipole at the feed point which penetrates into the medium. As the wave propagates along the dipole, its fringe fields penetrate deeper into the medium. Reflected signals from the medium are observed on a sampling scope either on the same dipole (direct mode) or on the second dipole (orthogonal mode) acting as a receiver. In the orthogonal mode, the probe is "blind" to homogeneous targets, e.g., horizontal stratifications, whereas in the direct mode both homogeneous and inhomogeneous targets are seen.

All measurements reported for this period were made with a 5 volt peak pulse generator (3 ns base, 2 MHz repetition rate). The fact that targets could be detected in both the overburden (depths to 5 feet) and hard rock (depths to 10 feet) using such low power is extremely encouraging. New pulse generators* and better baluns now available at the ElectroScience Laboratory will give us both higher power and lower frequencies in the spectrum (lower repetition rates); we anticipate successful target detection at significantly greater depths with this equipment.

~~At the specific request of the Technical Project Officer,~~ R.L.M. the experiments discussed herein are directed toward the detection and identification of buried cylinders. In addition to numerous probe tests and control or no-target measurements, the following targets have been measured using the probe in the orthogonal mode. 1, 3, 5 and 10 foot long hollow metal cylinders with diameters of 4 inches buried at a depth of 5 feet in the overburden. 2, 3, and 4 inch diameter extended plastic pipe (hollow) buried at a depth of 3 feet in the overburden. A "dummy" trench, i.e., a trench identical to those dug to install the cylinder targets was dug (5 foot depth) and then refilled. In all cases, the refilling was compacted. At a local limestone quarry, measurements were made of a hollow metal pipe, 1 foot in diameter whose top was buried 2.0 feet in a limestone medium, inhomogeneous stratifications in a limestone medium and a large tunnel (road) beneath some 30 feet of limestone. Several control measurements were also made for the limestone medium. On May 31, 1972, after this research and this report had been completed the authors were informed that the interest of the Technical Project Officer had shifted so that extended planar targets were of major interest. An immediate conclusion can be made, on the basis of scattering theory, that the scattered pulses for extended planar targets should be substantially larger than those from the cylinders treated in this report.

For both the limestone and overburden measurements, the target was detected in each case with the exception of the tunnel. We would not realistically expect to penetrate some 60 feet (2-way path) of limestone with only a 5 volt peak pulse with frequency content above 1 MHz. The presence of the tunnel should be easily evident with measurements using high power pulse generators. Presence of

*A Hewlitt Packard model 2/4A pulse generator was purchased with contract funds.

the target was evident both from a simple comparison of the target and control time domain waveforms and from examination of the spectral components of these waveforms. In addition, the reflected signals from the pipe and inhomogeneous stratification targets in limestone and the plastic pipe, cylinders and dummy trench were separable in the sense that the scattered waveforms and their associated spectra contained adequate information to identify the individual targets in the set of targets. However, with the simple processing used it was not conclusively evident that one could separate the different lengths of cylinder. This is expected since a theoretical analysis shows that the current distribution on a buried wire antenna is of a non-resonant form. Thus the only identifiable characteristic of the linear scatterers would be the relative magnitude of the scattered field and this is a very poor characteristic for the purposes of identification.

Since the cylinder diameter is quite small, less than 4 inches, separation of various cylinder diameters is not important for the purposes of this study. Measurements of a larger cylinder at the limestone quarry do indeed indicate that separation is possible in terms of cylinder diameter.

The analytical tools for the design of an electromagnetic pulse sounding probe and for the analysis of planar and spherical subsurface targets have been developed. Extensive computations using computer programs developed to exploit these analytical tools have been deferred, however, in order to concentrate on an initial series of experimental measurements. A "first generation" version of the pulse sounding probe has been designed and built. A mobile rig which permits measurements to be made at remote sites (removed from the computer and without available electrical power) has been refurbished. Using the "first generation" probe and a low power pulse generator, successful detection of conducting and dielectric cylinders at depths to 5 feet in the overburden and of a metallic cylinder and inhomogeneous stratifications to depths of 10 feet in a limestone medium has been demonstrated. The necessary equipment to operate the probe at significantly higher power with pulse generators having much lower spectral content has been acquired and is ready for testing. The feasibility of an electromagnetic pulse sounding technique has been established and we are now ready to refine our methods and equipment for specific applications to the hard rock tunneling problem.

II. PURPOSE

A unique electromagnetic pulse sounding probe for the detection, diagnosis and identification of geological and man-made anomalies within the earth is being developed. The immediate application of the probe is as a hazard detection device in advance of hard rock rapid tunneling operations, but numerous other applications in geophysical exploration, geophysical prospecting and in mining or drilling operations can be envisioned. During this contract period the objectives of the program are to; 1) design and demonstrate a probe structure capable of effectively coupling electromagnetic pulse energy into a ground or rock medium and at the same time be insensitive to obstructions located on the medium surface,

2) interrogate with this probe certain simple targets in ground and rock media and 3) establish preliminary bounds on the workable depths of electromagnetic pulse sounding via theoretical and experimental methods.

III. INTRODUCTION

The ultimate goal of the research on this program is to incorporate state-of-the-art advances developed at this laboratory, both in antenna systems and processing techniques, into a geological tool capable of delineating the size and shape of geological anomalies from the shape and spectral content of an echo pulse.

The detection of underground anomalies that represent hazards using a periodic video pulse radar system does not appear to present substantial difficulties. The problems that are of most importance are those associated with isolating the scattered pulse associated with buried target and then its identification. Pulses can be scattered from many different discontinuities including scattering from the balun, the input terminals of the antenna, the ground surface, targets above ground, etc. Much of our effort has been focussed on reducing these undesired scattered pulses so that the scattered pulses from the underground target (hazard) can be isolated. This effort has proven successful. Once the scattered pulse from the underground is properly separated from the clutter, there still remains the problem of identification. While only a limited effort has been expended for this purpose under the current contract, there has been developed at the ElectroScience Laboratory a variety of techniques for target identification. Since these techniques are required in a successful system, they have strongly influenced the choice of parameters of the system to be used for the electromagnetic hazard detection system.

Studies at this laboratory have conclusively demonstrated that if the gross features, i.e., the overall size and shape, of a target are to be deduced via electromagnetic interrogation then discrete frequencies over an 8 or 10:1 bandwidth with a fundamental such that the linear extent of the anomaly is approximately 1/10 of a wavelength in the ambient medium are dictated.[1] With a pulse sounding approach* to detection of subsurface targets, this fixes the characteristics (power, rise time, repetetion rate, etc.) of a pulse generator suitable for interrogation of a given range of anomaly sizes at a given depth. It does not necessarily follow that all of the higher spectral content are needed to obtain a viable signature, but our experience indicates that the lowest frequencies are essential.[2] Of course, the more high frequency content available, the more detail of the target is available, and the sharper the reflected pulses yielding an improved range gating. If follows that more detail and an improved

*An alternative system for radar applications uses discrete harmonically related cw measurements over the 10:1 bandwidth.[3]

range gating are to be expected when comparing measurements in a hard rock medium to those in the overburden since the high frequency energy is severely attenuated in the overburden. The use of low frequencies to interrogate the target is ideally suited to the problem of subsurface targets in either a ground or rock medium since it is precisely these frequencies which can penetrate to the target.

For the case of targets in free space, i.e., radar-type targets, studies at this laboratory have established three distinct techniques for processing low frequency scattering data to detect and identify the target. One of these uses harmonic spectral amplitude data in an n-dimensional space approach to target classification.[4] A second approach uses harmonic spectral amplitude and phase data to derive a small set of excitation-invariant target descriptors.[5] In the third approach, relationships between the size and shape of the target and its low frequency scattering characteristics are exploited to obtain 3-dimensional isometric images of the target from harmonic spectral amplitude and phase data.[3] Ultimately it is intended to apply these and similar sophisticated processing schemes to the analysis of electromagnetic pulse sounding data.* At this stage, however, we have confined ourselves to relatively simple averaging and differencing techniques with subsequent comparisons of target and control measurements in both the time and frequency domains. Once our probe designs have been optimized for a given medium and techniques for handling high power pulses with very broad spectral content established, we can properly begin to consider more advanced processing.

In Section IV of this report, the status of our analytical studies and the availability of computational programs are summarized. Details of the analytical studies have been given in a previous report,[7] which is included as an Appendix of this report.

Section V of this report describes the electromagnetic pulse sounding probe, reviews the probe design, tests and operation in both the direct and orthogonal modes; and describes the processing used on the pulse sounding data.

In Sections VI and VII respectively, experimental data on man-made targets in a lossy overburden and man-made and natural targets in a limestone medium are presented.

Section VIII of the report summarizes our conclusions regarding the feasibility and applicability of an electromagnetic pulse sounding system for interrogating subsurface targets and makes specific recommendations for future research in this area.

---

*The n-dimensional space approach has previously been used with shallow subsurface target measurements.[6]

IV. THEORETICAL STUDIES

Two types of theoretical studies have been conducted on the program. The first was a comprehensive analysis and computer program for all types of wire antennas and arrays of wire antennas in a homogeneous dissipative medium. The second type was plane wave scattering computations for planar and spherical conductivity and permittivity contrasts. In addition, closed form results for particular orientations for the transient fields of an infinite line source above a dielectric half-space were obtained. Approximate results estimating the effects of the overburden on the scattering from various targets were obtained. Illustrative results from the above studies were given in the Semi-Annual Technical Report[7] which is included as an Appendix of this report.

Listed below are brief descriptions of the computer programs which have been developed and are now available to provide probe design data and scattering computations.

1. Wire Antennas in a Homogeneous Dissipative Medium

The program handles all types of wire antennas including linear dipoles, V dipoles, rectangular loops, circular loops and arrays. The wire antenna can have a finite conductivity, and certain portions of the antenna can be enclosed by a thin dielectric sleeve. The output from the program provides a complete analysis of the system including self impedance, mutual impedance, current distributions, near-zone fields and far-field patterns. Solutions are via a piecewise-sinusoidal expansion for the unknown current distribution and Galerkin's method for reducing the integral equation formulation to a system of simultaneous linear equations. The present analysis and programs require the medium to be of infinite extent. For proper probe design data, these results need to be extended to include an air-dissipative medium interface. The first attempt to do this via an infinite array formulation with large interelement spacing was discarded because the required computer time became prohibitive. For finite antennas of arbitrary shape, the half-space introduces rather difficult problems even with numerical methods. An approximate quasi-static or image formulation may be the most feasible approach to the problem considering the present funding level and the necessity to continue an experimental program.

2. Homogeneous Dissipative Spherical Target in a Homogeneous Dissipative Medium

The program calculates the scattered fields (plane wave incidence) from an arbitrary homogeneous spherical target with constitutive parameters ε_1, σ_1, μ_0 immersed in an ambient medium with parameters ε_2, σ_2, μ_0. Solution is via a Mie series formulation.

3. Homogeneous Layered Dissipative Spherical Target in a Homogeneous Dissipative Medium

The program calculates the scattered fields (plane wave incidence) from an arbitrary homogeneous spherical target (ε_1,σ_1,μ_0)

with a homogeneous spherical layer ($\varepsilon_2,\sigma_2,\mu_0$) immersed in an homogeneous ambient medium ($\varepsilon_3,\sigma_3,\mu_0$). Solution is via a Mie series formulation.

4. Planar Contrasts

The program calculates the impulse response waveform (inverse transform of the frequency-dependent Fresnel reflection coefficient) for normal incidence at the interface of two homogeneous media ε_1, σ_1,μ_0 and $\varepsilon_2,\sigma_2,\mu_0$. The singularities and discontinuities in the waveform can be obtained in closed form. The program yields, via a Fourier synthesis procedure, the decay of the waveform from its initial value. Frequency-dependent constitutive parameters can be used.

5. Interface and Overburden Effects

The program calculates the back scattered field from a subsurface target assuming off-normal plane wave incidence on the air-ground interface and frequency-independent constitutive parameters for the ground medium. It is also assumed that the target scatters as a simple scaling of its free-space scattering characteristics. Output of the program is the ramp response waveform (impulse response waveform twice integrated with respect to time) of the target and this waveform is compared with the free space ramp response waveform of the target.

6. Convolution

The program calculates the convolution of two time domain waveforms. One waveform is completely arbitrary and is approximated by straight line segments. At present, the second waveform must be twice integrable analytically in closed form, e.g., a pulse, pulsed carrier, etc. The intended use of this program is primarily in conjunction with targets whose impulse or baseband pulse response is known only as a graph or plot, i.e., not analytically. Using the program, the targets response to other interrogating signals can be quickly obtained.

Another program used to control our pulse sounding measurements and to process and manipulate the measured data is described in a later section of this report. The programs listed above are used with a Datacraft 1600 computer. The control program is written for a small instrumentation computer (IBM Minimal Informer) which is presently used for on-line computer controlled measurements. The instrumentation and software to shift the on-line measurements to the more versatile modified Datacraft System are being prepared at this time.

a. Probe Design

The wire antenna analysis and programs provide a straightforward method for optimizing the probe design for a given target range, frequency range and medium conditions. These are based, at the

moment, or calculations for a homogeneous dissipative medium. Modifications of the program to account for the air-medium interface are not yet complete. Experimentally we have demonstrated that the mismatch due to the interface can be controlled by adjusting the shape of the dipole arms and the depth of grounding stakes. Once we have analytically accounted for the interface, the dipole arm shape and ground rod depth can be optimized for a wide variety of media.

The analyses and computer programs listed above assume that the conductivity and dielectric constant are constant with respect to frequency. It is recognized that these parameters are frequency dependent. The introduction of complex frequency dependent constitutive parameters is a simple matter of changing values for frequency domain computations. Periodic time domain waveforms can be constructed from these computations using the available Fast Fourier Transform (FFT) computer program, if needed. This cannot be readily achieved for the direct time domain computations of the waveforms. In most instances, this is not an essential flaw, however, since the major variation is of the form

$$\varepsilon^* = \varepsilon\left(1 + \frac{\sigma}{j\omega\varepsilon}\right)$$

where ε^*, the complex dielectric constant is frequency dependent.

In a previous report,[7] calculations using the wire antenna programs demonstrated that for shallow depths (< 4 feet) an uninsulated dipole produced field strengths an order of magnitude greater than those of an insulated dipole. However, at much greater depths only very slight differences in field strength are noted. In general, we are interested in targets at some distance and conclude that for our present applications, either insulated or uninsulated probes can be used.

In Fig. 1, the near-zone fields in the plane of a U-shaped dipole in a homogeneous ambient medium $\varepsilon_r = 9$, $\sigma = 0.003$ mho/meter are shown at ranges of 15 and 30 feet. The dipole has 15 foot insulated arms with 2.5 foot uninsulated ends perpendicular to the main arms. The results in Fig. 1 were obtained from the wire antenna program at a frequency of 10 kHz. It was found that the results remained essentially unchanged up to a frequency of 100 kHz. Note that the field component E_x which is parallel to the dipole arms has a sharp null which moves with range. This would be of no consequence for extended targets, but for finite objects the dipole would have a "blind spot" in the direct reflection mode for the x-component of the field. In Fig. 2, the same results are shown where the uninsulated portion of the dipole arms have been increased to 5 feet. Note that at the 15 foot range lengthening the uninsulated portion of the dipole arms has simply raised the level of the x and z components. The same is true at the 30 foot range. In each case a 3 to 4% increase in field strength is noted.

The wire antenna program permits one to calculate, for a homogeneous dissipative medium, the coupling between two arbitrary wire antennas separated by a given distance and in any orientation.

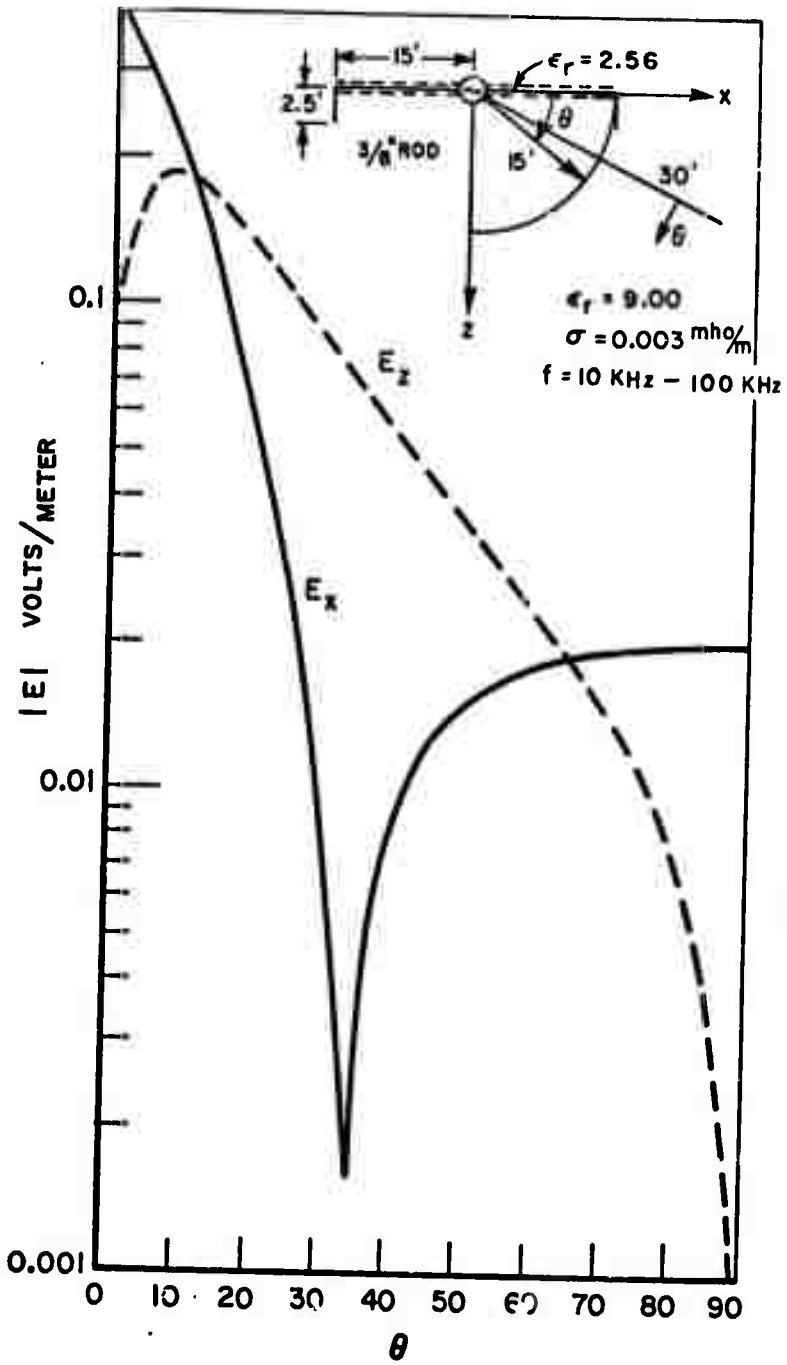

Fig. 1. Calculated near zone fields of a wire antenna in a homogeneous conducting medium.
(a) 15 foot range.

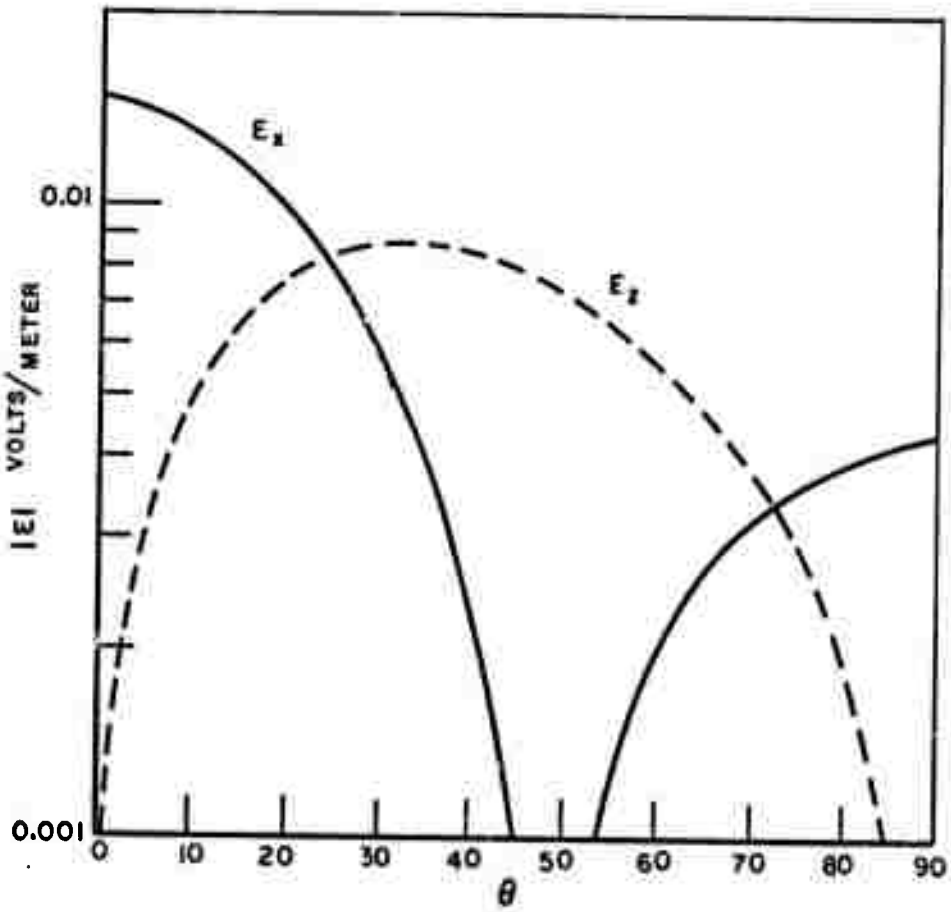

Fig. 1. Calculated near zone fields of a wire antenna in a homogeneous conducting medium. (b) 30 foot range.

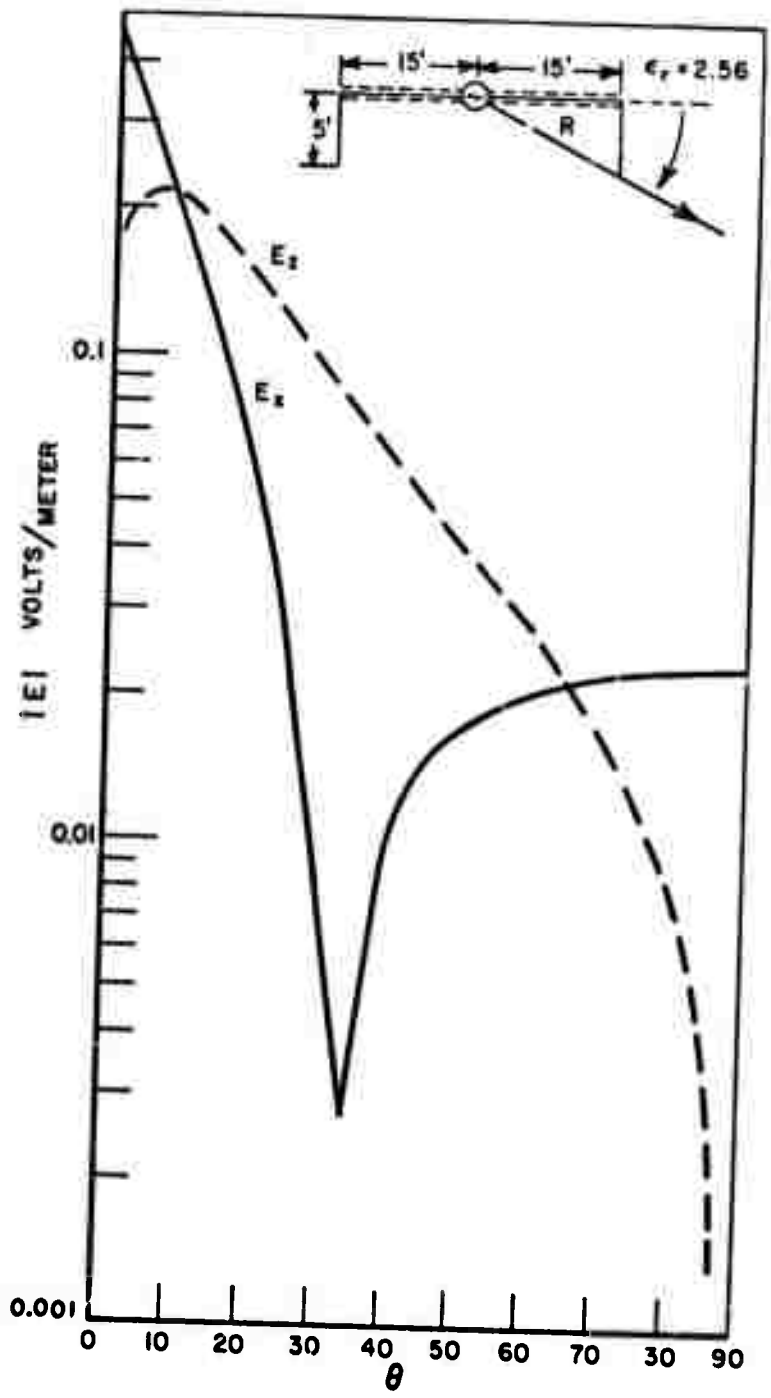

Fig. 2. Calculated near zone fields of a wire antenna in a homogeneous conducting medium.
(a) 15 foot range.

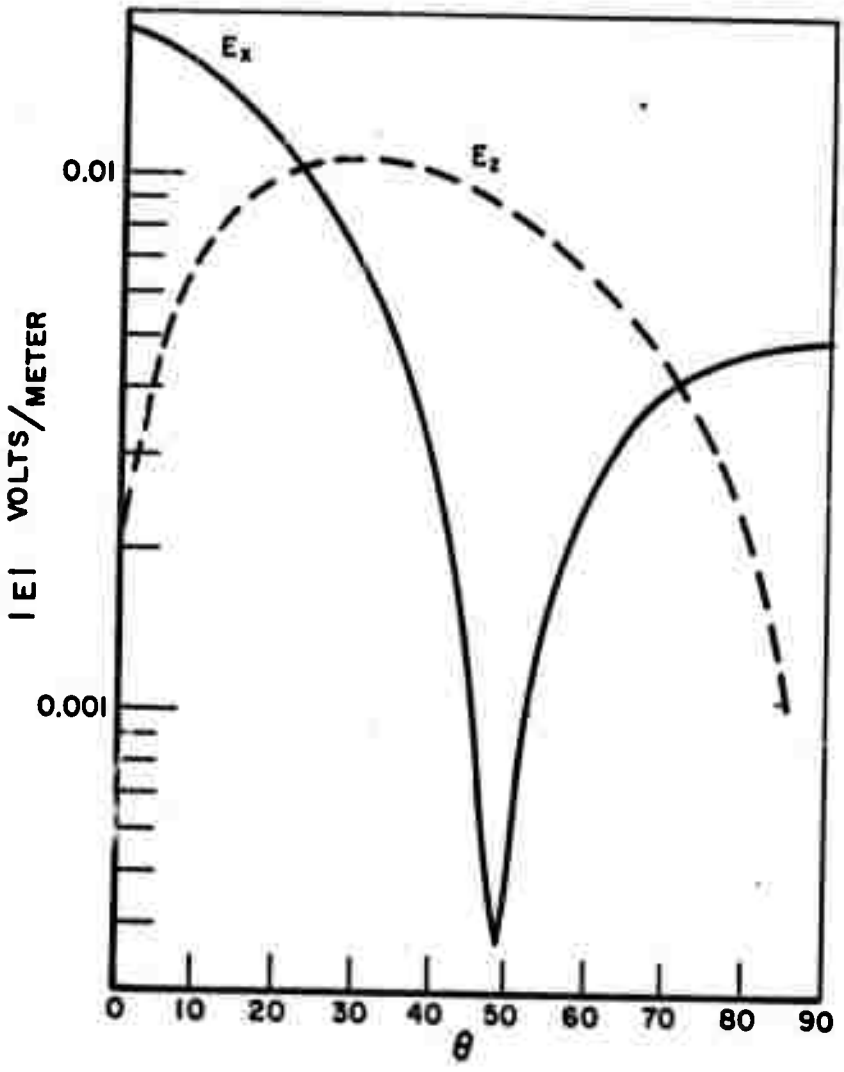

Fig. 2. Calculated near zone fields of a wire artenna in a homogeneous conducting medium.
(b) 30 foot range.

The received voltage at a second dipole when the first dipole is excited by a 1 volt input is shown in Figs. 3, 4 and 5 over a frequency range from 10 KHz to 10 MHz. The dipole configurations are shown in the figures, and results are shown for various assumed permittivities and conductivities for the medium. In Fig. 3, the relative permittivity is 15.0 and results for conductivities of 0.1, 0.05 and 0.01 mhos/meter are given. The dipoles have 10 foot arms and are separated by approximately 5.4 feet. In Fig. 4, the dipole arms are reduced to 5 feet, the relative permittivity is 15.0, and the same conductivities are used. Also shown is the result for a relative permittivity of 9.0 and conductivity of 0.01 mhos/meter illustrating that below 1 MHz the results are essentially independent of the dielectric constant. In Fig. 5, a portion of one antenna is insulated and the arms (10 feet) are in a U configuration. The relative permittivity is 9.0 and results for conductivities of 0.01, 0.006 and 0.003 mhos/meter are shown. Note from all three figures that over a lower portion of the spectrum, the received voltage actually increases with frequency to some peak value and then decreases. Also, this effect becomes more pronounced as the conductivity decreases.

Calculations such as those shown in Figs. 3, 4 and 5 permit one to predict the attenuation as a function of frequency for a medium with a given dielectric constant and conductivity by comparing calculations at 2 different ranges. In Fig. 6, the predicted attenuation in dB per foot is shown over the frequency range 10 KHz to 10 MHz for a medium with a relative permittivity of 15 and conductivities of 0.1, 0.05 and 0.01 mhos/meter. Note that over the frequency range 10 kHz to 400 kHz the curves are essentially flat, i.e., the attenuation is constant.*

The attenuation of the local ground has been measured in situ using pulse propagation data between a dipole buried at a depth of 5 feet in the overburden and 3 dipoles on the surface. An average (over several days) of these data are shown in Fig. 7 for frequencies from 10 kHz to 10 MHz. Actually, two pulse generators were used to span the frequency range and the two points shown for 1 MHz illustrate the spread of the data from the different generators. Comparing the data in Fig. 7 with the predicted attenuation curves in Fig. 6 it is clear that a qualitative agreement between predicted and measured attenuation is feasible. We would not anticipate quantitative agreement because of the air-earth interface.

---

*The dielectric constant and conductivity of the medium are assumed to be constant with frequency and the shape of the curves vs frequency will change with changes in the assumed load impedance of the receiving antenna. The results in Fig. 6 assume a constant load of 50 ohms. For a change of path length $\Delta\ell$, the total attenuation for $\Delta\ell$ feet is $20 \log_{10}(\frac{V_{\ell 2}}{V_{\ell 1}})$ where $V_{\ell 2}$ and $V_{\ell 1}$ are the voltages for paths ℓ_2 and ℓ_1 respectively and $\Delta\ell = \ell_1 - \ell_2$.

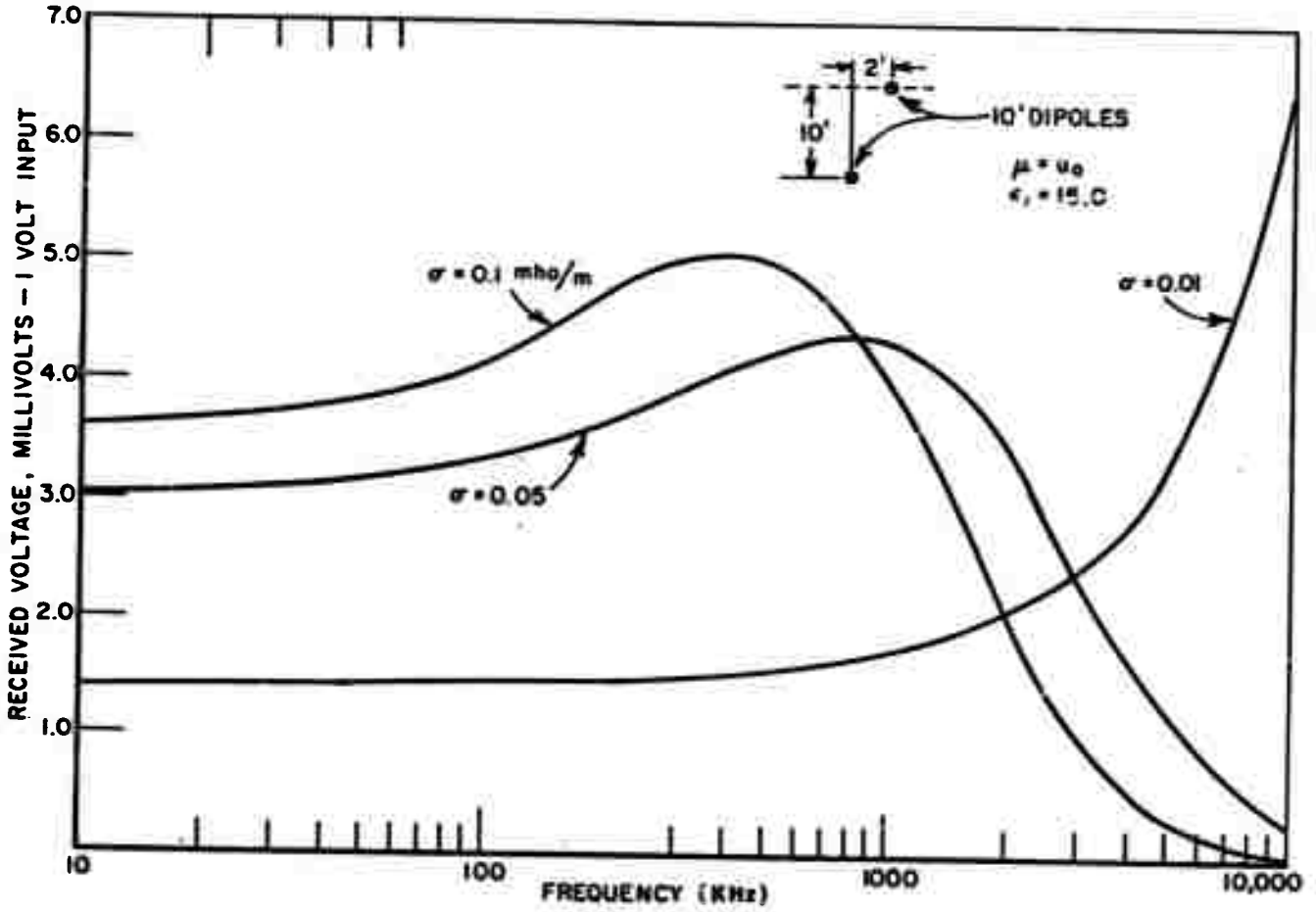

Fig. 3. Received voltage for transmission between two wire antennas in a homogeneous conducting medium, 1 volt input.

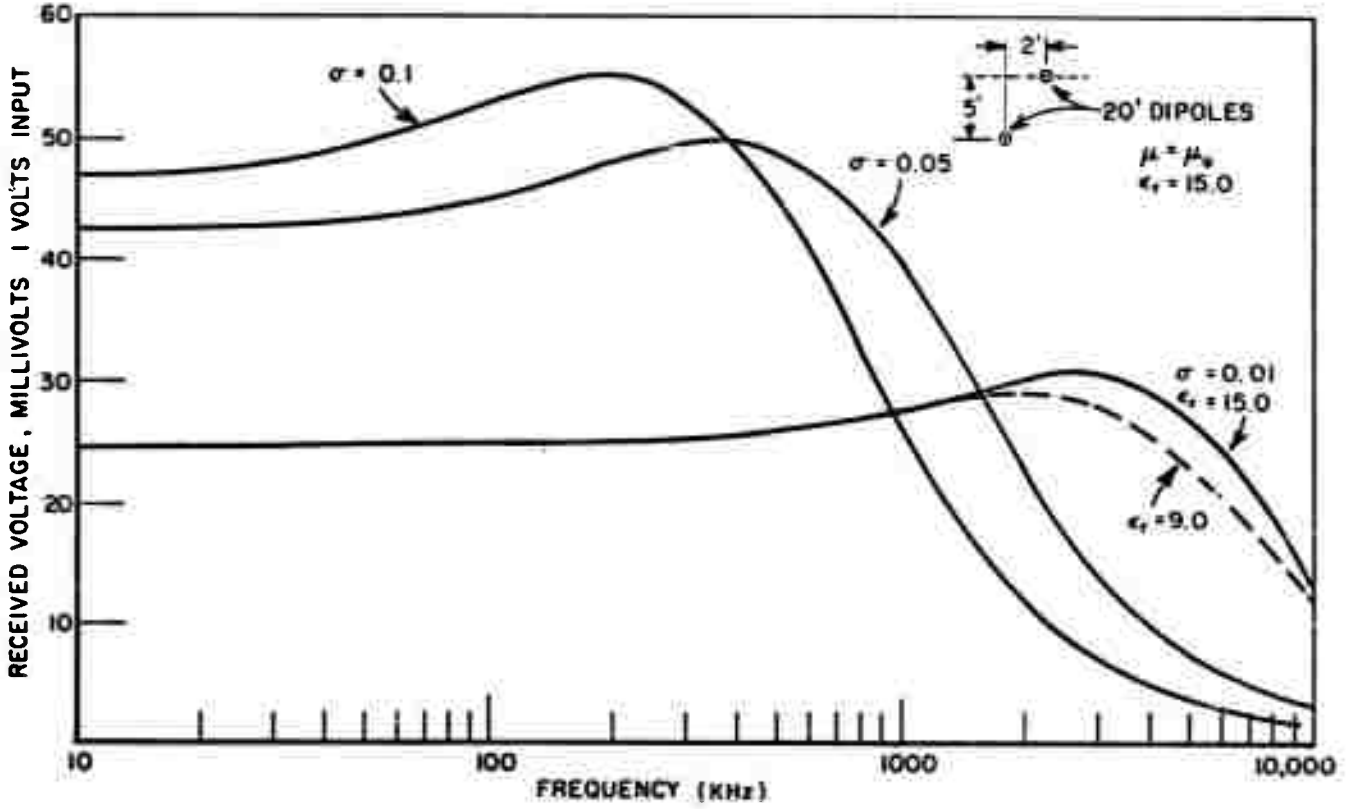

Fig. 4. Received voltage for transmission between two wire antennas in a homogeneous conducting medium, 1 volt input.

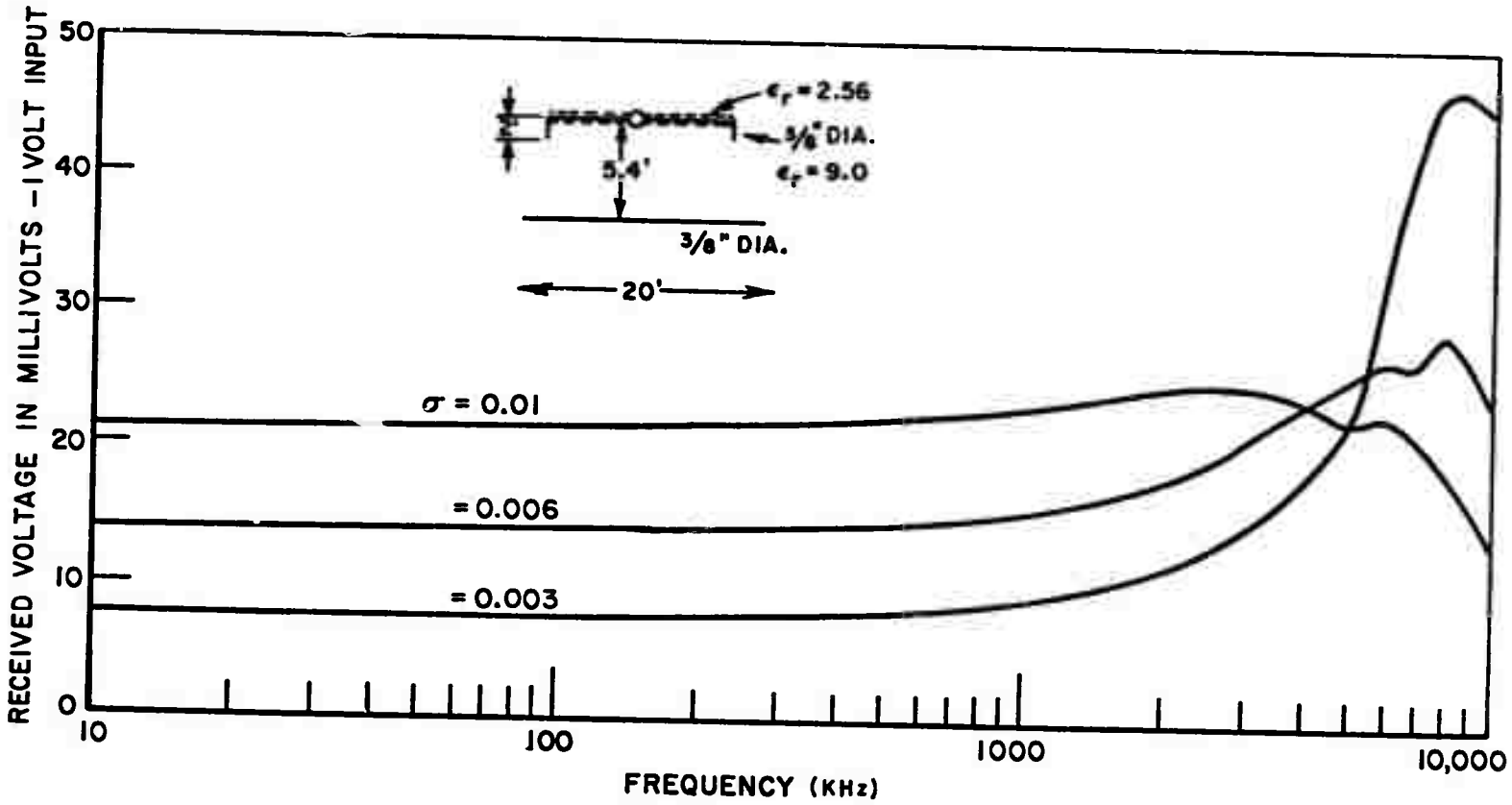

Fig. 5. Received voltage for transmission between two wire antennas in a homogeneous conducting medium, 1 volt input.

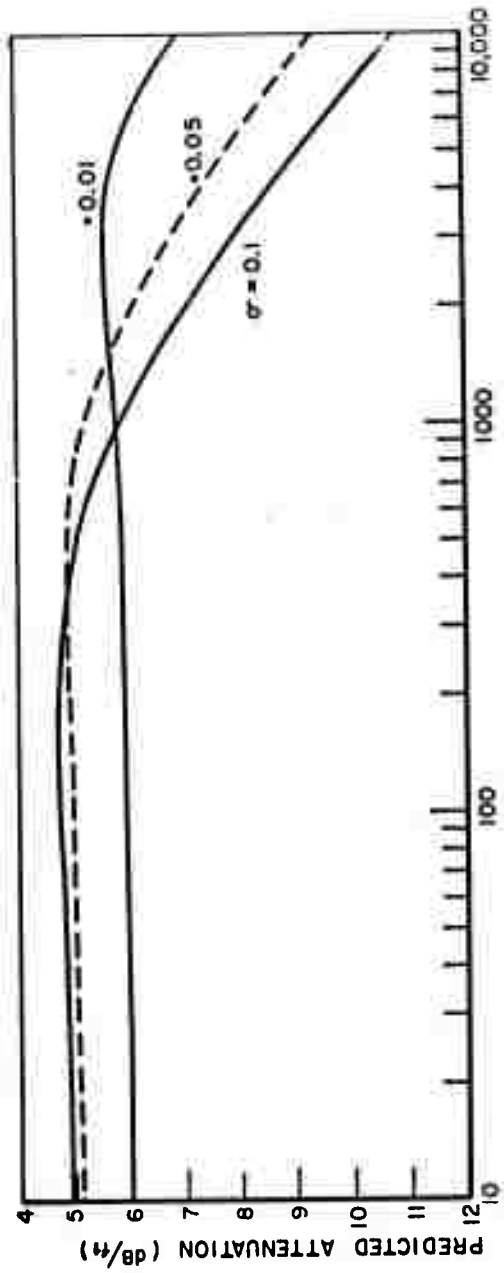

Fig. 6. Predicted attenuation for a homogeneous conducting medium.

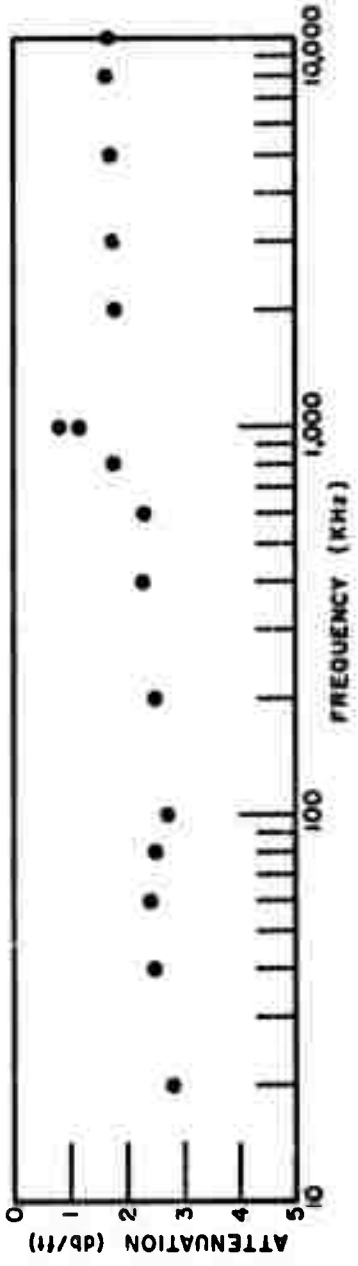

Fig. 7. Measured attenuation of the local ground.

It should also be noted that the wire antenna program was used to predict the input impedance of the buried antenna. Direct reflection measurements on the buried antenna demonstrated that the predicted value was within ±10% of the measured value.

Clearly, the comprehensive analysis and computer program can be used to generate a variety of probe design curves for given target ranges, media and frequency ranges. As noted earlier, we have deferred such an extensive computational program in favor of an experimental program.

Certain studies initiated during the first half of the contract and reported in the Semiannual Technical Report (see Appendix) were not continued during the second phase. The grounded monopole antenna used as a transmitter to make certain propagation tests was discarded for tunnel hazard detection applications for two basic reasons. First, this unbalanced antenna as a receiver has very severe noise problems. Second, it was found that the fields produced by the grounded monopole were confined to very narrow depths (essentially the depth of the monopole) and have a null along the axis of the monopole. While the grounded monopole is not appropriate for tunnel problems, the propagation mode using the monopole as a transmitter and a balanced dipole as a receiver would appear to have possible application for constitutive parameter measurements at shallow depths. An analysis of a line source above a half-space was also not continued. At the suggestion of the Technical Project Officer, our efforts were focussed on the experimental program. The limited budget made it impossible to complete both theoretical and experimental programs. Ultimately, it will be extremely important to evaluate the fields of various sources in functional form in order that the physical mechanisms can be understood. Numerical analyses such as that used for the wire antenna do not yield this information. The results reported in the Semiannual Report (see Appendix) were for the transient fields produced by a line source above a conducting half-space at locations either directly below the source or on the surface of the half-space. The dielectric constant and conductivity of the conducting medium are assumed to be constant with frequency and both short and long time results are given. That is, in the limit of high and low frequencies the wave number of the conducting medium ($\sqrt{j\omega\mu(\sigma+j\omega\varepsilon)}$) goes to $j\sqrt{\omega^2\mu\varepsilon}$ and $\sqrt{j\omega\mu\sigma}$ respectively. Analytical expressions for the transient fields for these cases are given. It may be possible to extend these results to an arbitrary observation point within the medium using numerical integrations. It does not appear feasible to consider a frequency-dependent dielectric constant or conductivity for the medium even if a mathematical model for the parameters were available - the analytical forms of the inverse transformations would become hopeless and render this approach invalid. This does not negate the result but does dictate caution in their interpretation.

V. ELECTROMAGNETIC PULSE SOUNDING SYSTEM.

A block diagram of the electromagnetic pulse sounding system with a direct interfacing to the computer is shown in Fig. 8 together with one version of the electromagnetic probe. The required instrumentation modifications for remote site measurements, i.e., divorcing the system from a direct interfacing with the computer, will be discussed later. The probe shown in Fig. 8 consists of two grounded, orthogonally oriented dipoles, where each dipole arm is a U arrangement of two wires. The probe dimensions shown are appropriate for interrogation of targets to depths of 30 to 40 feet in the overburden using the near-zone fields of the probe. For interrogation to the same depths in a different medium, the overall dimensions of the probe will remain constant but the shape of the dipole arms would be changed. If the medium is such that the use of ground rods is not practical, then an alternative arrangement using metal plates to obtain a capacitive coupling could be used. The purpose of the ground rods or plates is to match the low frequency energy in the interrogating pulse into the ground. In the next section the tuning achieved by both changes in the shape of the dipole arm and adjustments of the ground rod depths is demonstrated.

The pulse sounding system can be operated in two modes; a direct mode where one dipole is used for transmission and reception and an orthogonal mode where transmission is on one dipole and reception on the orthogonal dipole. In the orthogonal mode, the probe is "blind" to homogeneous targets including the air-medium interface and "sees" only inhomogeneous targets. The direct mode "sees" both homogeneous and inhomogeneous targets. It should not be inferred that the orthogonal mode will not "see" planar-type contrasts of infinite extent. If the contrast plane has some tilt with respect to the plane of the probe, the orthogonal mode will indeed respond. Thus the only planar discontinuity for which the probe is "blind" is one parallel to the probe plane - a seemingly remote possibility in tunneling. In operation as a hazard detection device in tunneling operations it is intended that for each location of the probe on the tunnel face, three measurements will be made - two direct modes using the two orthogonal dipoles individually and one orthogonal mode. This should provide excellent coverage without the necessity of moving the probe. During this contract period, effort has been primarily concentrated on orthogonal mode operation. This mode affords excellent transmitter-receiver isolation and is ideally suited for the type of targets considered. Also, true direct mode measurements using high voltage pulse generators will require some circuitry modifications in order to protect the sampling head of the scope from the high voltage pulse. The necessary circuitry is felt to be within the state-of-the-art. The baluns shown with the probe in Fig. 8 are special broadband baluns (Z-Line 50200E) which transform an unbalanced coaxial line with an impedance of 50 ohms to a balanced transmission line with an impedance of 200 ohms. A variety of such baluns are available for low power applications as "off the shelf" items. However, for high power applications the balun design to achieve broadbandedness is critical and must be individually tailored for specific pulse generators.

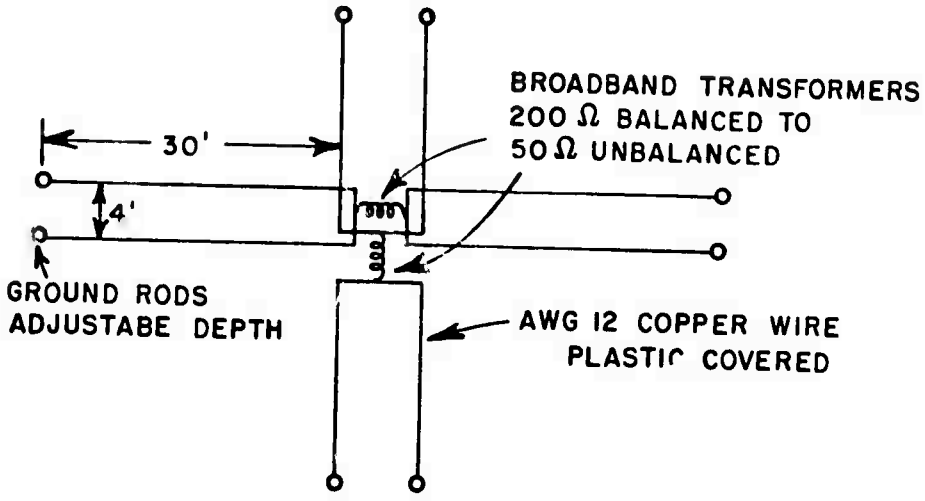

(a) ELECTROMAGNETIC PROBE

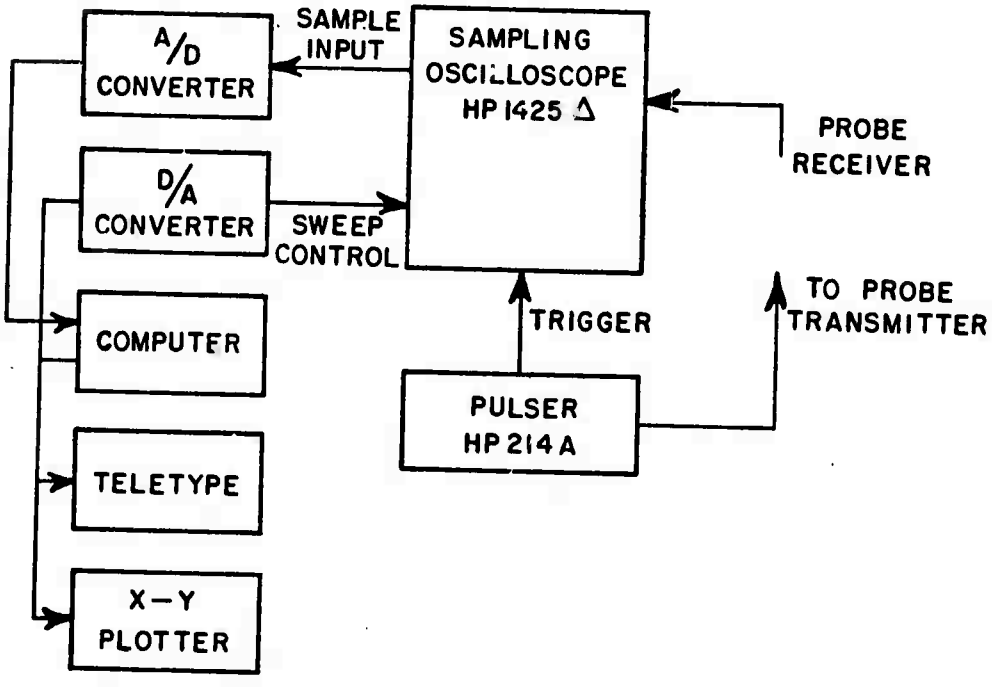

(b) BLOCK DIAGRAM — ORTHOGONAL MODE

Fig. 8. (a) Electromagnetic probe.
(b) Block diagram of pulse sounding system.

The electromagnetic pulse sounding system currently in use employs a pulse generator which produces a periodic train of video-type pulses. The pulses are coupled into the medium by the transmit arm of the broadband probe. Periodically, a wave is launched on the transmit dipole at the feed point which penetrates into the medium. As the wave propagates along the dipole, its fringe fields penetrate deeper into the medium. The dipole is not currently being employed as a radiating structure in the normal sense since it is the near fields which are being used. For this reason the dipole is referred to as a probe rather than as an antenna structure. Reflected signals from the medium are observed on a sampling scope acting as a receiver. The measurements are automated, i.e., the computer controls the scope sweep and records a response waveform which is an average of some 200 reflected waveforms. The purpose of averaging is to minimize noise problems. Once the averaged waveform is recorded it is available for further processing either in real time or at some later time. When the optimum processing schemes are fixed, the computer functions can be replaced by simple circuitry, but at this research stage the computer offers an irreplacable versitility.

The system modifications necessary for remote measurements are shown in Fig. 9. An external ramp generator controls the horizontal axis of the oscilloscope display providing a sweep rate independent of the sampling time base. The ramp generator also provides a gate signal which goes positive when the sweep begins and negative when the sweep is finished. The gate and ramp signals are recorded in parallel with the oscilloscope waveform on three channels of a multichannel FM tape recorder. In playback, the three channels recorded are connected to three analog/digital converter inputs for conversion of the oscilloscope waveforms into digital information.

The conversion technique is illustrated in Fig. 10. The ramp voltage at any point is proportional to the deflection across the screen of the oscilloscope waveform that has been recorded. Thus n evenly spaced samples may be taken by taking a sample at the start of the sweep and then monitoring the ramp and taking another sample each time the ramp voltage increases by $\Delta V = (V_2-V_1)/(n-1)$ until n samples have been taken. The gate voltage is used to provide a precise time mark for the first sample. From then on the sampling points are determined by the ramp voltage. This information is then fed into the digital computer and processed in the same manner as data from the local measurements.

A. Probe Configurations and Tests

A sketch of one version of the probe structure suitable for interrogation of targets at depths of 30 to 40 feet was shown in Fig. 8. In Figs. 11 and 12 the tuning mechanisms afforded by, respectively, the shape of the dipole arms and depth of the ground rods are illustrated. The results shown in Figs. 11 and 12 are direct reflectometry measurements on one dipole over the local overburden where the incident pulse is a step function with a 2 volt peak and a 15 ns rise time. The advantages of a dipole arm composed of two wires in a U or V arrangement as compared to an arm made up of a single wire are clearly evident in Fig. 11 where reflection waveforms for these dipoles are compared with those with an open circuit,

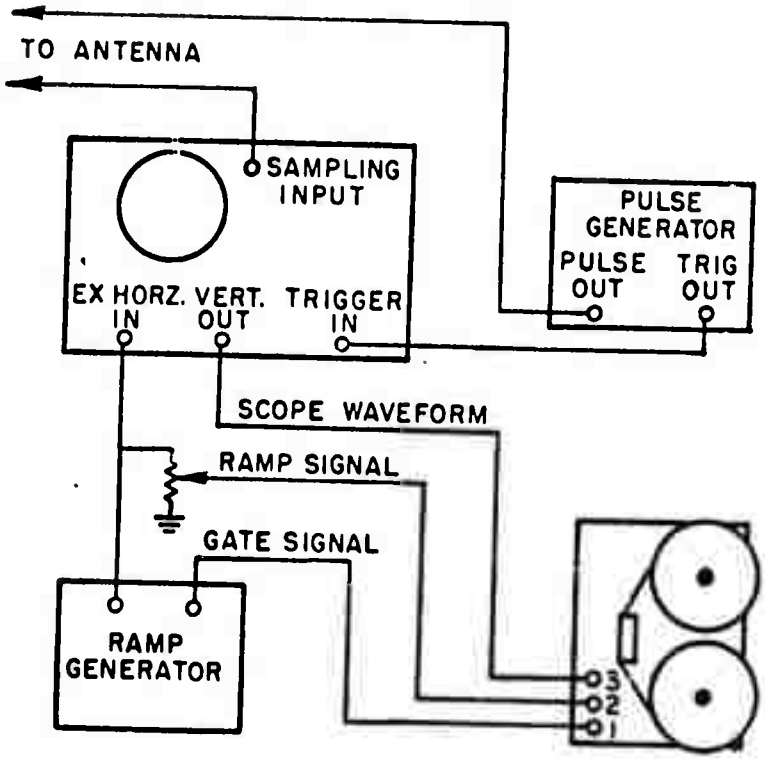

Fig. 9. Remote measurement system.
(a) recording
(b) playback.

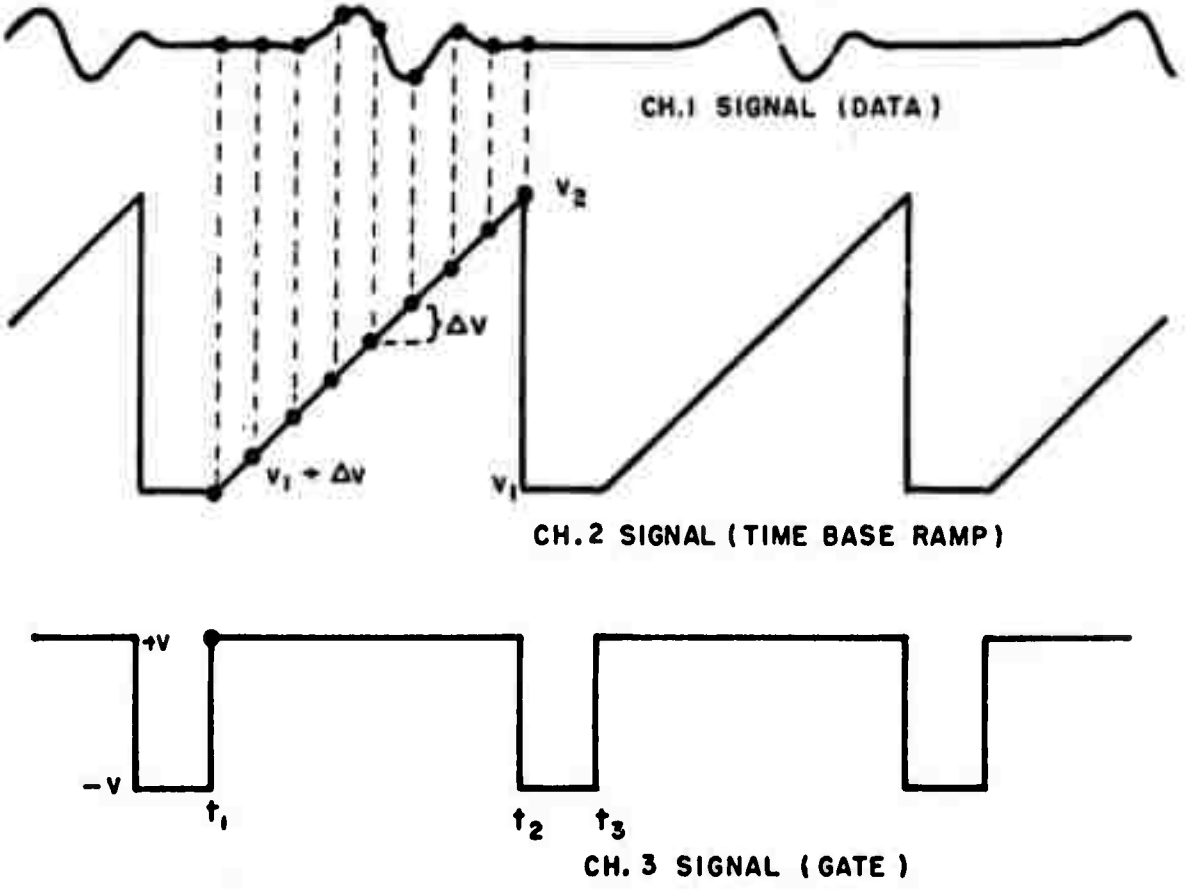

Fig. 10. Conversion of tape recorded data.

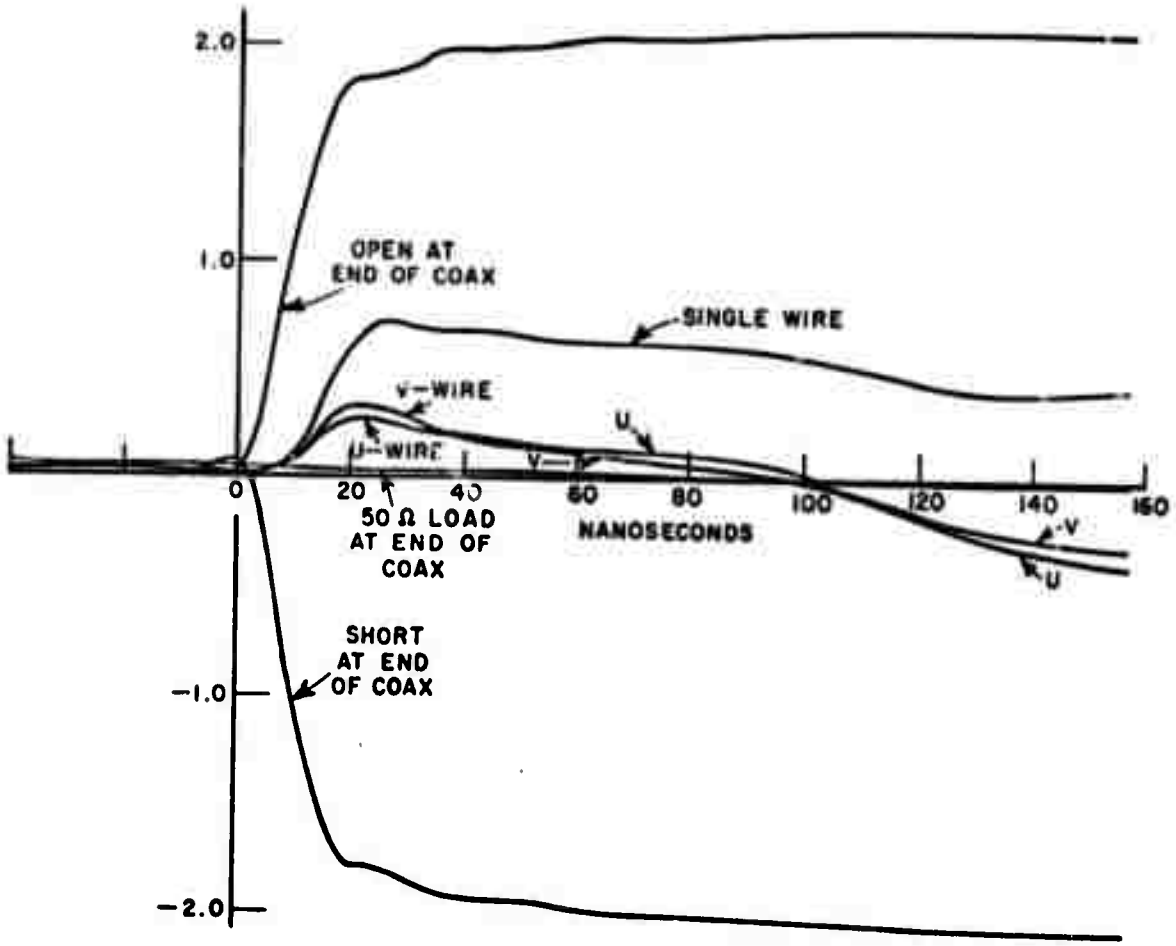

Fig. 11. Direct reflection mode of one probe, various termination and probe arm shapes.

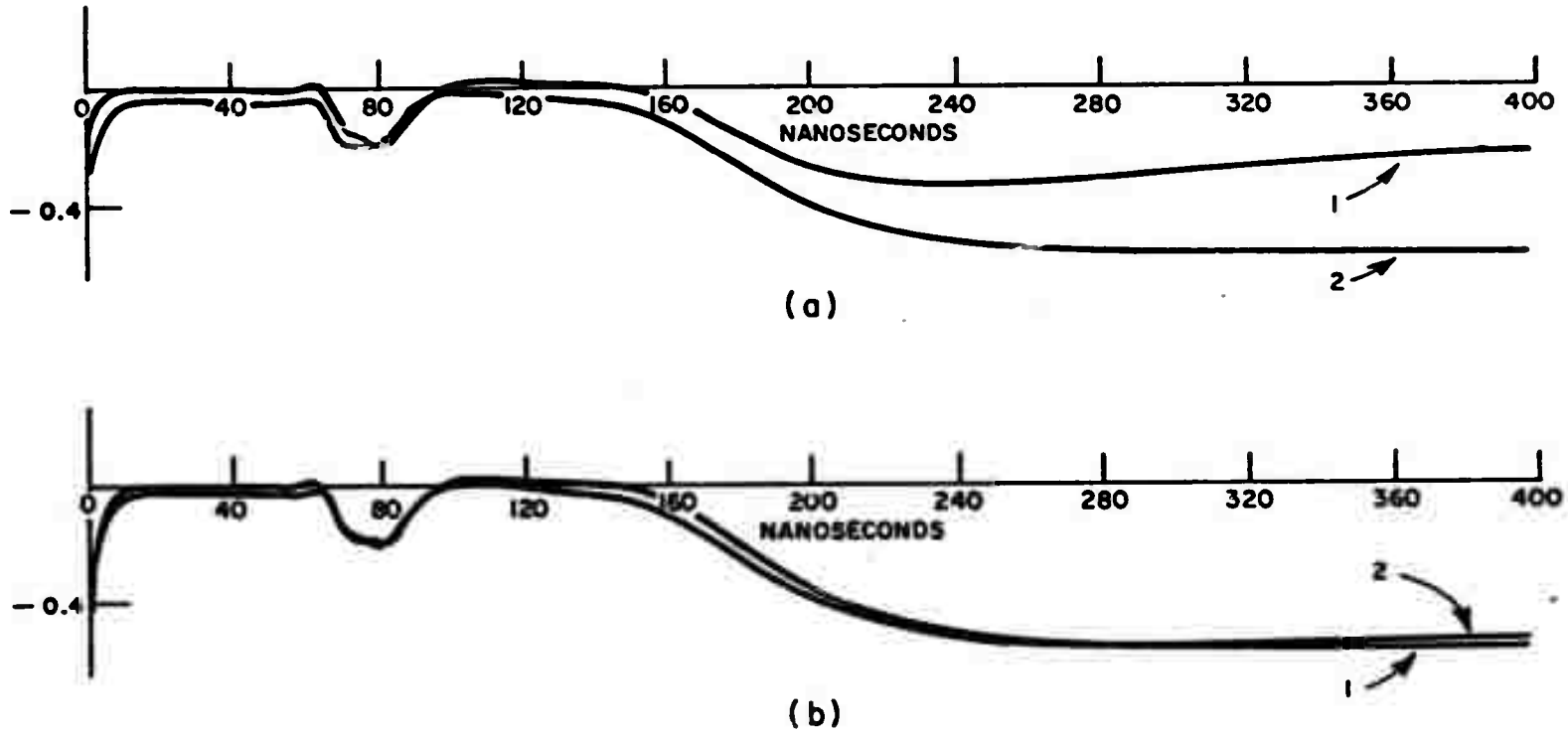

Fig. 12. Direct reflection mode of one probe, effect of ground rod depth.

short circuit and matched load at the probe feed point. In Fig. 12, the time scale is compressed in order to illustrate the tuning capabilities of the ground rods. By adjusting the ground rod depth, the later portion of the waveform can be matched to the waveform obtained when a matched load is placed at the end of the feed cable. Note that the waveforms shown in Figs. 11 and 12 are ample evidence that low frequency energy can be effectively coupled into the medium. When the probe configuration of Fig. 8 was tested in the orthogonal mode it was found that the system was extremely insensitive to surface obstructions. A station wagon driven between the probe arms had no effect on the response waveform.

The probe configuration in Fig. 8 was designed for use with an HP 214-A pulse generator purchased for use on this contract. The characteristics of the HP 214-A pulser (50 volt peak, 45 ns base, 10 KHz repetition rate) are appropriate for interrogation of subsurface targets with a maximum linear dimension of less than 10 times the repetition wavelength in the medium. Two other pulse generators; a laboratory built unit (5 volt peak, 3 ns base, 1-2 MHz repetion rate) and an Ikor generator (1000 volt peak, 250 ps base, 250 Hz repetition rate) are presently available at this laboratory. The Ikor unit became available less than one month ago.

After completion of a series of design measurements similar to those shown in Figs. 11 and 12, a series of direct and orthogonal mode measurements over the local overburden were initiated. It was found that when the Hewlett Packard pulser (HP214-A) was operated at peak power (50 volt peak pulse), the balun (50200E) on the transmit probe saturated. Saturation occurred, in fact, for pulse peaks less than 10 volts. Saturation of the transmit balun results in the appearance of false targets in the response waveform whose position is dependent on the incident pulse magnitude and duration. The balun problem does not in itself represent a basic limitation since baluns with a higher power handling capability can be built. At the same time, one should not underestimate the design difficulties inherent in building a balun to handle the HP 214-A pulse generator operating at peak power and to achieve a bandwidth from 10 KHz to 60 MHz. We seek to achieve reasonable pulse fidelity so that simply being able to force some power through the balun over this frequency range is not sufficient. It was decided, primarily because balun winding remains essentially an art rather than a science, to order appropriate baluns from a commercial specialist (Z-line Corporation) and circumvent the immediate difficulty either by eliminating the need for the balun or by using a lower power pulse generator. The decision not to attempt to wind our own baluns appeared to be a wise one since even for those with expertise in this area, a promised delivery date of 2 months extended to almost 5 months indicating some design difficulties. We now have baluns which meet the specifications of the HP214-A pulse generator. Unfortunately, the baluns were delivered too late to attempt a measurement sequence on subsurface targets during this contract period.

Attempts to eliminate the need for a balun were unsuccessful. In each scheme tested, it was found that when the baluns were

removed currents on the feed cables produced a sensitivity to feed cable position which was intolerable. Consequently, a series of measurements using a smaller version of the probe and the laboratory-built pulse generator were initiated. With a 1 to 2 MHz repetition rate and a 5 volt peak, this pulse generator is not appropriate for deep penetration of the medium. However, available 50200E baluns pass this pulse with good fidelity and thus the feasibility of the pulse sounding scheme could be tested on shallow targets, depths to 5 feet or so in the overburden, without encountering balun saturation problems. Accordingly, a series of measurements on conducting and dielectric cylindrical targets buried to depths of 5 feet in the local overburden were made. Results of these measurements are given in Section VI. The probe structure used for these measurements is shown in Fig. 13. Note that a section of 300 ohm twin lead has been inserted between the balun output and the feed point of the dipoles. The purpose of the twin lead is to clean-up, as far as possible, the range window for targets at shallow depths in the overburden. A direct or reflection mode measurement on one dipole of the probe in Fig. 13 is shown in Fig. 14. Note that the balun reflection is primarily high frequency and could be anticipated since the high frequency end of the 50200E balun is around 60 MHz. A second effect was noted from measurements similar to the one in Fig. 14. It was found that changing the ground rod depth had little effect on the response waveform. Comparing this result with those obtained for the larger prob. indicates that tuning via ground rod depth adjustment is primarily effective for frequencies below 1 MHz, at least when the probe is located on the overburden. On a less lossy medium, sensitivity to the ground rod depth should extend to higher frequencies.

Early in the contract period it was decided that some remote site measurements should be made at a nearby limestone quarry. The limestone medium ($\varepsilon_r \simeq 8.0$, $\sigma < 10^{-5}$ mhos/meter) was the most practical approximation to a hard rock medium (e.g., granite, $\varepsilon_r \simeq 7.0$, $\sigma < 10^{-6}$) within a reasonable distance from the laboratory.[9] Accordingly a mobile rig was outfitted (power to run the pulse generators and scopes was not available at the site) and instrumentation to divorce the system from the computer devised. Certain man-made and geological anomalies at the quarry appropriate for interrogation with the large probe and HP214-A pulse generator had been selected. When it became evident that the high power baluns would not be available during this contract period, it was decided to take a series of measurements at the quarry using the smaller probe and pulse generator. It was known in advance that certain of the targets selected were not appropriate using this pulse sounding system. The results of these measurements are given in Section VII.

Using flexible wires to construct the arms of the probe has the advantage that the wires can be made to conform to the individual undulations of the medium. A major disadvantage is that aligning the individual dipoles to achieve precise orthogonality is often a tedious and time-consuming effort. Alternatively, constructing the probe arms of rigid members automatically yields orthogonality, but now the height of the feed point can vary and the probe may well have

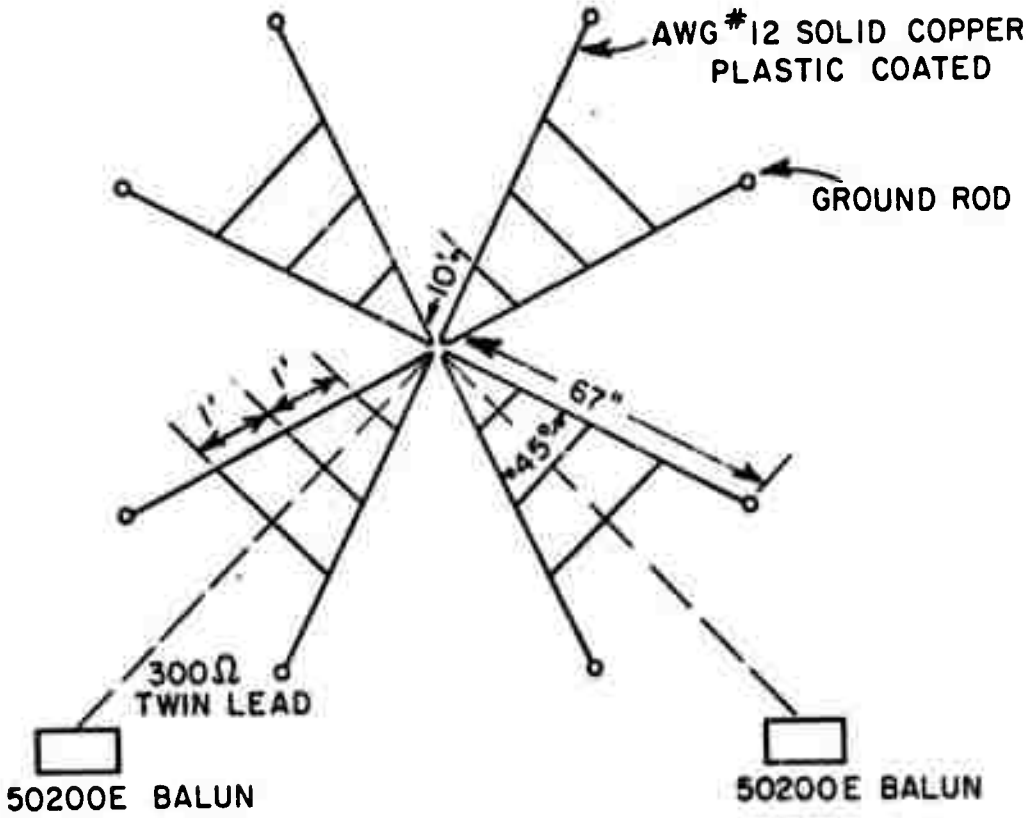

Fig. 13. Small electromagnetic pulse sounding probe.

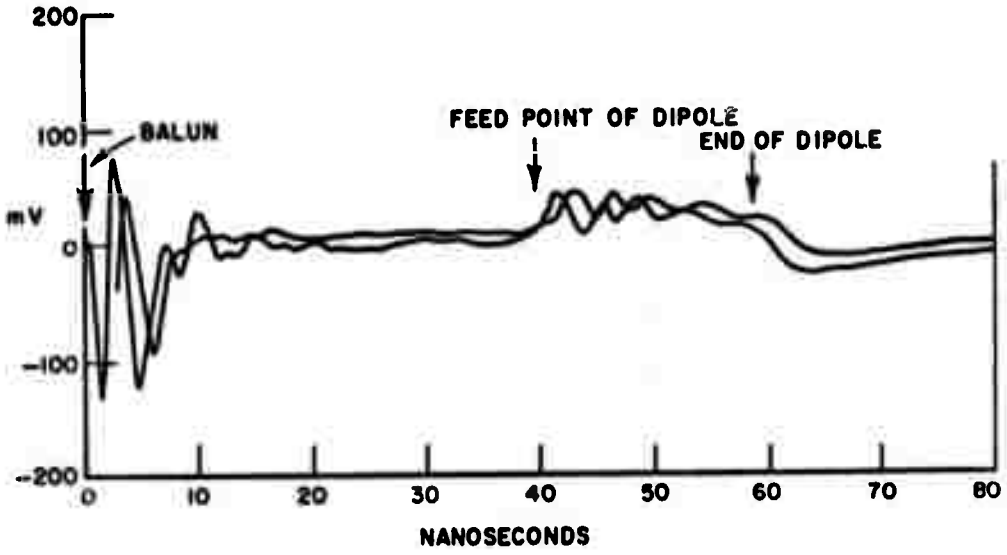

Fig. 14. Direction reflection mode of one probe.

some slope with respect to the medium's mean surface. Certain tests have been made of small probe configurations with respect to optimum arm configurations, feed point heights and the use of an absorbing material between the probe and the overburden (the vegetation above the overburden highly attenuates the high frequency energy in the pulse). The results of these tests are summarized below.

A preliminary study of probe parameters, including effects of varying conductor shape, height above the ground surface, and placing absorptive material between the probe and ground surface, has been made. In all cases an orthogonal transmit-receive probe pair was used. This approach seems to be the best way of isolating two probes which are very close to one another.

When a probe pair lies on a rough surface, it is known that isolation is degraded due to the asymmetry caused by the uneven ground. The frequency content of this coupling is inversely proportional to the average sizes of the ground irregularities, but in general lies above 40 MHz. For an application concerned with distant targets, where return with frequency content below about 40 MHz is expected, the ground irregularity problem is of little concern, since it can be virtually eliminated by filtering. It was found that raising the probes 2 to 3 inches above the ground and using absorptive material between the probe and ground, both improved the target return to clutter ratio for shallower targets where higher frequency returns were expected.

The effects of antenna geometry and conductor shape are seen at all frequencies. For the "bow-tie" (Fig. 15) configuration used in this study, the ends of the structure have been identified as the major source of coupling problems. Asymmetries in layout or ground parameters at the ends result in a degraded target return to clutter ratio. Initial tests have shown that the elimination of multiple reflections on the probe structure, and a "smoother" shape in general result in an improved performance. Further tests using models appropriate for distant targets are planned.

B. Processing Pulse Sounding Measurements

Simplified block diagrams for the electromagnetic pulse sounding probe in the orthogonal mode are shown in Fig. 16 for no-target (Fig. 16a) and target (Fig. 16b) configurations, where the block T indicates the presence of the target. Capitalized letters correspond to frequency-dependent quantities and the lower case counterpart to a time-dependent waveform. Each capital and lower case symbol are a transform pair. In terms of the complex variable $S = \sigma + j\omega$

$$E^o_{NT}(S) = C_t(S)\, P_t(S)\, G(S)\, P_r(S)\, C_r(S)\, E^i(S)$$

(1)

$$E^o_T(S) = C_t(S)\, P_t(S)\, G(S)\, T(S)\, P_r(S)\, C_r(S)\, E^i(S),$$

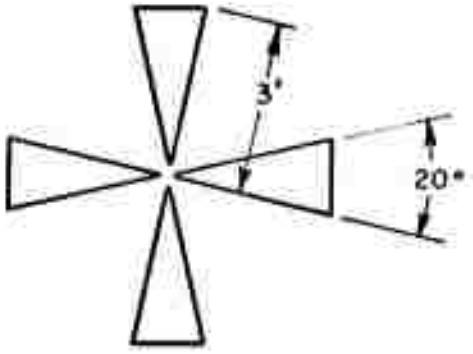

CROSSED DIPOLES

Fig. 15. Sketch of experiment probe geometry.

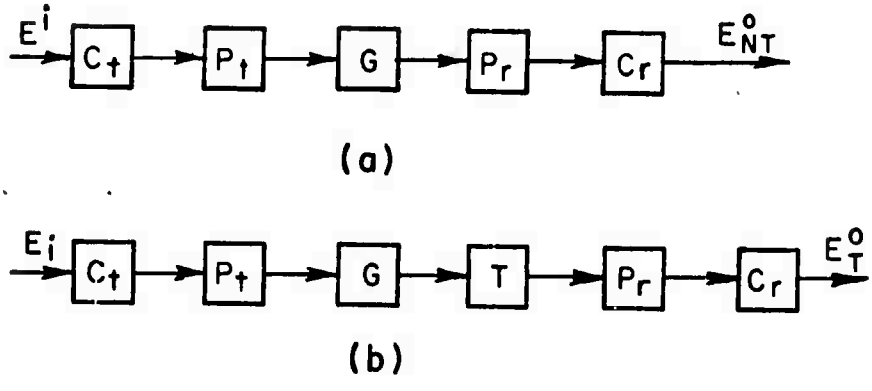

Fig. 16. Block diagram or pulse sounding probe in orthogonal mode.
(a) no-target
(b) target.

where C, P, G and T are the transfer functions of the cable, probe ground and target respectively and the subscripts t and r denote transmit and receive. The cable transfer functions include the baluns and short lengths of twin-lead line. Making the reasonable assumptions that the transmit and receive properties are identical, Eq. (1) simplifies to

$$E^o_{NT}(S) = C(S)^2\, P(S)^2\, G(S)\, E^i(S)$$

(2)

$$E^o_T(S) = C(S)^2\, P(S)^2\, G(S)\, T(S)\, E^i(S)\ .$$

By shorting the cables together including the baluns and twin-lead line, the normalizing response

(3) $$E^o_N(S) = C(S)^2\, E^i(S)$$

can be recorded. Ideally then

(4) $$\frac{E^o_T(S) - E^o_{NT}(S)}{E^o_N(S)} = P(S)^2\, G(S)\, [T(S) - 1]\ .$$

The normalizing response $E^o_N(S)$ is stable and repeatable. However, the no-target measurement is not precisely stable if the probe is moved to various ground locations. This is due to localized properties of the ground such as roughness, inhomogeneities, moisture content, vegetative cover, etc. which changes G(S). Some effect is also due to changes in P(S) which is somewhat sensitive to the height of the probe feed points above the ground. We choose to ignore the probe effect since most of this occurs in the direct coupling between the transmit and receive probes and, as will be seen later, can be gated out. At the jth location then the no-target response is more properly

(5) $$E^{oj}_{NT}(S) = C(S)^2\, P(S)^2\, E^i(S)\, [G_o(S) + N^i(S)]\ .$$

In practice, some M no-target measurements are made and an average

(6) $$\overline{E^o_{NT}(S)} = \frac{1}{M}\sum_{j=1}^{M} E^{oj}_{NT}(S) = C(S)^2\, P(S)^2\, E^i(S)\, [G_o(S) + \frac{1}{M}\sum_{j=1}^{M} N^j(S)]$$

is obtained. In a similar fashion an average target waveform

(7) $$\overline{E_T^o(S)} = \frac{1}{M}\sum_{j=1}^{M} E_T^{oj}(S) = C(S)^2\, P(S)^2\, E^i(S)\, T(S)\, [G_o(S) + \frac{1}{M}\sum_{j=1}^{M} \tilde{N}^j(S)]$$

is obtained either by moving along an extended target keeping the same probe-target geometry or by simply putting the probe down M times in the same location. Note that the ground transfer function has been written as

(8) $$G(S) = G_o(S) + N^j(S),$$

for the no-target case and as

(9) $$G(S) = G_o(S) + \tilde{N}^j(S)$$

for the target case. The reason being that the sampling is actually different in that for the target case the variations are restricted. The normalized difference of the averages is

(10) $$\frac{\overline{E_T^o(S) - E_{NT}^o(S)}}{E_N^o(S)} = P(S)^2\, G_o(S)\, [T(S) - 1] + \frac{P(S)^2}{M} \{ T(S) \sum_{j=1}^{M} \tilde{N}^j(S) - \sum_{j=1}^{M} N^j(S) \} .$$

If we make the assumption that $\tilde{N} = N$ then

(11) $$\frac{\overline{E_T^o(S)} - \overline{E_{NT}^o(S)}}{E_N^o(S)} = (T(S)-1)P(S)^2\, [G_o(S) + \frac{1}{m}\sum_{j=1}^{M} N^j(S)]$$

Let

(12) $$\frac{1}{M}\sum_{j=1}^{M} N^j(S) = N(S) ,$$

then

(13) $$\frac{\overline{E_T^o(S)} - \overline{E_{NT}^o(S)}}{E_N^o(S)} = (T(S)-1)P(S)^2\, [G_o(S) + N(S)] .$$

Interesting comparisons to Eq. (13) are

$$(14) \qquad \frac{E_{NT}^{oj}(S) - \overline{E_{NT}^{o}(S)}}{E_{n}^{o}(S)} = P(S)^2 \left[N^j(S) - N(S)\right] ,$$

and

$$(15) \qquad \frac{E_{T}^{oj}(S) - \overline{E_{T}^{o}(S)}}{E_{n}^{o}(S)} = P(S)^2 \, T(S) \left[\tilde{N}^j(S) - N(S)\right] ,$$

which essentially show the variance of the no-target and target measurements respectively.

Actually, the differencing and averaging are done in the time domain

$$\overline{e_{NT}^{o}(t)} = \frac{1}{M} \sum_{j=1}^{M} e_{NT}^{oj}(t)$$

$$(16) \qquad \overline{e_{T}^{o}(t)} = \frac{1}{M} \sum_{j=1}^{M} e_{T}^{oj}(t)$$

$$\overline{\delta(t)} = \overline{e_{T}^{o}(t)} - \overline{e_{NT}^{o}(t)} = \frac{1}{M} \sum_{j=1}^{M} e_{T}^{oj}(t) - \frac{1}{M} \sum_{j=1}^{M} e_{NT}^{oj}(t)$$

The fast Fourier transform of the difference waveform is then normalized by the pulse and cable spectrum. It has been demonstrated that the transform of the difference waveform is the difference of the transformed waveform, thus no aliasing errors are present. Usually, the difference waveform, $\delta(t)$, is gated before being transformed. That is, the difference waveform, $\delta(t)$, is multiplied by a gate waveform

$$(17) \qquad \begin{aligned} g(t) = {} & a(t-T_1) \left[u(t-T_1) - u(t-T_2)\right] + \\ & 1 \left[u(t-T_2) - u(t-T_3)\right] + \\ & \left[1 - a(t-T_3)\right] \left[u(t-T_3) - u(t-T_4)\right] , \end{aligned}$$

where a, T_1, T_2, etc. are real constants. The time durations T_2-T_1 and T_4-T_3 are equal, and can be zero. The purpose of the gate is to remove the leading portion of the difference waveform which has rather high frequency content and can be attributed to direct coupling between the transmit and receive probes. It can also be used to isolate the scattered fields from different reflection mechanisms. Examples

of the ungated and gated difference waveforms will be shown later. A trapazoidal gate is used in order to avoid placing artifically generated step discontinuities in the gated waveform.

Processing the data then involves the following steps:

1) averaging the target and no-target time domain waveforms.

2) Obtaining the time domain difference waveform, i.e., the target average minus the no-target average.

3) Gating the difference waveform to remove the direct coupling between transmit and receive probes.

4) Transformations of the gated difference waveform to the frequency domain, i.e., a fast Fourier transform.

5) Normalization of the transformed difference by the pulse-cable transfer function.

6) Inverse transformation of the normalized spectrum in 5) back to the time domain - inverse fast Fourier transform.

Four signatures of the target are available for study; the amplitude and phase characteristics in the frequency domain (5 above), the time domain difference waveform before normalization (3 above) and the time domain difference waveform after normalization (6 above). From a comparison of these signatures for various targets, one can begin to consider the separation of targets and the recognition of a given target. We have confined our results for the present to examinations of the normalized amplitude spectrum and the gated difference waveform before normalization. The phase spectrum does have information content but it is generally more difficult to utilize. Also, we will generally need more power and lower frequencies in the interrogating pulse spectrum in order to obtain reasonable phase spectrums. With more advanced processing schemes we would begin to combine the amplitude and phase data at several frequencies to synthetically produce waveforms uniquely characteristic of the target and possibly intimately related to the physical properties of the target. As was demonstrated earlier,[7] obtaining waveforms predictably dependent upon the target's physical properties may not be possible in a highly dispersive medium but this does not negate obtaining a characteristic waveform.

In the next two sections of this report, certain of the waveforms and spectra discussed above for cylindrical targets in the overburden and for targets in a limestone medium are presented.

C. Manipulation of Time Domain Reflectometry Data

It was noted earlier (Section IVB) that an extremely versatile program for the automated measurement and processing of pulse sounding data was used with a directly interfaced instrumentation computer. This software has been developed on a number of programs including this contract. The main features of the program are described below.

Program for Manipulation of Time Domain Data

This program provides a means of recording time domain data from a sampling oscilloscope, drawing it on the plotter, storing it on the disc and performing various manipulations including Fourier transforms.

Data files consist of a single disc track and must be created with the DAT command prior to program execution. They consist of 256 data words followed by 10 file description words and finally a code word which is equal to integer 1 for a frequency domain file and zero for a time domain file.

The program actually consists of three complete programs which are interchanged by the core swapping subroutine SWAP. To load the program:

First load TDRSS in the regular way and execute.
Then load TDRS in the regular way and execute.
Finally load TDRM in the regular way and execute.

The program has its own operating system and when TDRM is executed it will respond with a # sign. It will then accept any of the following commands (only the first three characters are significant).

CALibrate - The sampling 'scope is set to the upper scale limit and a carriage return is typed. Repeat for lower scale limit. Computer gives instructions. These points will be ±4 inches on the plotter.

RECord - 256 samples are recorded from the sampling 'scope (average of 200 sweeps) and converted to a ±4 scale in terms of the calibration points.

WRIte file- Writes the 256 data points currently in core on the disc. Program responds with NAME: The file name is then typed in. Program then prints DESCRIPTION. Up to 30 characters of description may then be typed in which are written on the file. Program follows with INSTRUMENT SETTINGS. A further 30 characters may be used to indicate these. The file is written after the final carriage return.

READ file - NAME is requested and the previously written file read back into core.

DEScription-Prints out the 30 character description and the 30 characters indicating instrument settings of the most recently read or written file.

WHAT is? - Program requests NAME. The 30 character description of the named file is then printed out without affecting the main core buffer. Used to check whether an old file is wanted before writing over it.

PLOT - Draws the current contents of the core buffer on the plotter. In the time domain the scale is simply ±4 inches. In the frequency domain only the amplitude of the d.c. term and the first 100 harmonics is plotted on a 0 to -80 dB scale.

XSHift - INCHES is requested. The data points are then shifted in core by the indicated amount. Points are shifted to the nearest core location; there is no interpolation. Points lost at one end of the trace are added to the other end. (Do not use for frequency domain data.)

YSHift - INCHES in DBS are requested for the time or frequency domains respectively. The data in core is then shifted by the indicated amount. In the frequency domain only the amplitude data is shifted. The angles remain unchanged.

GRId - Draws a grid on the plotter. The computer requests the number of divisions required in each direction.

ADVance - Moves the plotter forward one page.

REVerse - Moves the plotter back one page.

FFT - Takes the fast fourier transform of the contents of the core buffer. The data output is stored so that the odd number points are amplitudes on a dB scale starting with the d.c. term and continuing to the 127th harmonic in location 255. The even number points are phase angles in radians. The 0 dB level corresponds to the d.c. power represented by a constant 4 inch deflection in the time domain.

IFFt - Takes the inverse Fourier transform.

FILter - Used to process a time domain waveform through a band pass filter. The program requests the highest and lowest harmonics to be saved (0 to 127, 0 being the d.c. term).

COMbine files - Provides for adding or subtracting files in any manner. FILES (NAME AND MULTIPLIER) is printed followed by a colan (:). The file name is typed in followed by a carriage return. An X is then printed. Any real multiplier is then typed in followed by a carriage return. This sequence is repeated as many times as desired. A carriage return in response to: terminates the sequence leaving the weighted sum in the core buffer (e.g., to obtain a difference curve a multiplier of 1. could be used for the first file and -1. for the second. Multipliers of 5. and -5. would produce a magnified difference. A multiplier of 0.25 for each of four files would produce an average, etc.) Taking a difference of two frequency domain files produces a ratio since amplitudes will be subtracted in dBs and phases in radians. (A multiplier used here would amount to raising to a power). This permits impulse responses to be found by dividing a response waveform by that of an incident pulse; also reflection coefficients by dividing a response by that of a short circuit.

PRInt - Prints all or part of the current core buffer on the teletype. The starting element number will be requested. Printing may be interupted with the BREAK button. A control D will then return to the # sign. The scale of the print out is in inches of plotter movement in the time domain and dB and radians in the frequency domain (see FFT for data arrangement).

LABel - Draws the current DESCRIPTION, INSTRUMENT SETTINGS and FILE NAME on the plotter. LABEL NUM: will be requested. The first label will be in the top left hand corner of the page. If a second, third, etc. label is required it will be moved down 1" each time. A carriage return has the same effect as typing number 1 for the label number.

GATE - Gates out a portion of the time domain waveform. The GATE OPEN and GATE CLOSE positions in inches are requested. All points before OPEN and after CLOSE are set to zero.

VI. PULSE SOUNDING DATA FOR CYLINDRICAL TARGETS BURIED IN THE OVERBURDEN

Pulse sounding measurements of various cylindrical targets buried in the overburden close to the ElectroScience Laboratory have been made. The measurements were made using the small probe shown in Fig. 13 and the laboratory-built (5 volt peak, 3 ns base, 1.5 MHz repetition rate) pulse generator. The targets consisted of 2, 3 and 4 inch diameter hollow dielectric (ϵ_r = 2.56) pipes at a depth of 3 feet in the over-

burden and 4 inch diameter conducting hollow pipes, 1, 3, 5 and 10 feet long at a depth of 5 feet in the overburden. The dielectric targets were some 20 feet long or greater. Other conducting pipes in the same sequence, i.e., lengths of 1, 3, 5 and 10 feet, are also buried at depths of 1 foot and 3 feet and have been measured, but the data presented here will be confined primarily to the 5 foot depth.

In Figs. 17 and 18, respectively, the interrogating pulse and its spectrum are shown. The pulse and spectrum shown corresponds to propagation through both feed cables (roughly 150 feet each), both baluns (50200E) and two sections of 300 ohm twin lead shorted together. The balun characteristics shown in Figs. 17 and 18 will not change when the twin lead is attached to the probe. The balun operation is separated in time from the probe and it is the characteristic impedance of the line, not the total impedance seen at the output port of the balun, which is important for the short time response of interest. Clearly the pulse shown in Fig. 17 is not the waveform being transmitted into the ground - it is however the waveform at the feed point of the probe. Ideally, the normalization of the response waveforms should be by the actual transmitted pulse, but this waveform cannot be measured. To obtain this waveform requires an absolute calibration of the system and this in turn requires both an experimental measurement of a known target geometry and an analytical solution must be obtained using the near-zone fields of the probe. Thus, an extention of the wire antenna analysis is needed to provide a complete calibration of the system. Note that the spectrum shown in Fig. 18 has been normalized by setting the magnitude of the harmonic with the peak amplitude to unity. One must carefully distinguish between this type of normalization and that suggested to remove the incident pulse, cables and baluns from the spectral and temporal responses. The spectrum in Fig. 18 corresponds to the quantity $E_R^N(S)$ in Eq. (3), where it is assumed that all other spectra will be normalized to unity first in the same way.

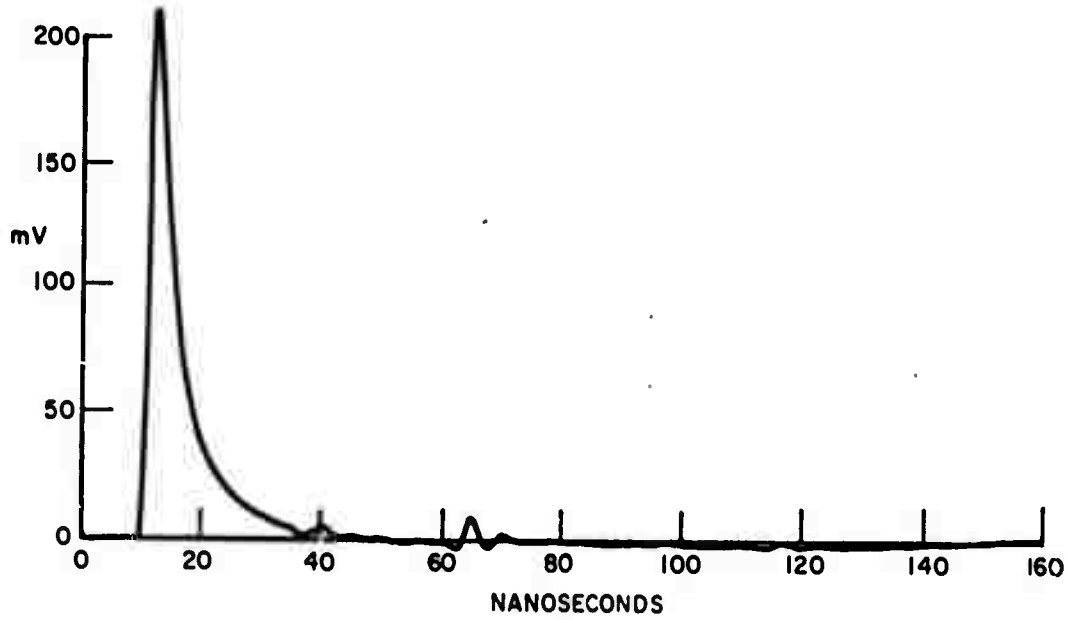

Fig. 17. Interrogating pulse waveform.

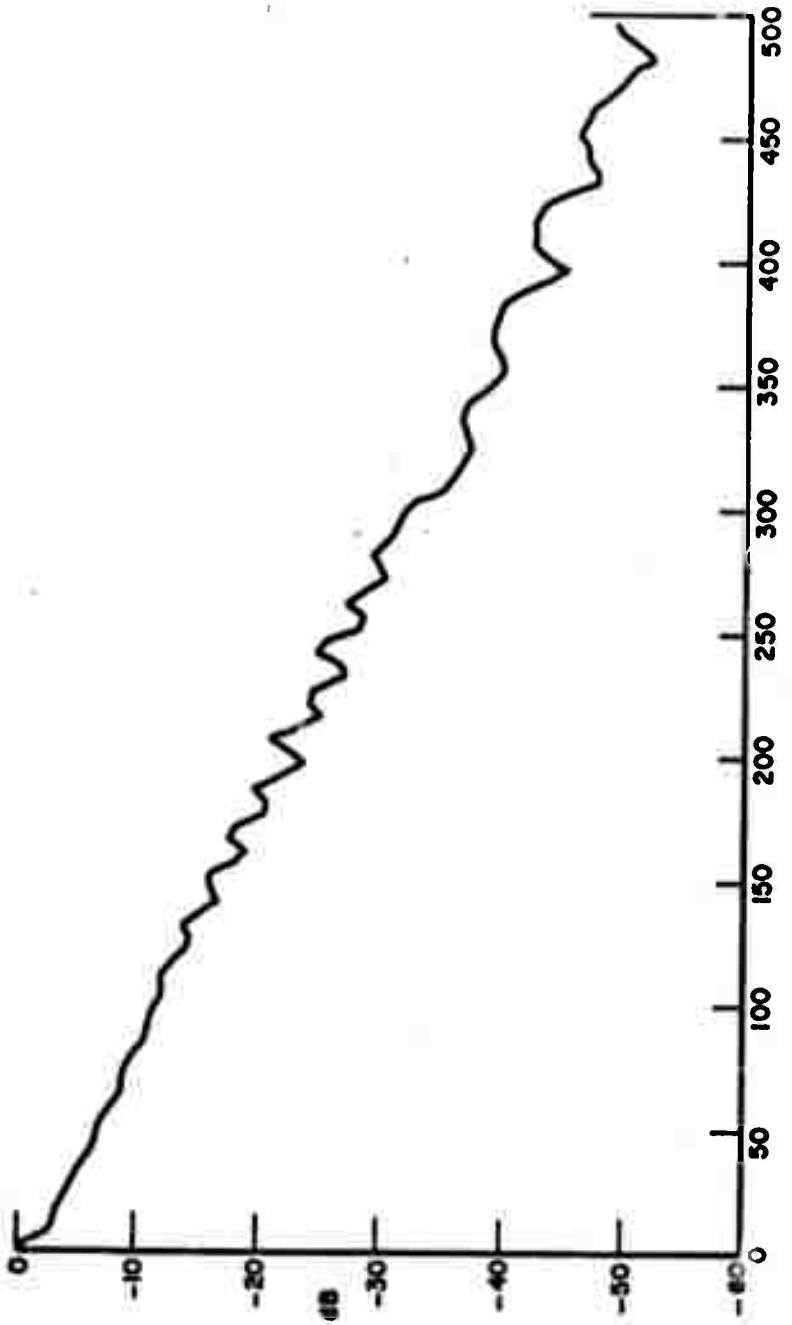

Fig. 18. Amplitude spectrum of interrogating pulse.

It was stressed in Section VB, that it was important to secure averages of both the no-target and target response waveforms because of possible individual variations. In Figs. 19a and 19b respectively, 4 measurements (orthogonal mode) of a no-target configuration at 4 different locations and 3 measurements of a 3 foot conducting cylinder (4 inch diameter) at a depth of 3 feet are shown. For a cylindrical target, maximum response in the orthogonal mode occurs when the cylinder axis bisects the angle between the transmit and receive dipoles. The orthogonal data reported here and in Section VII were made using this configuration. Shown in Fig. 19c and Fig. 19d respectively are the average waveforms for the no-target and target configurations. Deductions based on comparisons of any selected pair from Figs. 19a and 19b might be inconclusive, but a comparison of the averaged waveforms leaves little or no doubt as to the presense of a target.

On the following pages, measured and processed waveforms and spectra for the following targets are given in Figs. 20 to 28, respectively.

1. 2 inch diameter dielectric pipe.
2. 3 inch diameter dielectric pipe.
3. 4 inch diameter dielectric pipe.
5. 4 inch diameter x 1 foot length conducting pipe
6. 4 inch diameter x 3 foot length conducting pipe
7. 4 inch diameter x 5 foot length conducting pipe
8. 4 inch diameter x 10 foot length conducting pipe
9. a dummy trench (5 foot depth x 10 foot length), i.e., a trench dug and then refilled
10. No-target results.

In each figure, with certain obvious exceptions, the following waveforms and spectra are shown.

a. the difference waveform, target average - no-target average
b. the gated difference waveform.
c. the unnormalized amplitude spectrum of the gated difference waveform.
d. the normalized amplitude specturm of the gated difference waveform.
e. the normalized amplitude spectrum of the gated difference waveform with the spectrum of the incident pulse, cables and baluns removed.

Several general points should be noted. The difference waveform (a) has been gated to basically remove the direct coupling between transmit and receive probes. A rectangular gate was used and the on-point of the gate selected to avoid introducing step discontinuities. The off-point of the gate was 160 nsec in each case. The characteristics of the amplitude spectrum of the incident pulse (Fig. 18) are such that when it is subtracted from the target spectrum (d) an enhancement of the high frequencies results since the process involves division by small numbers. Realistically, the spectra in e in each figure should be disregarded above roughly 300 MHz.

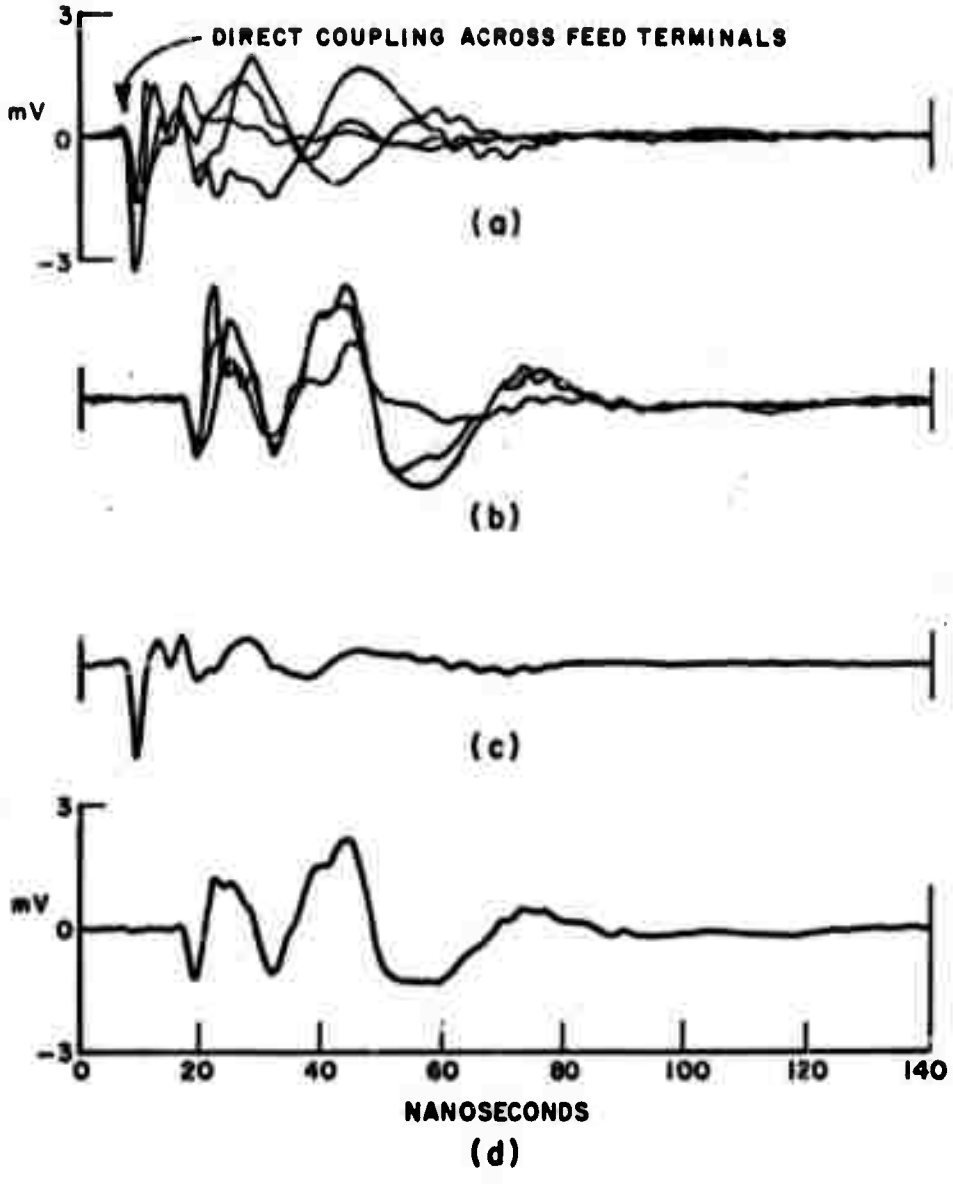

Fig. 19. Orthogonal mode response waveforms.
(a) no-target
(b) 3 foot cylinder target
(c) no-target average
(d) target average.

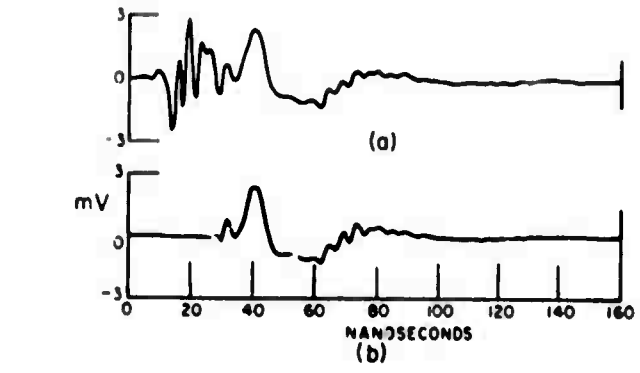

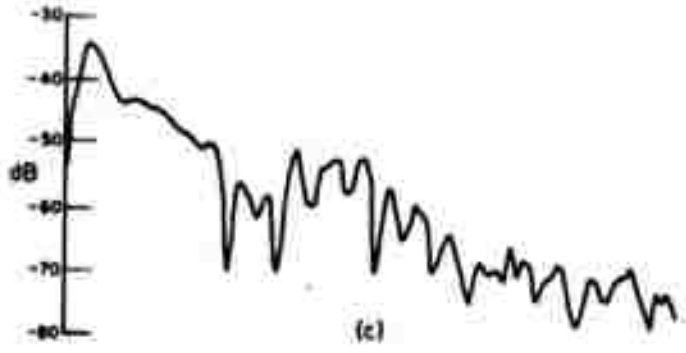

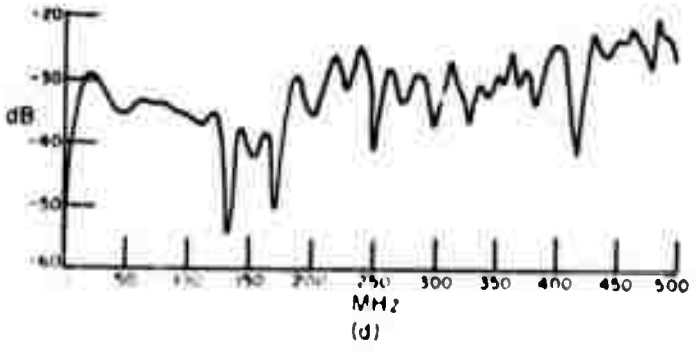

Fig. 20. Orthogonal mode response 2" dielectric pipe.
(a) difference waveform
(b) gated difference waveform
(c) normalized amplitude spectrum
(d) normalized amplitude spectrum with incident pulse removed.

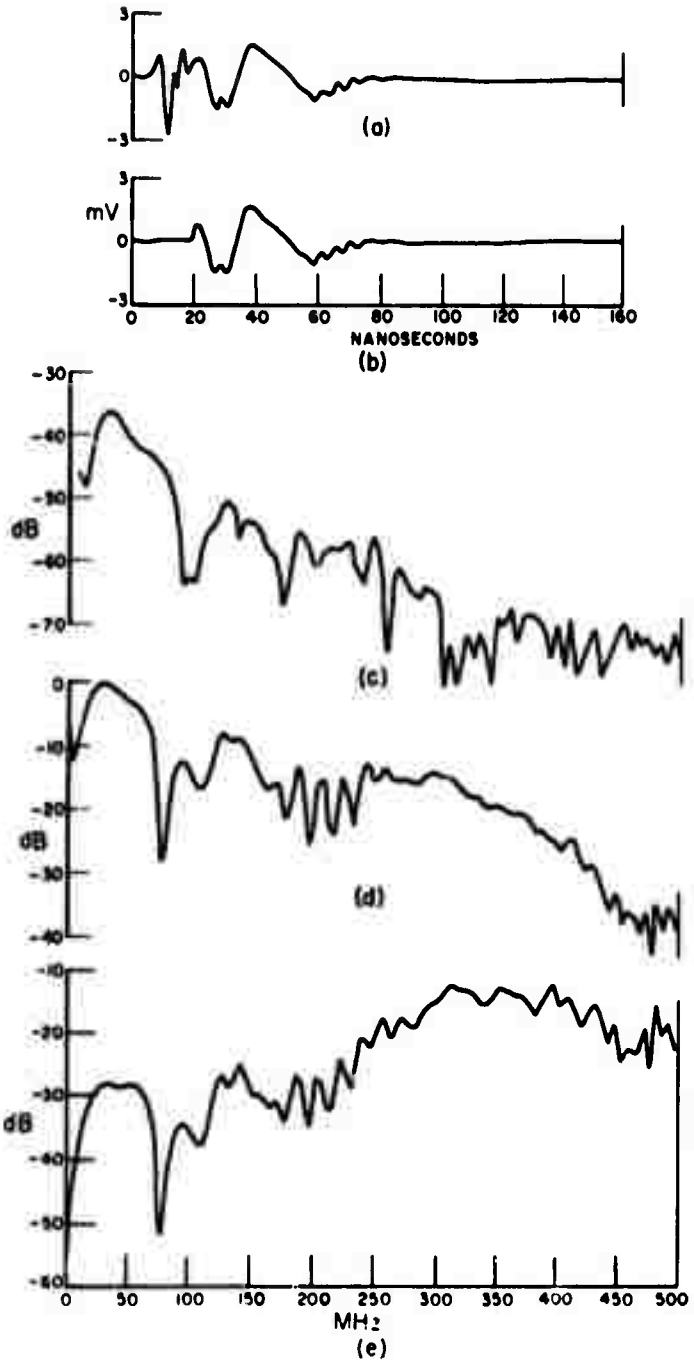

Fig. 21. Orthogonal mode response 3" dielectric pipe.
(a) difference waveform
(b) gated difference waveform
(c) unnormalized amplitude spectrum
(d) normalized amplitude spectrum
(e) normalized amplitude spectrum with incident pulse removed.

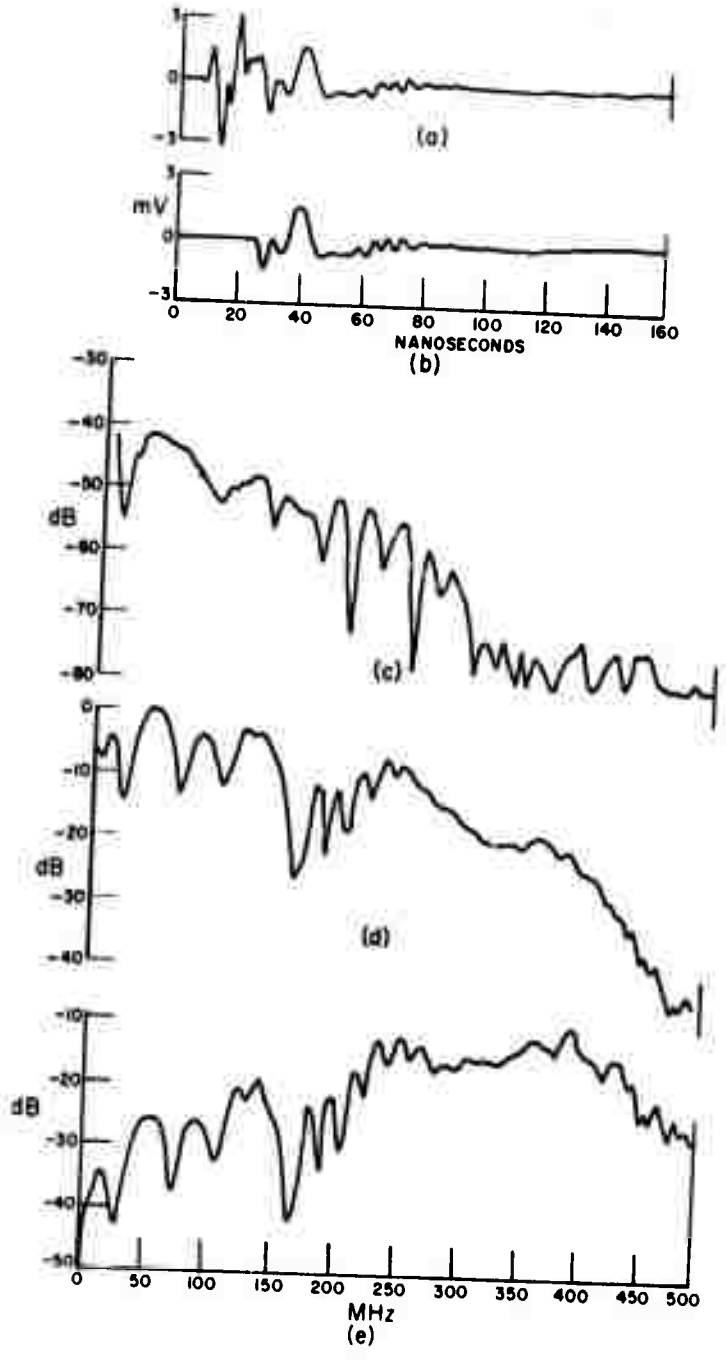

Fig. 22. Orthogonal mode response 4" dielectric pipe.
(a) difference waveform
(b) gated difference waveform
(c) unnormalized amplitude spectrum
(d) normalized amplitude spectrum
(e) normalized amplitude spectrum with incident pulse removed.

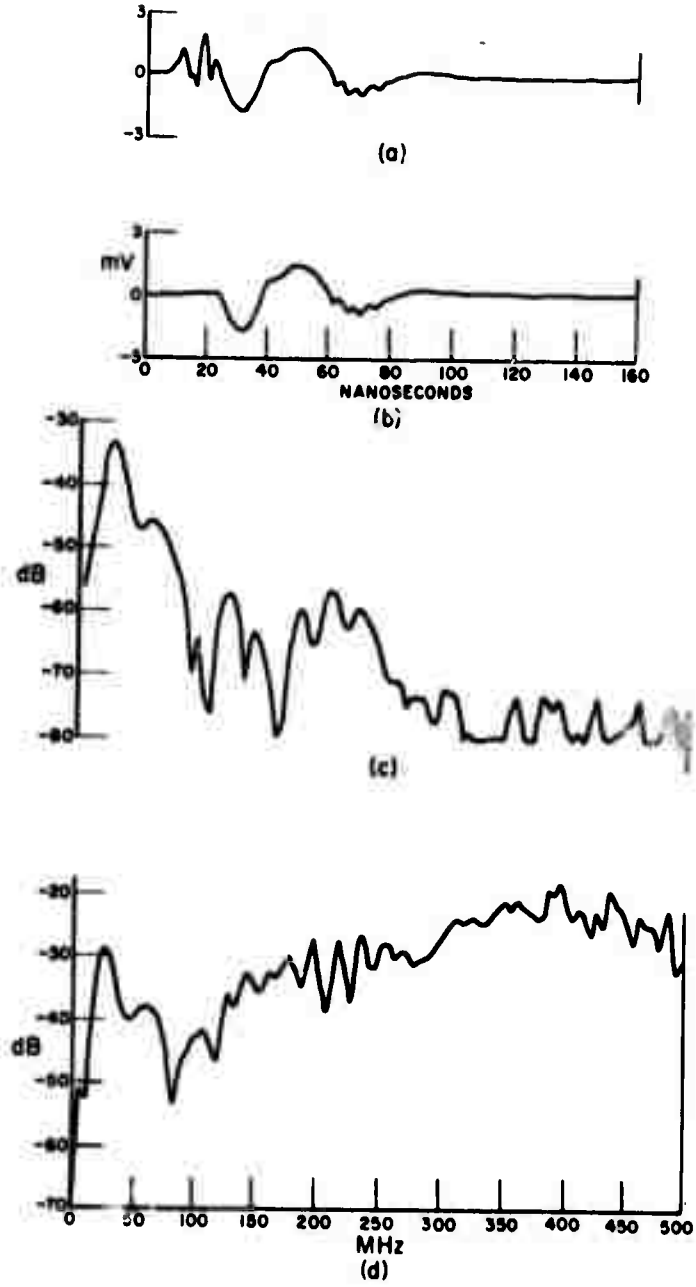

Fig. 23. Orthogonal mode response 1' cylinder.
(a) difference waveform
(b) gated difference waveform
(c) normalized amplitude spectrum
(d) normalized ampl itude spectrum with incident pulse removed.

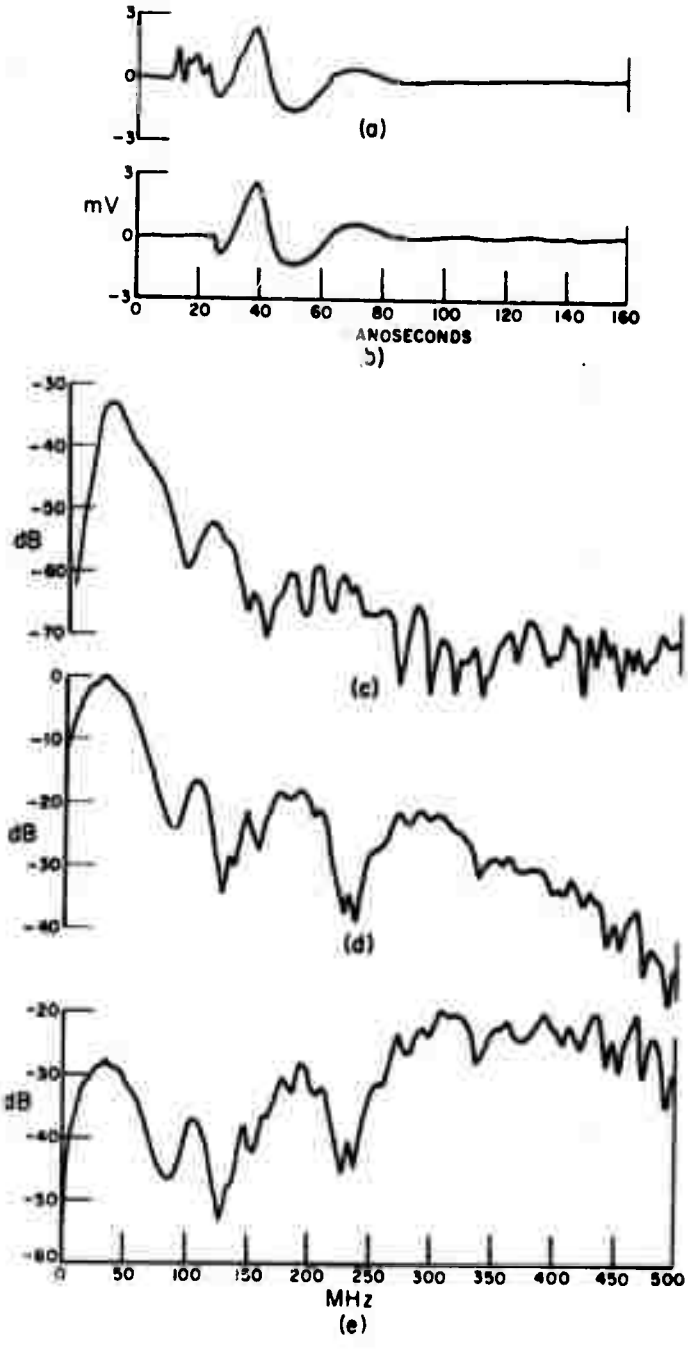

Fig. 24. Orthogonal mode response 3' cylinder.
(a) difference waveform
(b) gated difference waveform
(c) unnormalized amplitude spectrum
(d) normalized amplitude spectrum
(e) normalized amplitude spectrum with incident pulse removed.

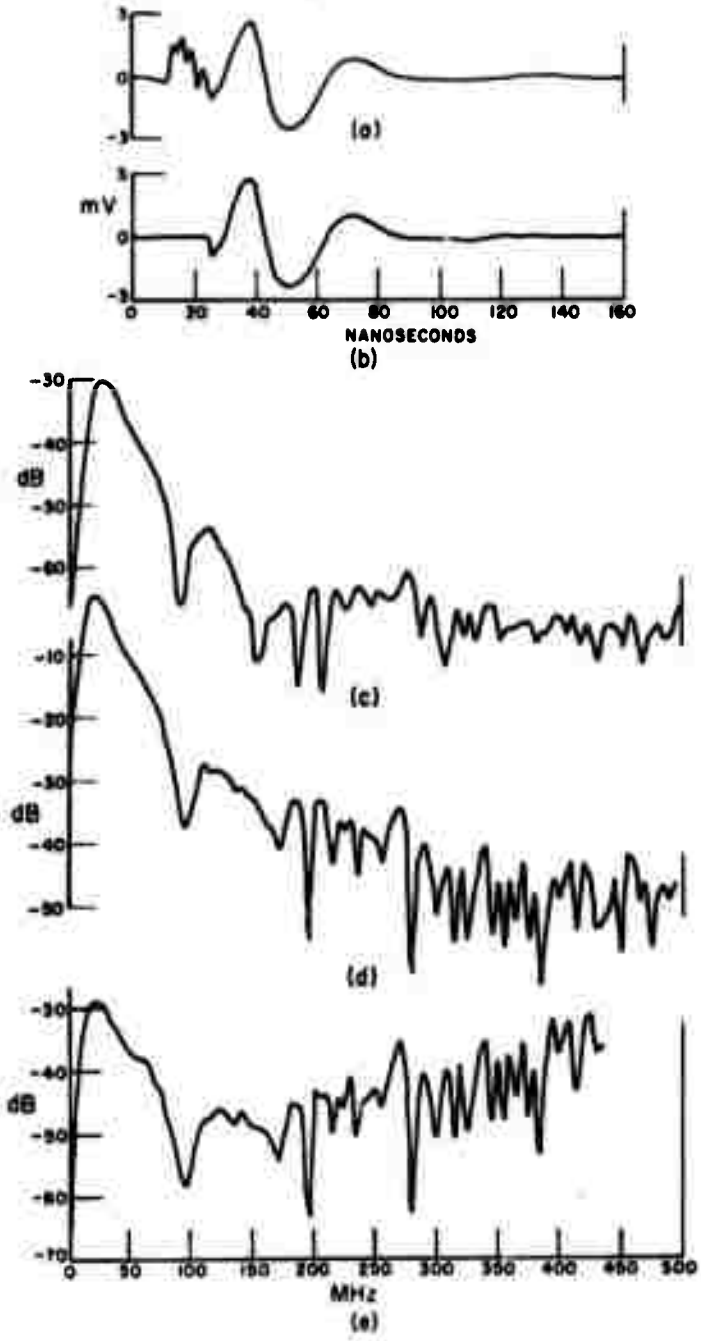

Fig. 25. Orthogonal mode response 5' cylinder.
(a) difference waveform
(b) gated difference waveform
(c) unnormalized amplitude spectrum.
(d) normalized amplitude spectrum
(e) normalized amplitude spectrum with incident pulse removed.

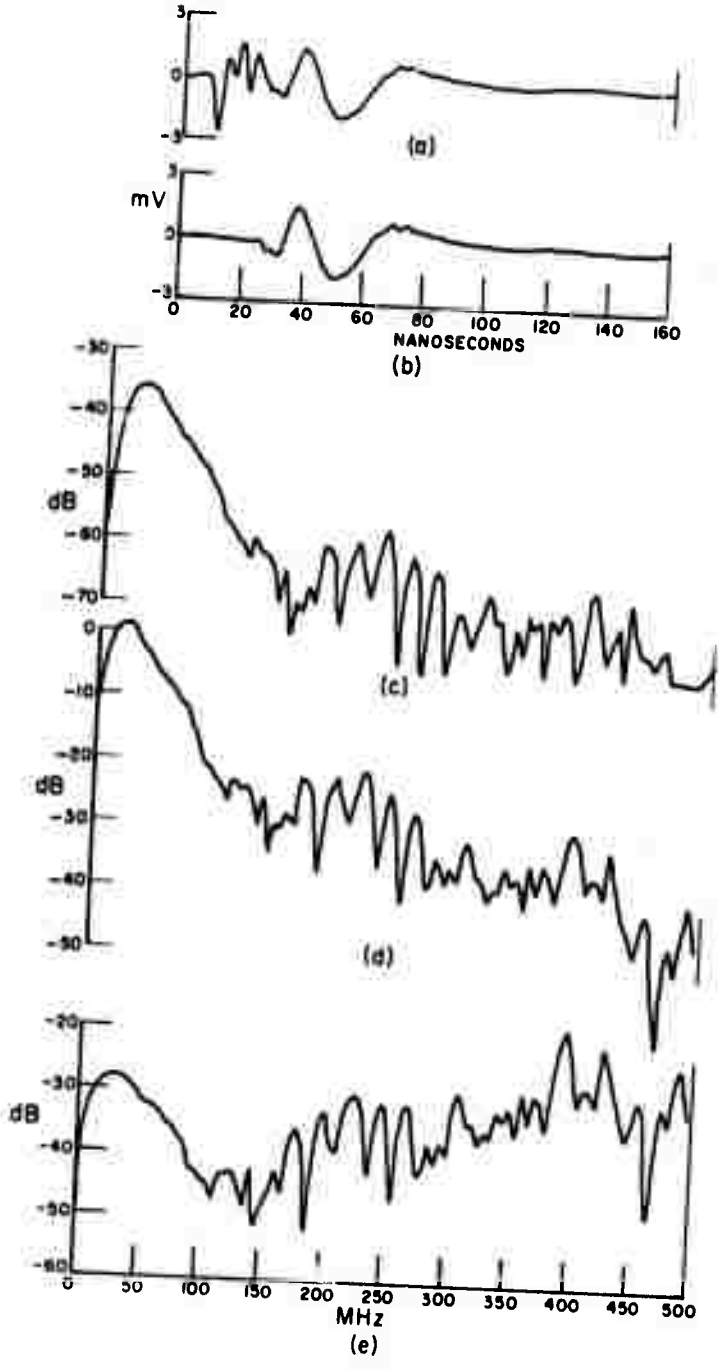

Fig. 26. Orthogonal mode response 10' cylinder.
(a) difference waveform
(b) gated difference waveform
(c) unnormalized amplitude spectrum
(d) normalized amplitude spectrum
(e) normalized amplitude spectrum with incident pulse removed.

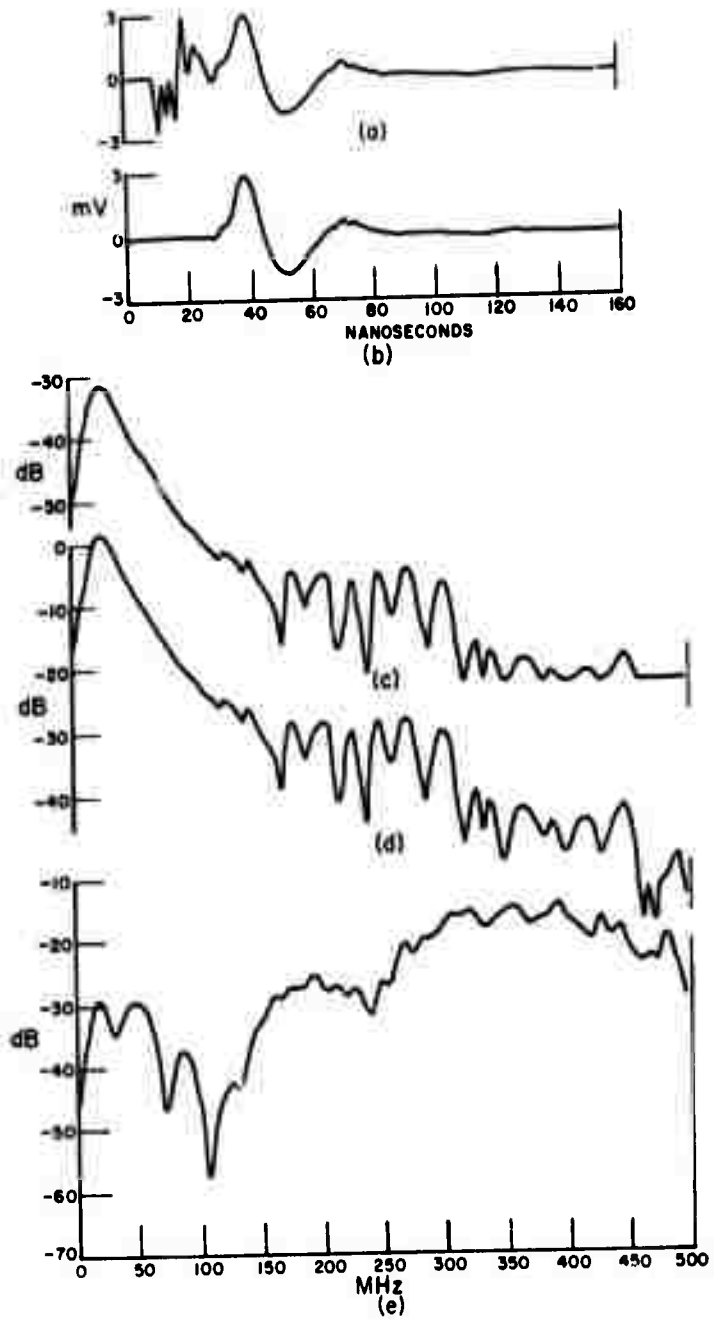

Fig. 27. Orthogonal mode response dummy trench.
(a) difference waveform
(b) gated difference waveform
(c) unnormalized amplitude spectrum
(d) normalized amplitude spectrum
(e) normalized amplitude spectrum with incident pulse removed.

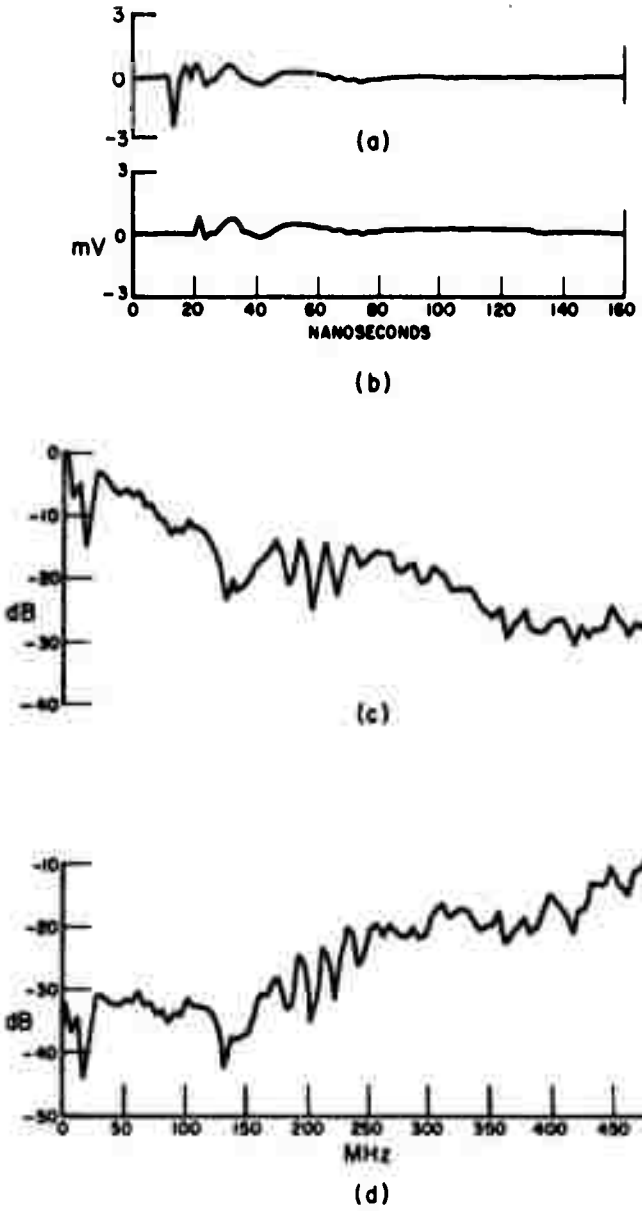

Fig. 28. No-target response, orthogonal mode.
(a) time waveform (average)
(b) gated time waveform
(c) amplitude spectrum
(d) amplitude spectrum with incident pulse removed.

Consider first the gated difference waveforms, b, for each target. It is clear in each case that a target is present. This was also clear when the average target response was compared to the average no-target response, e.g., Figs. 19c and 19d. Note that the presence of the dummy trench, Fig. 27, is also evident. At the time this series of measurements was taken, the buried targets had been in place for approximately 3 months. When the targets were installed, the fill was compacted in each case. It will be interesting to observe, on a continuing basis, how long the dummy trench continues to differ significantly from the no-target response. The response of the dummy trench also indicates that the target response waveforms are really a combination of the target and trench responses. Of course, no such dummy trench will exist in advance of any hard rock tunneling operation. It is interesting to note however that perturbations that one would usually assume to be insignificant are detectable.

From an examination of the gated (b) or ungated (a) difference waveforms the following conclusions can be drawn;

1) the class of dielectric targets can be separated from the class of conducting targets, and both can be separated from the dummy trench response.

2) From the difference waveforms, separation of the conducting target lengths or the dielectric target diameters does not appear feasible.

3) the direct coupling between transmit and receive probes (a) appears significantly different for the dielectric targets and dummy trench than it does for the conducting targets. This difference is the result of the way the individual measurements to secure an average response were made. Because the dielectric targets were extended, the individual measurements were made by moving along the target keeping the same probe-target geometry. For the conducting targets, the probe was simply replaced several times in the same location. The result of the local influence of the grounds on the direct coupling is particularly noticeable for the perturbed ground.

4) the ungated difference waveforms (a) for the dielectric targets endure for roughly 100 ns and the waveforms for the conducting targets and dummy trench for approximately 140 ns. This is reasonable considering the difference in depth of the targets. It also indicates that in the case of the dummy trench, the bottom of the trench is seen; although the response is clearly very small.

A casual observation of the normalized spectra of the gated difference waveforms with the incident pulse removed would indicate that all of these targets appear separable. However, as will be discussed, the influence of the trench is the major source of the differences, particularly since the returns from the trench and from the target are not completely coherent.

The amplitude spectra for the gated difference waveforms, with and without the incident pulse removed, show much the same type of separations and distinctions as those deduced from the time domain waveforms. In general, however, the differences for target classes are much less distinct. We have, however, discarded the phase spectrum. Clearly both the real, time-dependent response waveform and its complex, frequency-dependent transform contain the same information. Visually, in these cases, the time waveforms seem more simple to interpret.

For cylindrical targets of length L we would anticipate dipole-type resonances in the amplitude spectra at the following frequencies

$$f_n = \frac{c(2n-1)}{2L\sqrt{\varepsilon_r}} \text{ Hz},$$

which yields the following frequencies in MHz for the conducting targets assuming $\varepsilon_r = 10.0$[6]

n	1 foot	3 foot	5 foot	10 ft
1	158	53	32	16
2	464	159	96	48

A creeping wave-type resonance (cylinder radius r)

$$f \approx \frac{c}{r\sqrt{\varepsilon_r}} \cdot 0.15$$

for $\varepsilon_r = 10.0$ yields (for a 4 inch diameter)

$f = 286$ MHz and a second creeping wave-type at

$f \simeq 572$ MHz.

For extended dielectric cylinders in a lossy medium, the resonances are complicated but constructive interference of reflections from the front and rear of the cylinder yields

$$f_n = \frac{cn}{4r\sqrt{\varepsilon_r}} ,$$

which for an ε_r of 10 yields (in MHz)

n	2 inch	3 inch	4 inch
1	3164	2128	1580
2	6328	4256	3160

The width of the trenches dug to bury the targets was 1.33 feet for the dielectric targets and 2 feet for the conducting targets and the dummy trench. Reflections from the side walls of the trench would yield resonances

$$f_n = \frac{c(2n-1)}{2w\sqrt{\varepsilon_r}} \quad \text{Hz},$$

where w is the width of the trench. Again for an ε_r of 10 (in MHz)

n	1.33 feet	2 feet
1	119	79
2	357	237

There is also the possibility of parallel plate waveguide-type resonances associated with the depth of the trench. This effect would produce resonances at frequencies

$$f_n = \frac{cn}{2d\sqrt{\varepsilon_r}} \quad ,$$

where d is the trench depth. Resonances at multiples of 33 MHz for the 5 foot depth and 11 MHz for the 3 foot depth would be predicted. We would also anticipate seeing at least the first resonance of the probe structure which in free space would be at 50 MHz. An examination of the various spectra shows an invariant resonance at roughly 25 MHz, and this resonance is attributed to the probe structure when it is on the ground. One possible means for reducing the effect of this resonance is the use of lossy wire so that the signal reflected from the end of the probe is attenuated an order of magnitude before reaching the feed.

Examining the spectra in terms of the above predicted resonances, there appears to be a correlation between the trench width and the resonances. That is, the spectra corresponding to dielectric targets all have a resonance near 119 MHz, and the conducting targets near 79 MHz. We would not anticipate seeing creeping wave-type resonances for conducting targets with the power and target depths involved,

and clearly the predicted resonances for the dielectric targets are beyond our capability at this time. There is some correlation between the predicted and measured dipole-type resonances for the conducting targets, e.g., the 1 foot and 10 foot (Figs. 23 and 26), but it is not consistent. The spectra for the conducting targets are indeed different, but the differences are not consistently related to the difference in target length.

The various predicted resonances for subsurface cylindrical targets can, at best, be considered first order approximations to more complicated mechanisms. Other processing of the spectra is possible, e.g., a matched filter approach using predicted resonances for a given target or the spectrum of the dummy trench. Properly, however, it is felt that such schemes should await data from a new set of measurements where higher power and lower frequencies are available.

VII. PULSE SOUNDING DATA FOR A CYLINDRICAL TARGET, INHOMOGENEOUS STRATIFICATIONS AND A CYLINDRICAL VOID IN A LIMESTONE MEDIUM

As noted earlier, the original research plan included remote measurements on a full scale basis at a limestone quarry* located some 5 miles from the ElectroScience Laboratory. Since electrical power at this site was not available, it was necessary to refurbish a mobile rig originally used for terrain cross section measurements.[8] This mobile facility consisting of a 2½ ton van with an independent internal combustion generator is now operational; thus electromagnetic pulse sounding data at a variety of sites remote from the ElectroScience Laboratory are now possible.

The mobile facility has been used to obtain initial pulse sounding data for particular targets in a limestone medium. Because of the balun problems discussed earlier, the initial measurements were made using the identical probe structure and pulse generator utilized for the overburden measurements. A photograph of the mobile rig which houses a generator, stabalines, as well as the pulse generator, sampling scope and recording equipment is shown in Fig. 29.

A photograph showing the typical stratifications of the limestone medium is shown in Fig. 30. The photograph also shows a large tunnel which was originally selected as one of the geological features to be measured. Note that the medium is by no means solid and homogeneous, the stratifications, which are primarily inhomogeneous, are typical of

---

*Marble Cliff Quarries Company, 2100 Tremont Center, Columbus, Ohio 43221

Fig. 29. Photograph of mobile pulse sounding rig.

Fig. 30. Photograph of tunnel and typical stratifications at the limestone quarry.

the medium in the locations where measurements were made. In Figs. 31a and b, the response of the medium (no target) in the direct reflection mode, both probes, is shown. Note that the response waveform is larger in magnitude by roughly a factor of 10 than that for the same probe and pulser over the overburden. The mismatch at the balun and probe feed point is larger, and a large reflection from the end of the probe is clearly evident. It is obvious from these waveforms that considerably more high frequency energy is arriving at the end of the probe than was the case for an overburden medium. Figure 31c shows the orthogonal mode response in the same location (stratifications only). Note again the increase in the magnitude of the response. Figure 32 shows the same sequence of response waveforms when the probe is located near a target consisting of a 1 foot diameter hollow metal pipe whose top is some 2 to 2.5 feet below the limestone interface. The sketch in Fig. 32 shows the probe and pipe configuration. Some evidence of the target is apparent if these waveforms are compared to the no-target set. Finally, in Fig. 33, the same sequence of waveforms when the probe is directly over the pipe target is shown. The sketch in Fig. 33 shows the probe and target geometry. Note that the probe is positioned for maximum response in the orthogonal mode and one would not anticipate a large target response in the direct mode. In the orthogonal mode, the presence of the pipe is very evident. Figure 34 shows the amplitude spectra of the cross polarized response with the incident pulse removed for a) the no-target case and b) over the pipe. The presence of the target is also evident from a comparison of the spectra. Assuming an ϵ_r of 9 for the limestone medium, creeping wave-type resonances for the pipe would be predicted at 100 MHz, 218 MHz, etc. The 100 MHz resonance can be seen in Fig. 34b. The same sequence of measurements was repeated with the probe located above the tunnel shown in Fig. 30, these waveforms are shown in Fig. 35. While both the direct and orthogonal waveforms indicate responses from the homogeneous and inhomogeneous stratifications, there is no evidence of a response from the tunnel. The distances are such that a response from the tunnel would occur at a time well beyond the observed duration of the waveform. This was not unexpected considering the probe and pulser which were used. The limestone quarry* has a number of interesting geological features suitable for tests of a full scale probe and a pulse generator with higher power and lower frequencies. An extensive series of measurements at these locations is planned for the next contract period.

---

*It is appropriate to acknowledge the excellent cooperation of Mr. Max Werner and his staff at the quarry site. Not only was free access to the site provided, but Mr. Werner also conducted tutorial-type tours of the quarry for our education.

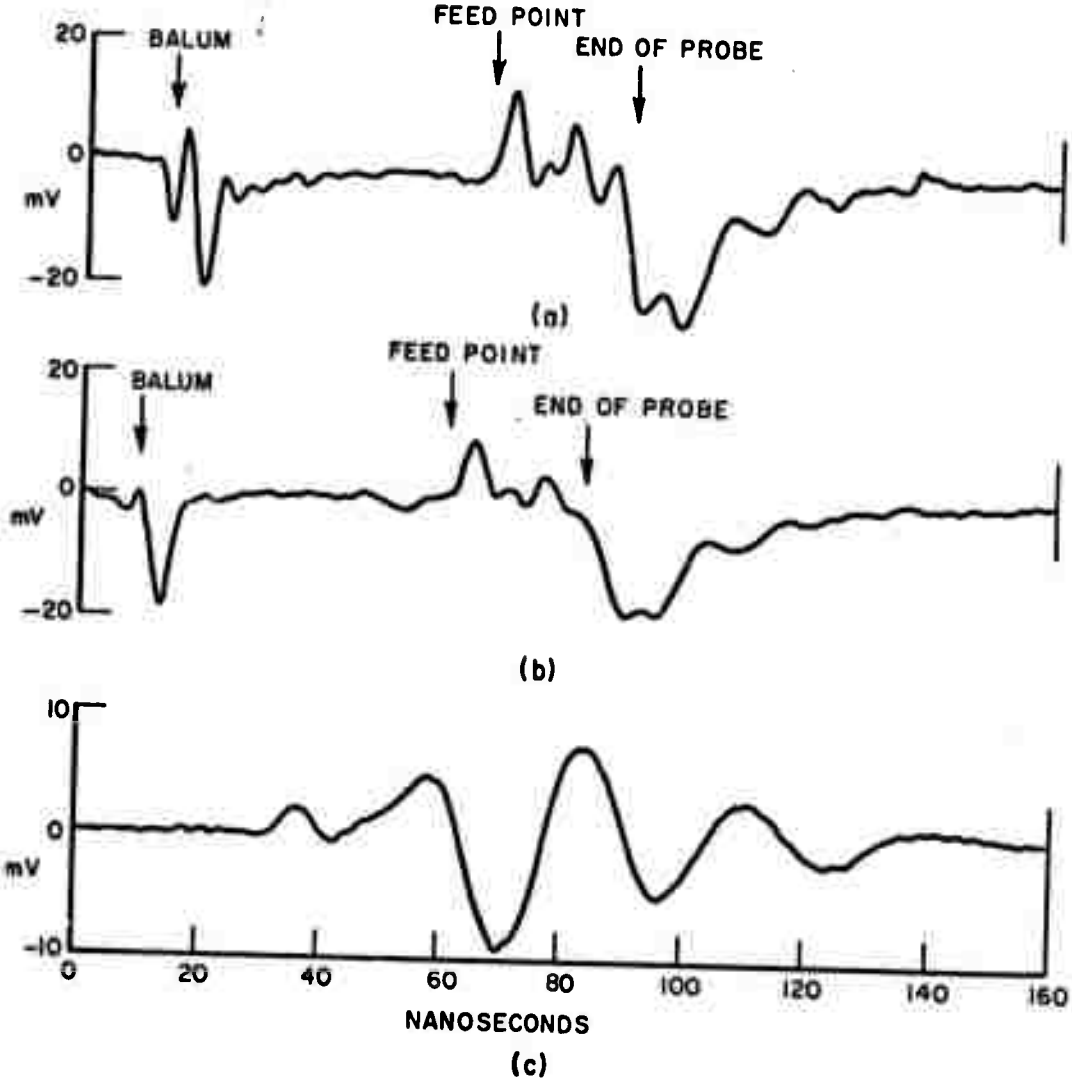

Fig. 31. No-target response waveforms for limestone medium.
(a) direct mode
(b) direct mode
(c) orthogonal mode.

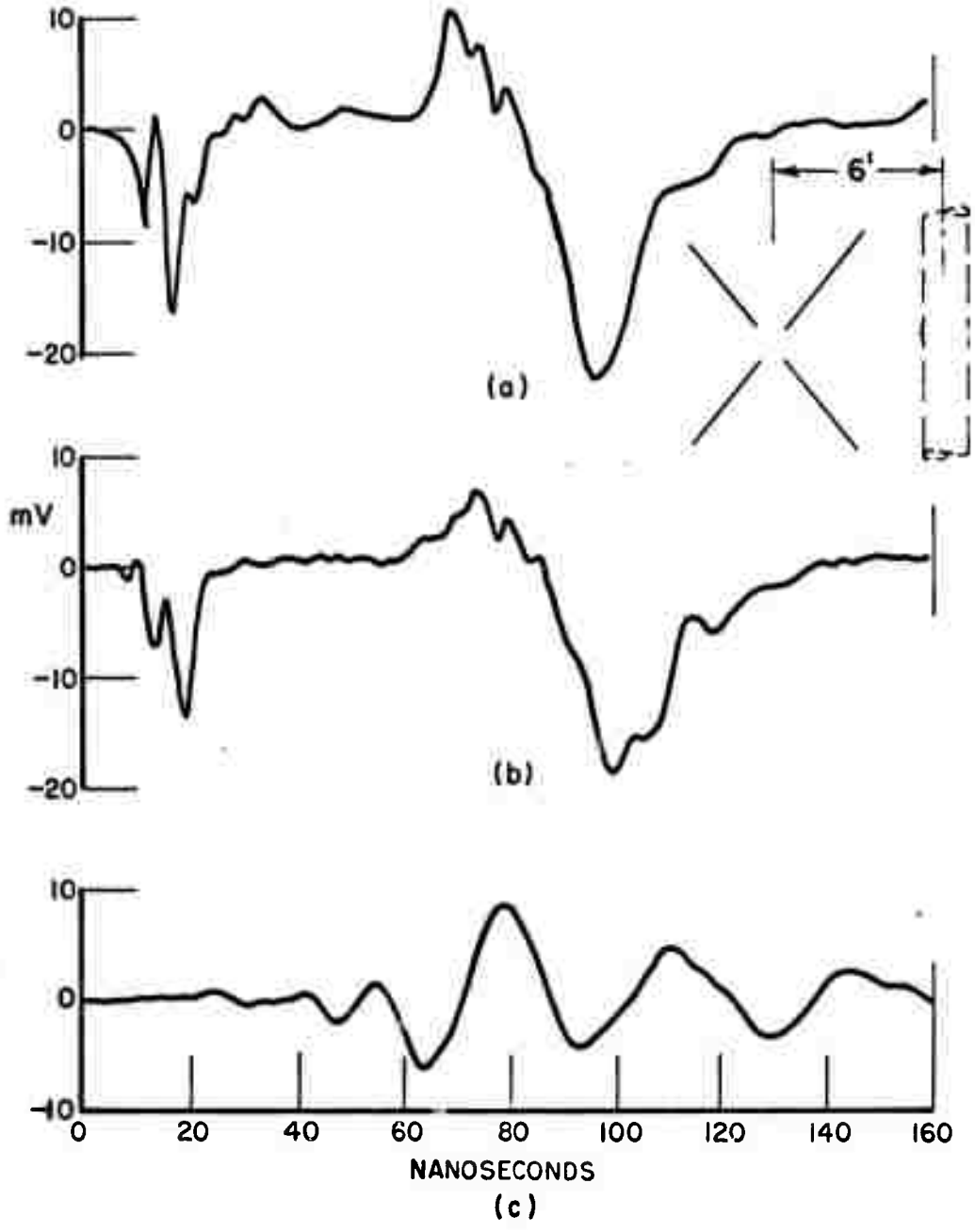

Fig. 32. Response waveforms near cylinder target in limestone medium.
(a) direct mode
(b) direct mode
(c) orthogonal mode.

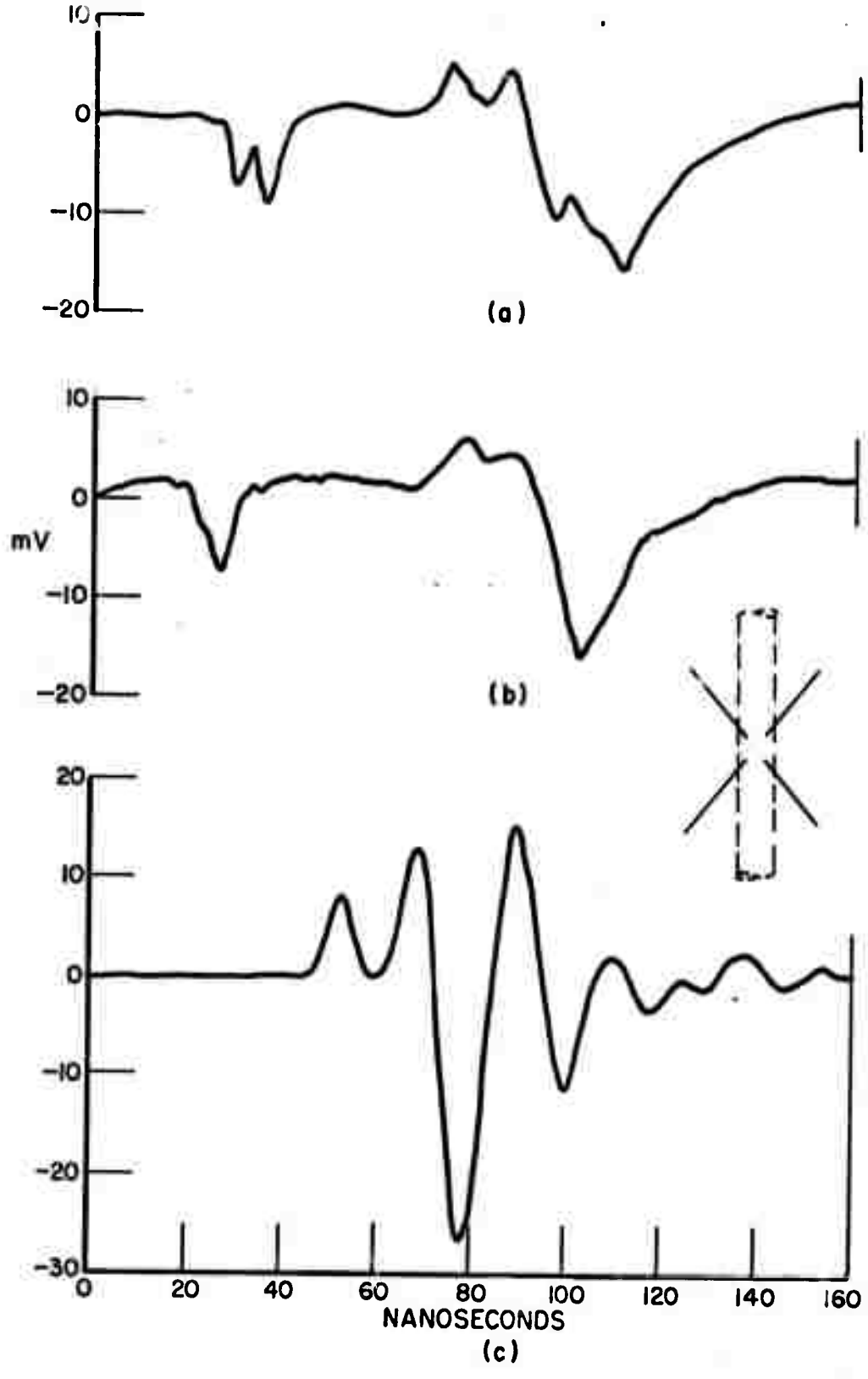

Fig. 33. Response waveforms over cylinder target in limestone medium.
(a) direct mode
(b) direct mode
(c) orthogonal mode.

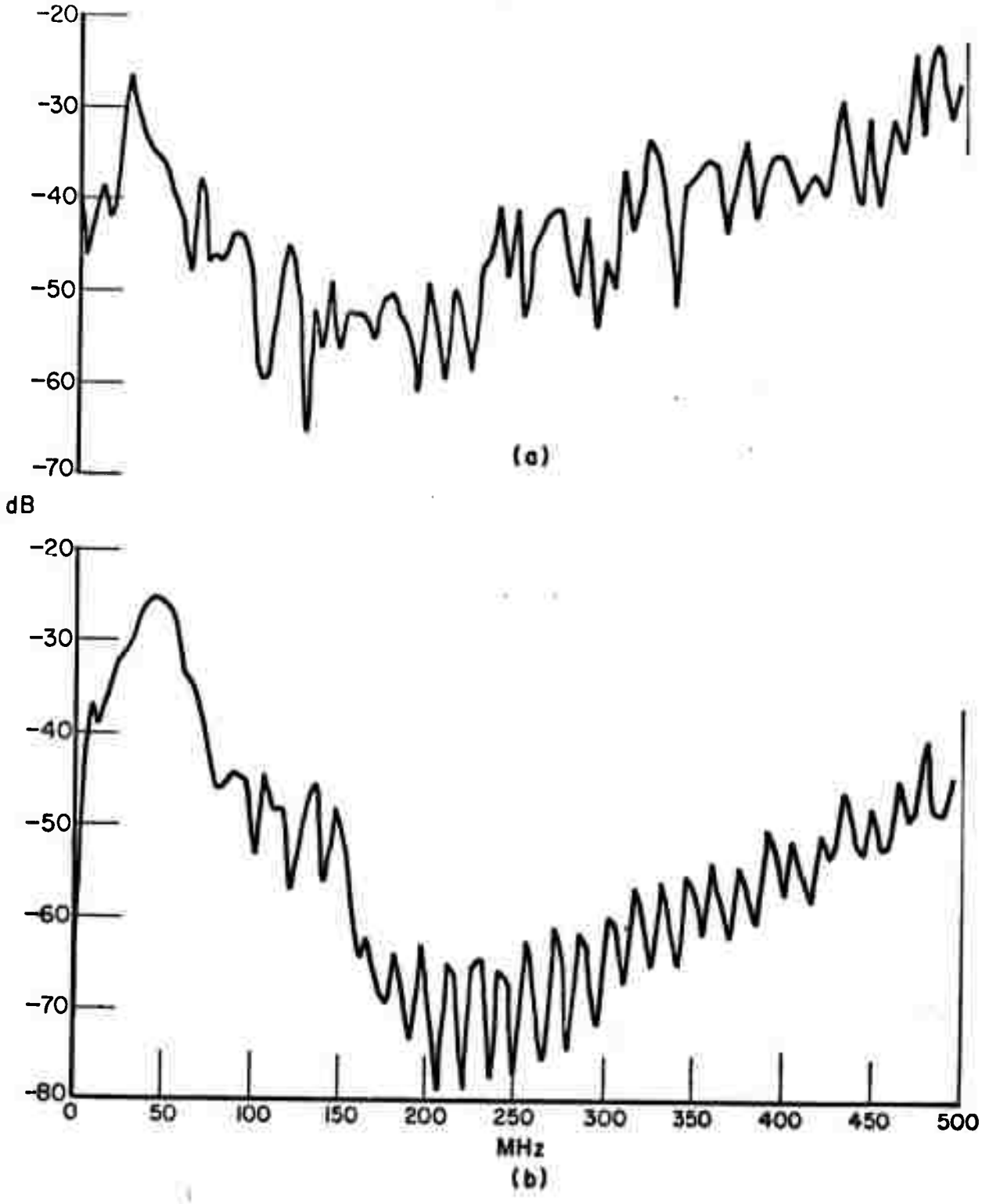

Fig. 34. Amplitude spectra for orthogonal mode response over limestone medium.
(a) no-target
(b) cylinder target.

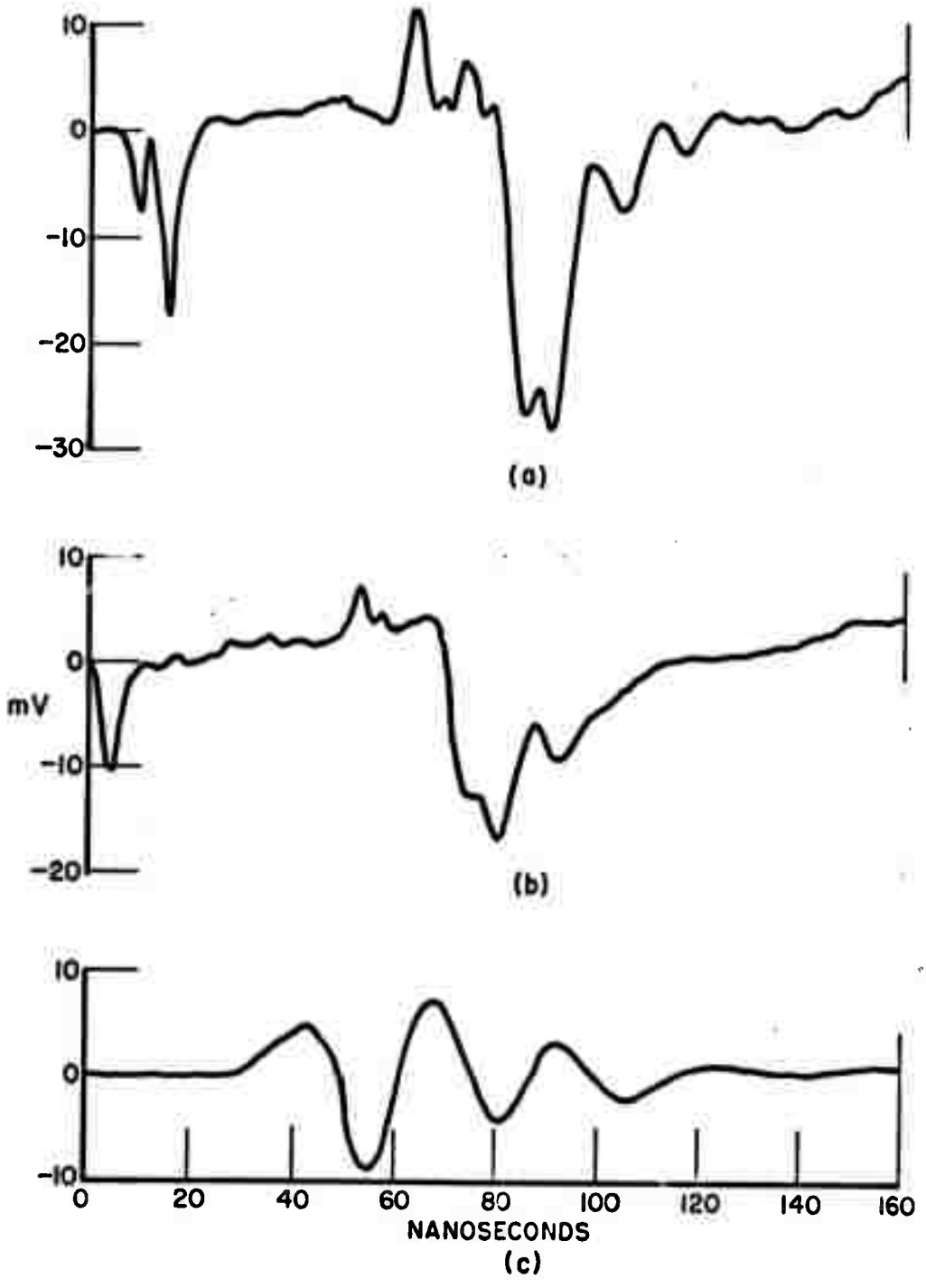

Fig. 35. Response waveforms over tunnel in limestone medium.
(a) direct mode
(b) direct mode
(c) orthogonal mode.

Some further comments concerning data processing methods for this particular electromagnetic system are appropriate. The point was made earlier that a proper processing must await an analytical capability for a specific target geometry, i.e., a calibration capability. With this in hand, one can then begin to secure refined estimates of the impulse response of the scatterer from measured response waveforms. Note that even this waveform will be range dependent, not only because of the changing characteristics of the medium with depth but because we are using the near-zone fields of the probe. No attempt has been made here to optimize the processing used. Our goal, at this stage, was simply to illustrate the system capability. Two obvious things could be done to further demonstrate the detection and identification capability of the system. First, a bandpass filtering of these same data based on the predicted resonances given earlier is feasible.* This assumes a priori knowledge of the basic target geometry. Second, a much more refined gating of the target and no target waveforms or the difference waveform could be used. With this approach a measured or estimated delay time for the medium is used with the gate to isolate a particular portion of the waveform. This approach has been successfully used by Sullivan[6] on subsurface targets at shallow depths. An a priori knowledge of the target geometry is not required. It was not felt that even these refinements were justified.

A few conclusions are in order to relate the system discussed in this report to conventional radar systems. The major difference lies in the fact that present studies have not involved targets in the far field of the antenna and that the limit on sensitivity is imposed by ground clutter, not the signal noise level. This means that the received power level does not vary as the fourth power of the range and also that the ambient noise is not a significant factor. These factors will indeed become important as the range is increased. The fact that clutter is the factor that limits sensitivity also implies that correlation techniques will not be useful in improving the signal to clutter ratio unless the characteristics of the scatterer and the clutter are well established. This is, of course, our goal but these data at this time are not available.

*Successful filter-type processing of these same data has subsequently been reported.[10]

VIII. CONCLUSIONS AND RECOMMENDATIONS

The feasibility of an electromagnetic pulse sounding system for the detection of subsurface targets has been demonstrated, in the field, from measurements of conducting and dielectric cylinders buried in the overburden and from measurements of a conducting cylinder buried in a limestone medium. A full scale version of a probe suitable for use with the system has been designed and tested with low power. These tests demonstrated that electromagnetic pulse energy could be effectively coupled into a lossy medium and that the probe was very insensitive to obstructions on the surface. Because of delays in the delivery of special high power, broad band baluns needed to operate the full scale probe with a high power pulse generator, the field measurements were made with a scaled down version of the probe and a low power pulse generator. The pulser output power and spectrum were inappropriate for interrogation of large targets at deep depths, nevertheless, the measurements conclusively demonstrate the feasibility of the pulse sounding approach.

Analytical studies conducted during the first portion of the contract have developed computational tools for the analysis of various probe geometries and the analysis of plane wave scattering from planar and spherical conductivity contrasts. The comprehensive analysis and computer programs for arbitrary wire antennas in a homogeneous dissipative medium are felt to be a major advance in the state-of-the-art. It remains to add a half-space correction to these programs.

In summary, excellent progress has been made toward the development of a geological tool suitable for the detection and delineation of geological or man-made anomalies within the earth. A major demonstrated feature of the tool is its ability to either "see" or be "blind" to homogeneous geological features.

It is recommended that during the next contract period an extensive series of measurements be made in a local limestone quarry using a full scale probe and high power pulse generators. The necessary equipment for these tests, including a mobile rig and special high power, broad band baluns, are now in hand. The computational programs developed from our analytical studies for probe design and scattering analysis should be improved and extended. In particular, a half-space correction for the wire probe analysis and scattering analysis for cylindrical and other less regular targets are needed. Assuming the measurement program outlined above yields good data, more advanced processing schemes including the generation of target-characteristic response waveforms should be tested. Finally, during the latter stages of the next contract period, the necessary plans and budget estimates to permit the transport of our equipment to a mine or tunnel site to obtain pulse sounding data at such a location should be made.

REFERENCES

1. Kennaugh, E. M. and D. L. Moffatt, "Transient and Impulse Response Approximations," Proc. IEEE, Vol. 53, No. 8, August 1965, pp. 893-901.

2. Final Summary Report 2467-5, 13 March 1970, The Ohio State University ElectroScience Laboratory, Department of Electrical Engineering; prepared under Contract F44620-67-C-0095 for Air Force Cambridge Research Laboratories. (AFCRL-69-0402) (AD 870 169)

3. Young, J. D., "Target Imaging from Multiple-Frequency Radar Returns," Report 2768-6, June 1971, The Ohio State University ElectroScience Laboratory, Department of Electrical Engineering; prepared under Grant AFOSR-69-1710 for Air Force Office of Scientific Research.

4. Repjar, A. G., "The Linear Separability of Multiple-Frequency Radar Returns, with Application to Target Classification," Report 2768-5, 16 November 1970, The Ohio State University ElectroScience Laboratory, Department of Electrical Engineering; prepared under Grant AFOSR-69-1710 for Air Force Office of Scientific Research.

5. Moffatt, D. L., "Time Domain Electromagnetic Scattering from Highly Conducting Objects," Report 2971-2, May 1971, The Ohio State University ElectroScience Laboratory, Department of Electrical Engineering; prepared under Contract F19628-70-C-0125 for Air Force Systems Command, Laurence G. Hanscom Field. (AFCRL-71-0319)

6. Sullivan, W. B., Jr., "Short Pulse Measurements of Targets Immersed in a Lossy Half-Space," M.Sc. Thesis, The Ohio State University, 1970.

7. Moffatt, D. L., "Electromagnetic Pulse Sounding for Geological Surveying with Application in Rock Mechanics and Rapid Excavation Program," Report 3190-1, 18 October 1971, The Ohio State University ElectroScience Laboratory, Department of Electrical Engineering; prepared under Contract H0210042 for Bureau of Mines.

8. Peake, W. H., Cosgriff, R. L., and Taylor, R. C., "Terrain Scattering Properties of Sensor Systems Design," Bulletin 181, The Ohio State University Engineering Experiment Station, May 1960.

9. Parkhomenko, Electrical Properties of Rocks, Plenum Press, New York, 1967.

10. Moffatt, D. L. and Peters, L., Jr., "An Electromagnetic Pulse Hazard Detection System," Proceedings of 1972 North American Rapid Excavation and Tunneling Conference, Chicago, Ill., June 5-7.

APPENDIX

ELECTROMAGNETIC PULSE SOUNDING FOR GEOLOGICAL SURVEYING WITH APPLICATION IN ROCK MECHANICS AND RAPID EXCAVATION PROGRAM

Semiannual Technical Report 3190-1

ElectroScience Laboratory
The Ohio State University

This research was supported by the Advanced Research Projects Agency of the Department of Defense and was monitored by Bureau of Mines under Contract No. H0210042

ABSTRACT

A concise discussion of research progress on Contract H0210042 for the period 22 February 1971 to 22 August 1971 is presented. Analytical results on the scattering by various planar and spherical conductivity contrasts and on design data for an electromagnetic pulse sounding probe are described and illustrated. A first generation version of the probe is given and initial measured data demonstrating certain features of the probe are presented.

TABLE OF CONTENTS

I. TECHNICAL REPORT SUMMARY

A unique electromagnetic pulse sounding technique for the detection and diagnosis of geological and man-made anomalies within the earth is being investigated. The immediate application of this technique is as a hazard detection tool in advance of hard rock rapid tunneling operations, but other potential uses can be envisioned. The goals of the program during this contract period are to design and build an electromagnetic probe which effectively couples electromagnetic energy into the ground, is insensitive to surface targets and with this probe measure the scattered fields from cylinders in a rock medium.

The primary goal of this effort is the detection of discontinuities that represent hazards for hard rock tunneling operations. The effort has been separated into two approaches, one theoretical, the other experimental. While it is recognized that the experimental work is the most important part of the project, the theoretical program has been initiated first while equipment has been obtained and interfaced so that the experimental aspects of this research effort can be successfully pursued. The system that has been used consists of a source which produces a periodic train of video pulses. These are coupled to the ground by a broadband probe. The probe does not respond to the ground interface and the pulsed energy has been successfully coupled into the ground over the broad frequency band contained in the transmitted pulse. Nor does it appear to respond to large structures above the ground. A station wagon has not been detected when driven between the antenna elements. Techniques are currently being pursued to achieve the same goal for a rock subsurface medium. The probe consists of a pair of orthogonally oriented balun fed dipoles stretched over the surface of the earth. A wave is launched on one dipole at the feed point that penetrates into the ground. As it propagates along the dipole, its fringe fields penetrate deeper into the earth. The shape of the dipole has been modified to reduce reflections from the antenna structure itself. It is then terminated by a ground wire at the antenna terminals. Reflections on the wire are minimized by this termination which shows that almost all of the energy is indeed being coupled into the ground. Both the transmitter probe and the orthogonal probe can be used to receive reflected signals. These are observed on the sampling scope which acts as a receiver. In our present system, the computer monitors the sampled voltage and stores this information for further processing and can plot any received waveform. The orthogonal probe "sees" only non-homogeneous targets and hence is ideal for detection of any cylindrical obstruction.

Our measurements revealed that a component of the probe system (balun) which matches the output characteristics of the pulse generator to the input characteristics of the probe was not capable of handling the higher power ranges of the generator for any significant pulse width. This made the actual detection of subsurface targets with this present probe difficult. This is not a basic problem because other components with higher power handling capability are available and have been ordered. A different feed arrangement which eliminates the need for the matching component, albeit with a somewhat higher mismatch, has also been devised. In the meantime, a smaller version of the probe and a much narrower pulse with a higher frequency operating band have been used to demonstrate the feasibility of the pulse sounding approach with measurements of a clay drain tile at a depth of 3 feet. This probe has not at this time been properly matched. However by means of a differencing process in the computer, it has been used to obtain a very distinct scattered pulse from the three foot deep drain. This differencing is a very valuable tool which can be retained in the final system by a simple memory and a simple circuit as a final tuning mechanism. The technique used here was to measure the apparent reflections obtained when the probe is placed over a section of ground in which there are no targets. These reflections from the probe are then subtracted from those when the probe is placed over the drain tile. The reflected pulse obtained in this manner is 10 dB above the residual noise. This new probe eliminates the need of grounding the ends of the dipole and would be adequate for penetration of the hard rock medium. Preparations for measurements at a nearby site which offers anomalies characteristic of hard rock tunneling hazards have been made. These preparations primarily involved equipment and circuitry for non-real time use of the computer. The versatility of the computer is essential in establishing the proper parameters to be monitored and to fix the proper data processing steps, i.e., design of the system can be achieved and verified using computer software without the expense of hardware construction. Once the proper data processing steps are established, these should be replaced by devices designed for those specific tasks in the final system for hazard detection.

Preparations are also being made at the nearby quarry for measurements above a rocky media with no lossy soil layer. This has several advantages and disadvantages. The advantage is that losses and dispersion effects will be reduced and consequently a more distinct scattered pulse will be received from buried objects. The disadvantage is that the system can not be as easily matched and above ground reflection could be more apparent.

The feasibility of electromagnetic pulse sounding as a tool for eliciting the size and shape of geological anomalies within the earth is also to be established. A pulse sounding approach for the interrogation of subsurface targets is predicated on certain advances in identification and discrimination of radar targets and on advances

in antenna design for coupling energy into a lossy medium; both of which were pioneered at this laboratory. The approach also utilizes available computer technology for averaging, differencing and other processing of periodic signals. In a field version system, the computer functions would be replaced by circuitry, but in the research phase the computer again offers an irreplacable versatility in processing techniques.

Simply stated, it has been demonstrated that the physical properties of an object (size, general shape and composition) are adequately defined by the interactions of the object with electromagnetic waves over a frequency range where the object size ranges from small to that comparable to the interrogating wavelength. In terms of geological anomalies of reasonable size, this dictates low frequencies and it is precisely these frequencies which can penetrate the earth to significant depths. Thus the approach is ideally suited for the interrogation of subsurface targets.

At this stage of the contract, analytical tools for studying the scattering of electromagnetic waves by planar and spherical approximations of geological anomalies and for the analysis of electromagnetic probe structures have been developed and are being applied. The need for these calculations is to establish better design parameters for the system and to provide additional data for target identification purposes. The latter study, essentially an analysis of arbitrary wire structures in a dissipative medium, is felt to represent a significant advance in the state-of-the-art. A pulse generator (H.P. 214A) with pulse characteristics suitable for interrogation of anomalies of the order of 10 to 100 feet at depths possibly over 100 feet has been purchased.

In summary, the analytical tools for the design and analysis of an electromagnetic pulse sounding probe have been developed. These same tools will serve to define the basic limitations of the pulse sounding technique. A first version of the probe has been constructed, a power handling problem revealed and solved, and the feasibility of the pulse sounding approach demonstrated via measurements of a shallow subsurface target. The program is proceeding in agreement with the original research plan and no deviation from this plan except possibly a slight delay in the initiation of remote site measurements is anticipated.

II. PURPOSE

A unique electromagnetic pulse sounding technique for the detection and diagnosis of geological and man-made anomalies within the earth is being investigated. The immediate application of this technique is as a hazard detection tool in rapid excavation operations in a hard rock medium. During this contract period the objectives of the program

are to; 1) design and demonstrate a probe structure capable of effectively coupling electromagnetic pulse energy into the ground and at the same time be insensitive to surface scatterers, 2) interrogate with this probe certain simple subsurface targets such as voids and discontinuities representative of rapid excavation hazards, and 3) establish preliminary bounds on the workable depths of electromagnetic pulse sounding via theoretical and experimental methods.

III. INTRODUCTION

The ultimate goal of the research on this program is to incorporate state-of-the-art advances developed at this laboratory, both in antenna systems and processing techniques, into a geological tool capable of delineating the size and shape of geological anomalies from the spectral content of an echo pulse.

If the gross features, i.e., overall size and shape of an anomaly are to be deduced via electromagnetic interrogation then frequencies over an 8 or 10:1 bandwidth with a fundamental such that the linear extent of the anomaly is approximately 1/10 of a wavelength in the medium are dictated.[1] With a pulse sounding approach,* this fixes the characteristics (rise time, repetition rate, etc.) of a pulse generator suitable for a given range of anomaly sizes. It does not necessarily follow that all of the higher spectral content are needed to obtain a viable signature,[2] but the lowest frequencies are essential. Of course, the more high frequency content available the sharper the reflected pulses and consequently an improved range gating. This is an advantage of the hardrock medium over the soil media currently being used in our experimental studies. Thus the approach is ideally suited for subsurface interrogation where low frequencies are needed to obtain significant penetration. Clearly, the attenuation and dispersion of the ground as well as the size and scattering characteristics of a given anomaly bound the maximum working depth of a pulse sounding system. Analytical studies to secure estimates of these limiting effects via plane wave scattering computations for planar and spherical conductivity contrasts are described in Section IV.A of this report.

In Section IV.B, a comprehensive analysis of wire antennas in a homogeneous, dissipative medium is described. Considerable effort has been expended on this study since realistic estimates of penetration depths, dispersion effects and surface target sensitivity for practical probe geometries are a vital requirement of the program. A major feature of the computational programs developed is that the speed and accuracy are sufficient to permit pulse type excitation studies via Fourier synthesis.

*An alternative system for radar applications uses discrete harmonically related cw measurements over the 10:1 bandwidth.[3]

Certain exact, closed form results which can be obtained for the transient fields of an infinite line source in the presence of a half-space are given in Section IV.C. These two-dimensional results are less directly applicable to the immediate problems and have not therefore been extended at this time.

The first generation version of the pulse sounding probe and the results of measurements on this probe are described in Section V. These initial tests were made in the immediate vicinity of the laboratory but the necessary circuitry and equipment for remote site operation are now nearly completed.

A summary of the present status of this research effort and our plans for the remaining contract period are given in Sections VI and VII respectively.

IV. ANALYTICAL STUDIES

A. Scattering Computations

1. Planar contrasts

The plane wave scattering characteristics of a planar contrast between two dissipative media are most simply studied in terms of the impulse response waveform at the interface, i.e., the inverse Laplace transform of the frequency-dependent Fresnel reflection coefficient. For normal incidence and assuming the constitutive parameters of both media are frequency independent, the form of the impulse response waveform is shown in Fig. 1. The response to any other incident waveform is given by convolution as is discussed later. The plane wave is incident from medium 1 into medium 2. The response consists of an impulse singularity of weight

$$A = \frac{\sqrt{\varepsilon_{r1}} - \sqrt{\varepsilon_{r2}}}{\sqrt{\varepsilon_{r1}} + \sqrt{\varepsilon_{r2}}} , \tag{1}$$

a jump discontinuity of magnitude

$$B = \frac{2\sqrt{\varepsilon_{r1}\varepsilon_{r2}}}{\varepsilon_0\left(\sqrt{\varepsilon_{r1}} + \sqrt{\varepsilon_{r2}}\right)^2}\left[\frac{\sigma_2}{\varepsilon_{r2}} - \frac{\sigma_1}{\varepsilon_{r1}}\right] , \tag{2}$$

and then a smooth decay to zero in a time less than the relaxation time (ε_2/σ_2) of medium 2. Note that both the singularity and discontinuity can be of either sign depending upon the relative permittivity and conductivity contrasts. In Fig. 2, the weight of the singularity, A, is shown for permittivity contrasts, $\varepsilon_{r1}/\varepsilon_{r2}$, from 0.1 to 10.0. Fig: 3 shows the quantity $\varepsilon_0\,\varepsilon_{r1}\,B/\sigma_1$ for conductivity contrasts σ_2/σ_1 from 0.1 to 10.0 with the permittivity contrast, $\varepsilon_{r2}/\varepsilon_{r1}$, as a parameter.

IMPULSE RESPONSE WAVEFORM FOR PLANE WAVE REFLECTION AT THE INTERFACE OF TWO LOSSY MEDIA. NORMAL INCIDENCE.

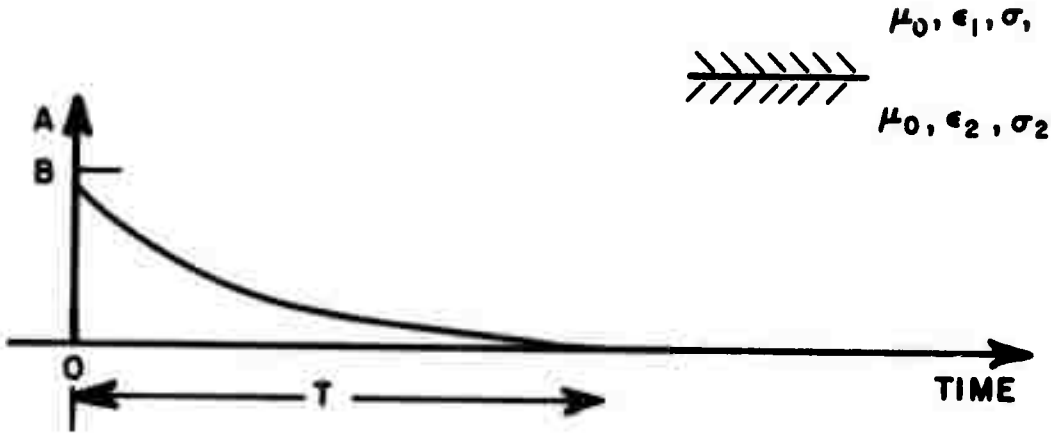

A - WEIGHT OF IMPULSE SINGULARITY, $A = \dfrac{\sqrt{\epsilon_{r1}} - \sqrt{\epsilon_{r2}}}{\sqrt{\epsilon_{r1}} + \sqrt{\epsilon_{r2}}}$

B - INITIAL VALUE OF WAVEFORM, $B = \dfrac{2\sqrt{\epsilon_{r1}\epsilon_{r2}}}{\epsilon_0\left(\sqrt{\epsilon_{r1}} + \sqrt{\epsilon_{r2}}\right)^2}\left[\dfrac{\sigma_2}{\epsilon_{r2}} - \dfrac{\sigma_1}{\epsilon_{r2}}\right]$

T IS LESS THAN THE RELAXATION TIME $\left(\dfrac{\epsilon_2}{\sigma_2}\right)$ OF THE MEDIUM

Fig. 1. Sketch of impulse response waveform of planar contrast.

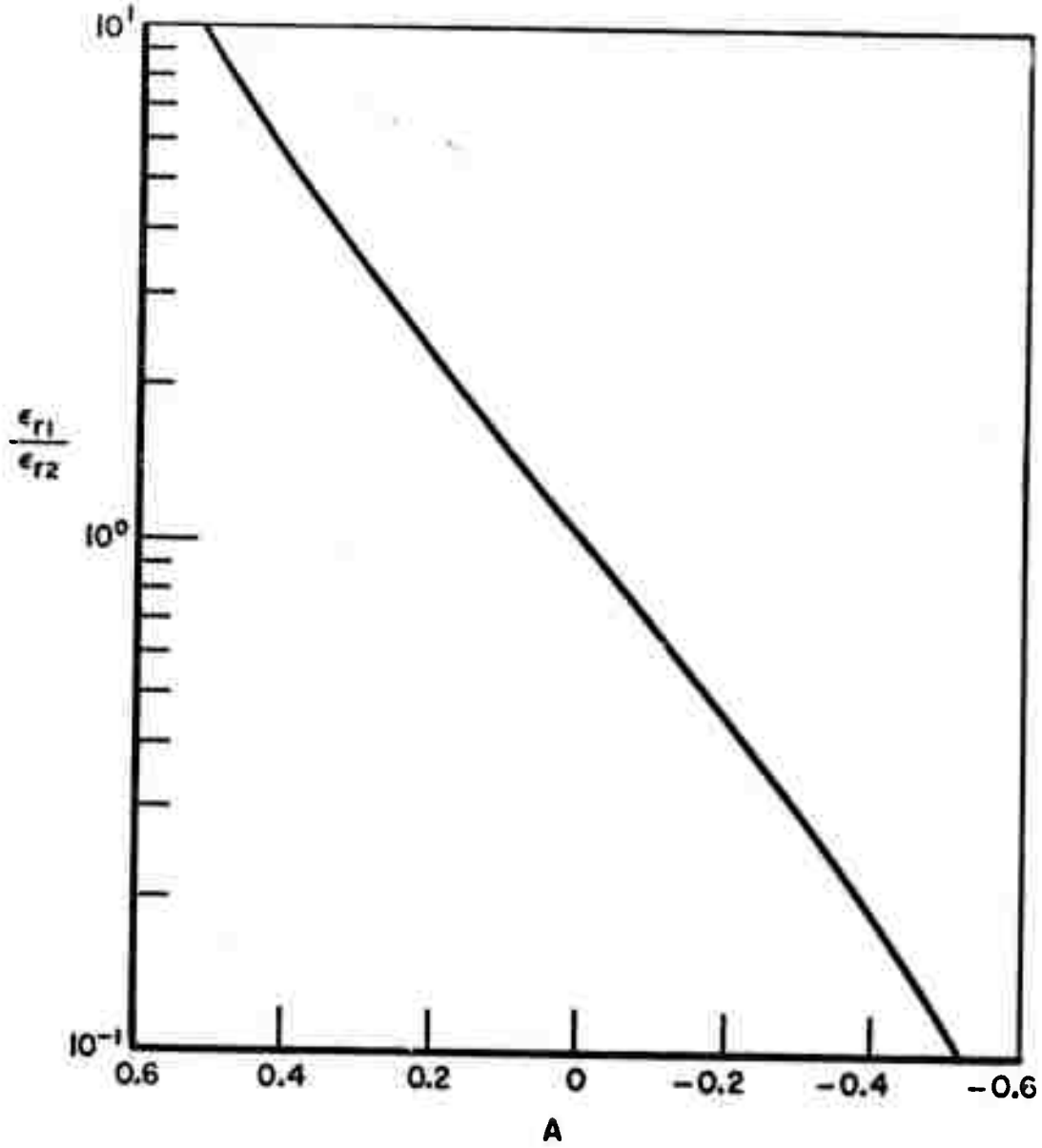

Fig. 2. Weight of impulsive singularity.

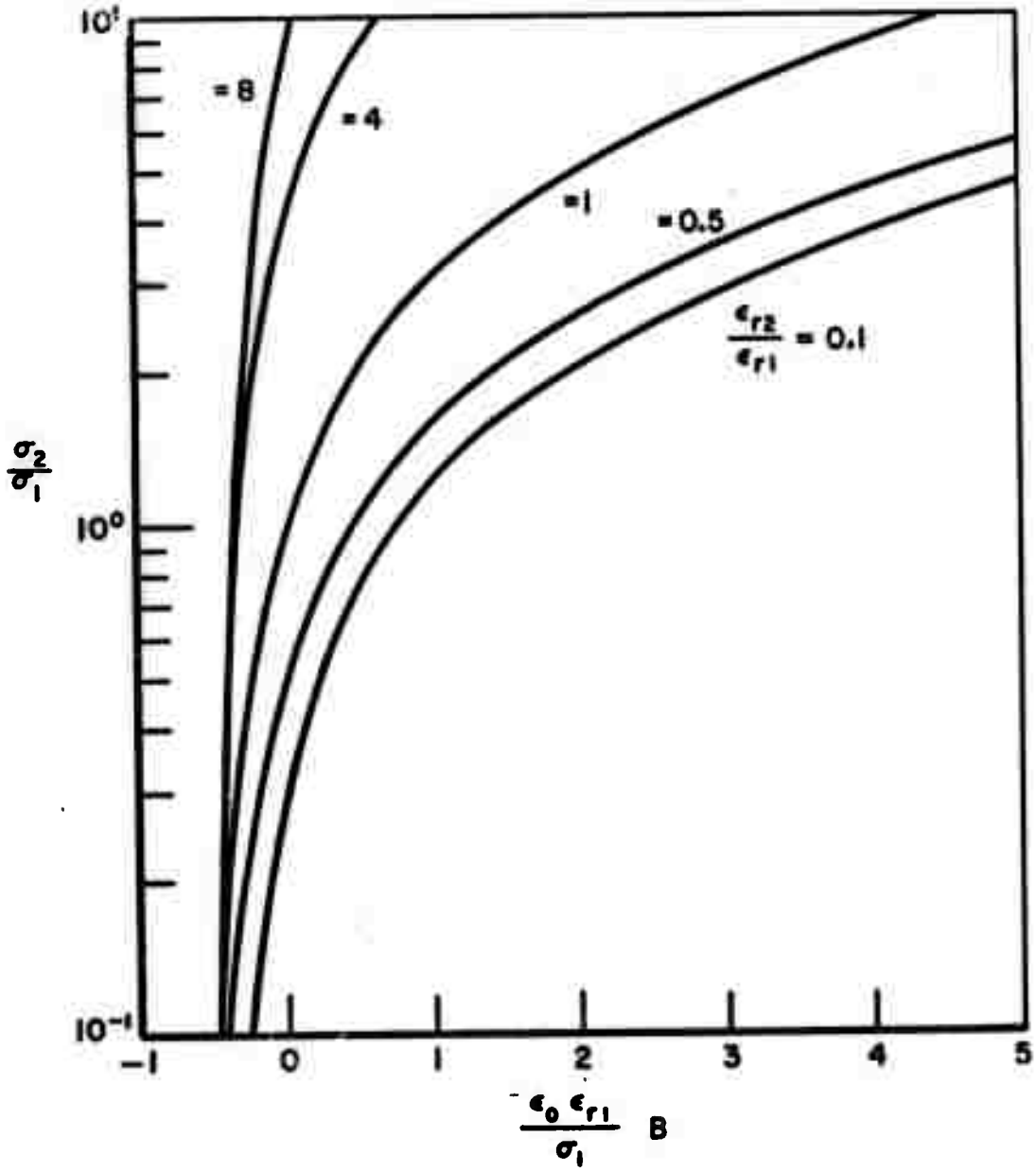

Fig. 3. Magnitude of step discontinuity.

Details of the decay rate of the waveform are best obtained via a Fourier synthesis procedure[4] where the response waveform is constructed from calculations of the frequency-dependent reflection coefficient at harmonically related frequencies. Examples of such waveforms are shown in Figs. 4 and 5. To simplify the synthesis procedure, the impulse singularity has been subtracted from the reflection coefficient before synthesis. The synthesis procedure also permits one to introduce frequency-dependent constitutive parameters in both media since calculations of the reflection coefficient at discrete frequencies are made. In this case the constitutive parameters used to calculate the quantities in Eqs. (1) and (2) should be those the media approach in the high frequency limit.

Given the impulse response waveform for a planar contrast, the response for an interrogating plane wave with an arbitrary time dependence is easily obtained by convolution.[1] Note specifically that the convolution computations do not require analytical expressions for the impulse response waveform, which are obviously not obtained when the Fourier synthesis procedure is used. The most serious drawback to the results given here is the assumption of an impulsive plane wave incident from medium 1. If this medium is very lossy then the assumption is poor when one considers an air-earth interface above medium 1. This could be corrected if the dispersive properties of the medium are known. However, if medium 1 is essentially a dielectric, e.g., hard rock which might be expected at the face of a tunneling operation, then the impulsive assumption is a good one.

The planar contrasts have a distinctive signature which has diagnostic features in the sign and magnitude of both the impulsive singularity and the jump discontinuity and in the effective duration of the waveform. it is clear that a reasonable approximation for the impulse response waveform is

$$F_I(t') \approx A\delta(t) + Be^{-\alpha t/T_r}\mu(t), \tag{3}$$

where A and B are defined in Eqs. (1) and (2), T_r is the relaxation time for medium 2. ($T_r = \varepsilon_2/\sigma_2$) and α is an adjustable parameter. Sufficient computations to estimate α over a range of contrast parameters will be made.

2. Spherical contrasts

The Mie series resulting from a modal solution of the plane wave scattering by a spherical target has been programed for the IBM 360 computer for 2 cases: a lossy sphere in a dissipative ambient medium and a lossy sphere with a lossy layer in a dissipative ambient medium.

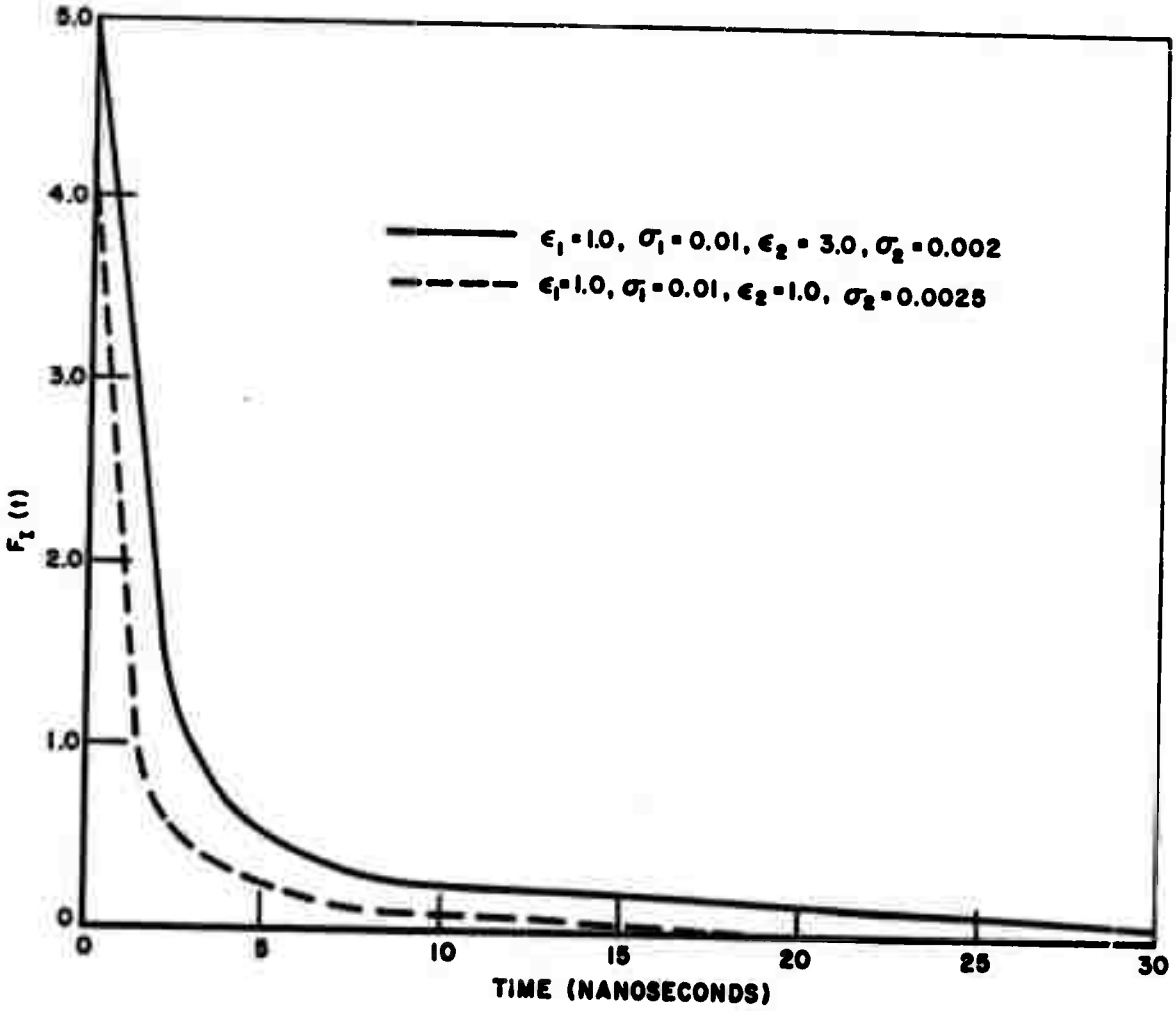

Fig. 4. Impulse response waveforms of planar contrast, impulse singularity removed.

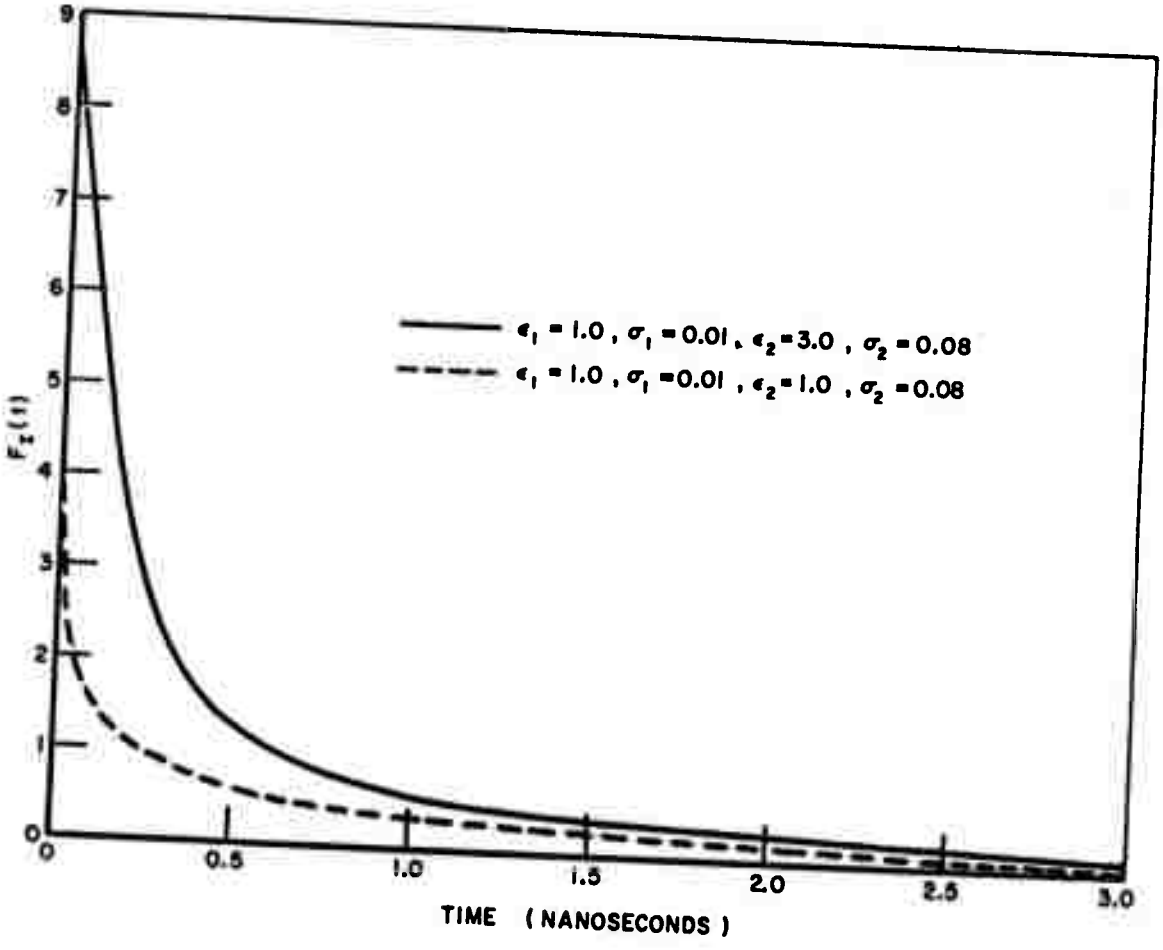

(a)

Fig. 5a,b. Impulse response waveforms of planar contrast, impulse singularity removed.

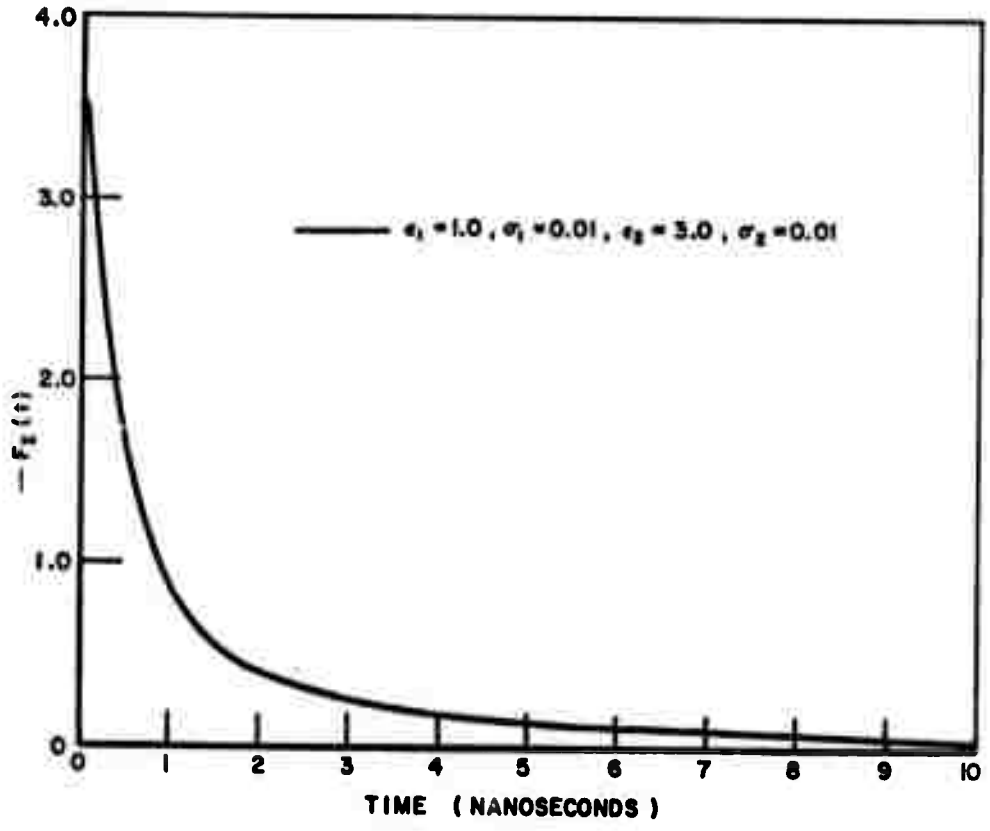
4.0
3.0
2.0
1.0
0
$-F_2(t)$
$\epsilon_1 = 1.0$, $\sigma_1 = 0.01$, $\epsilon_2 = 3.0$, $\sigma_2 = 0.01$
0
1
2
3
4
5
6
7
8
9
10
TIME (NANOSECONDS)

(b)

Fig. 5. (Cont.)

As with the planar contrast, the assumption of a plane wave incident on the target places restrictions on the ambient medium. With these programs, formulation of the transient response waveforms via Fourier synthesis is feasible. At present the computations have been confined to single frequencies, primarily to ensure that all bugs have been removed from the programs.

Examples of the computations for spherical targets are shown in Figs. 6, 7, and 8. In Fig. 6 the E-plane (6a) and H-plane (6b) patterns showing the magnitude of the scattered field squared as a function of bistatic angle are shown. Zero degrees is backscatter. The sphere in Fig. 6 is a lossless dielectric, $\varepsilon_r = 2.8$, with a radius of 5 cms. The ambient medium has a wavenumber $k_m = 99.48 + j0.2973$ so that the index of refraction for the sphere is $1.056 - j0.003$. The frequency is 3.0 GHz. Patterns are shown in Fig. 6 for observer ranges of 0.1, 0.3 and 0.5 meters. In Fig. 7, similar results for a lossy sphere ($\varepsilon_r = 11.0$, $\sigma = 0.385$, loss tangent = 0.210) with a radius of 5 cms are shown. The ambient medium and the frequency are the same as those in Fig. 6. Finally, in Fig. 8, results are shown for the same conditions as Fig. 7 but a lossy layer 1 cm thick ($\varepsilon_r = 11.0$, $\sigma = 0.0025$, loss tangent = 0.00136) has been added to the sphere. It should be noted that for economy reasons the angular increment for these computations (Figs. 6, 7 and 8) was quite large (30°), thus some fine detail of the curves may not be shown. The data shown were primarily run to check out the computer programs. These programs are efficient, but the cost of such calculations is not trivial. Thus, some effort to estimate parameters for the ambient medium and spherical targets which are realistic models of tunneling hazards will be expended before extensive calculations are made.

3. Overburden effect estimates

The effects of the air-earth interface and propagation in the ground on the plane wave interrogation of a buried target has been estimated in the following manner. A plane incident wave at an off-normal angle from the earth surface is assumed. The transmitted field at a given depth is calculated under the assumption of frequency independent constitutive parameters for the earth. This field is then modified by the known scattering characteristics (amplitude and phase) of the target in free space at an equivalent (same electrical size) frequency. The propagation path to the surface is retraced and the field then transmitted through the earth-air interface. It is desired to compare the ramp response waveform of the target in free space and in the earth. This is done via a Fourier synthesis procedure with calculations as described above at discrete harmonically related frequencies. For the ramp response waveform (twice integrated impulse response) only a very few frequencies are needed.[2] It is interesting that two different ramp response waveforms for the target

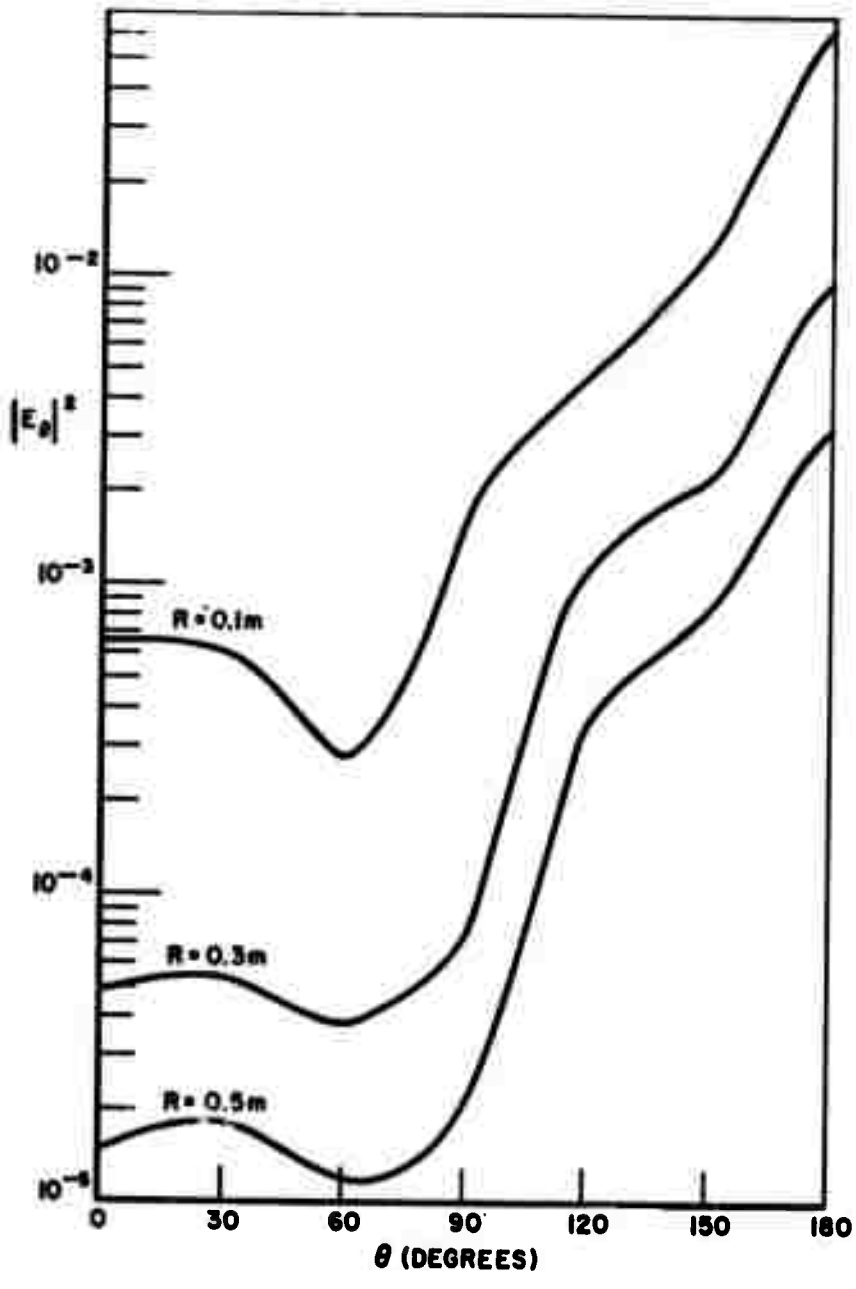

(a)

Fig. 6. Magnitude squared of scattered field vs bistatic angle lossless dielectric sphere in a lossy medium. (a) E-plane, (b) H-plane.

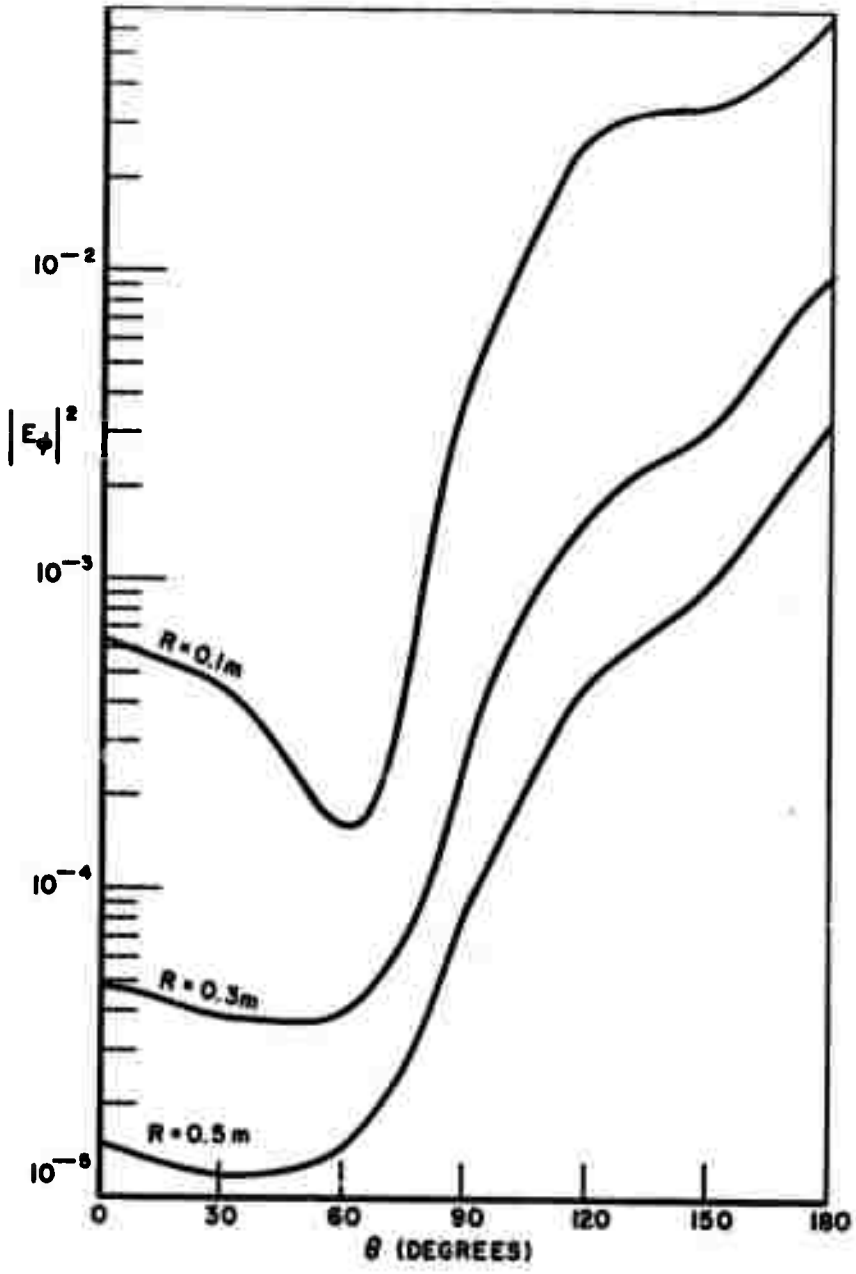
10^{-2}
$|E_\phi|^2$
10^{-3}
R=0.1m
10^{-4}
R=0.3m
R=0.5m
10^{-5}
0
30
60
90
120
150
180
θ (DEGREES)

(b)

Fig. 6. (Cont.)

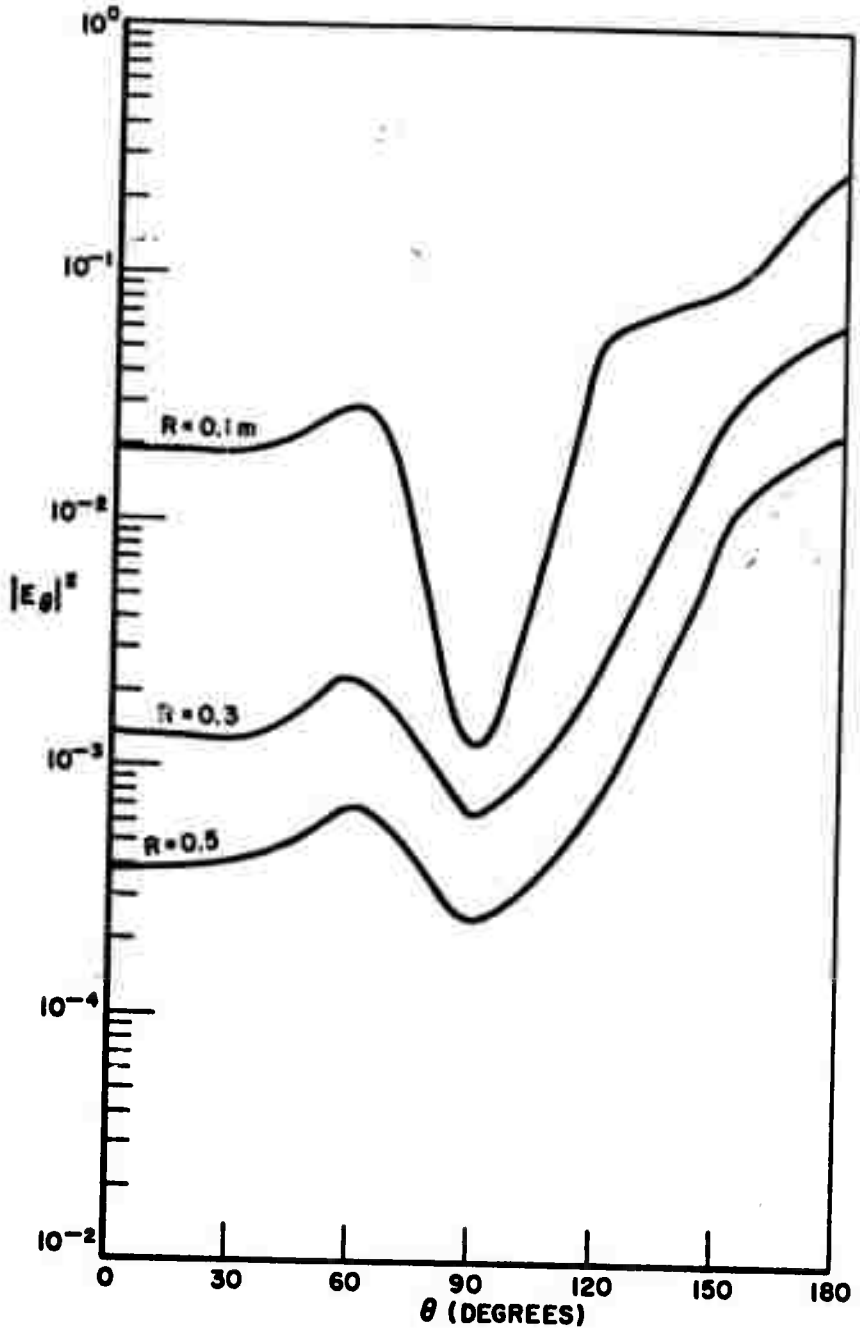

(a)

Fig. 7. Magnitude squared of scattered field vs bistatic angle for a lossy dielectric sphere in a lossy medium. (a) E-plane, (b) H-plane.

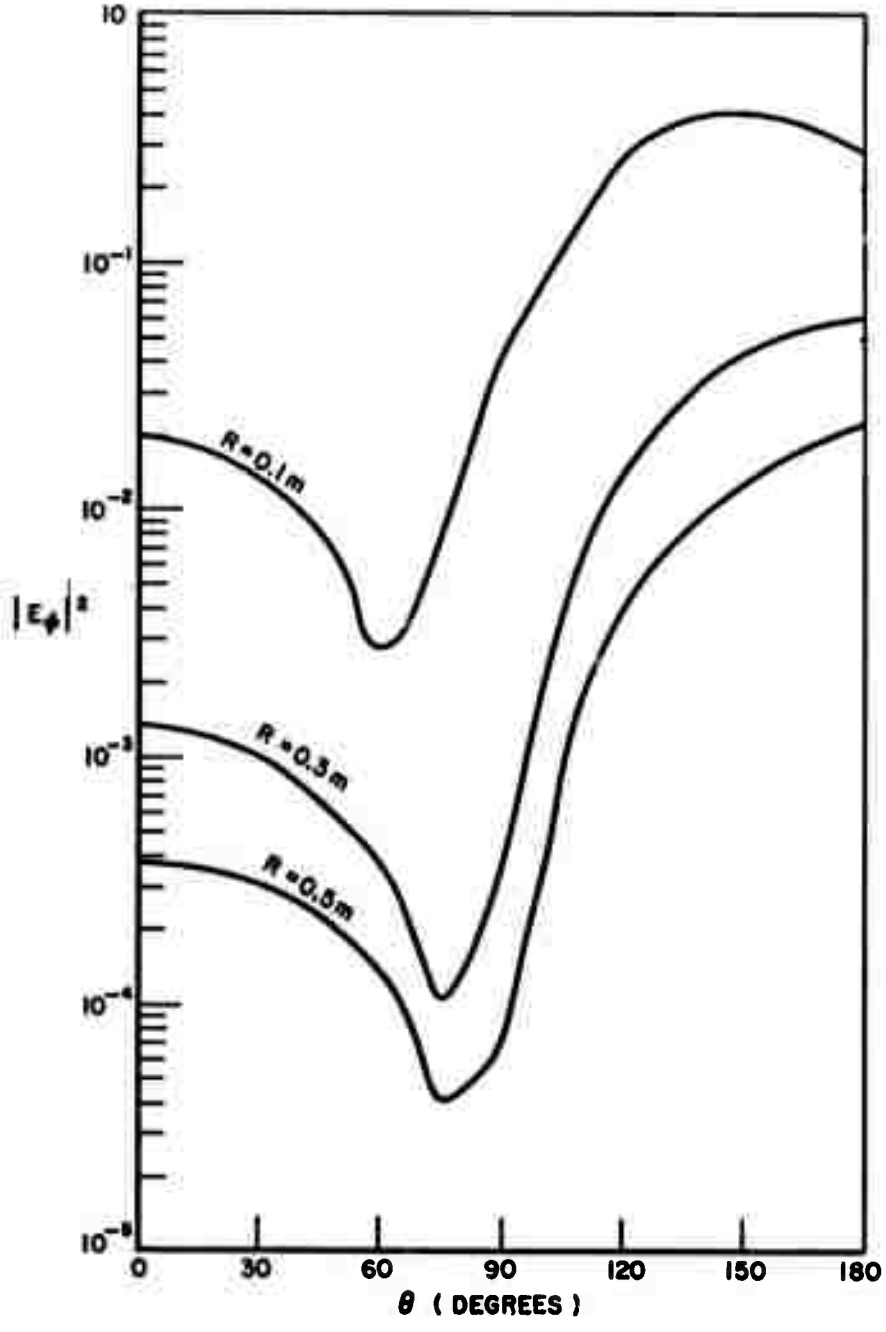
10
10^{-1}
10^{-2}
10^{-3}
10^{-4}
10^{-5}
$|E_\phi|^2$
R=0.1m
R=0.3m
R=0.5m
0
30
60
90
120
150
180
θ (DEGREES)

(b)

Fig. 7. (Cont.)

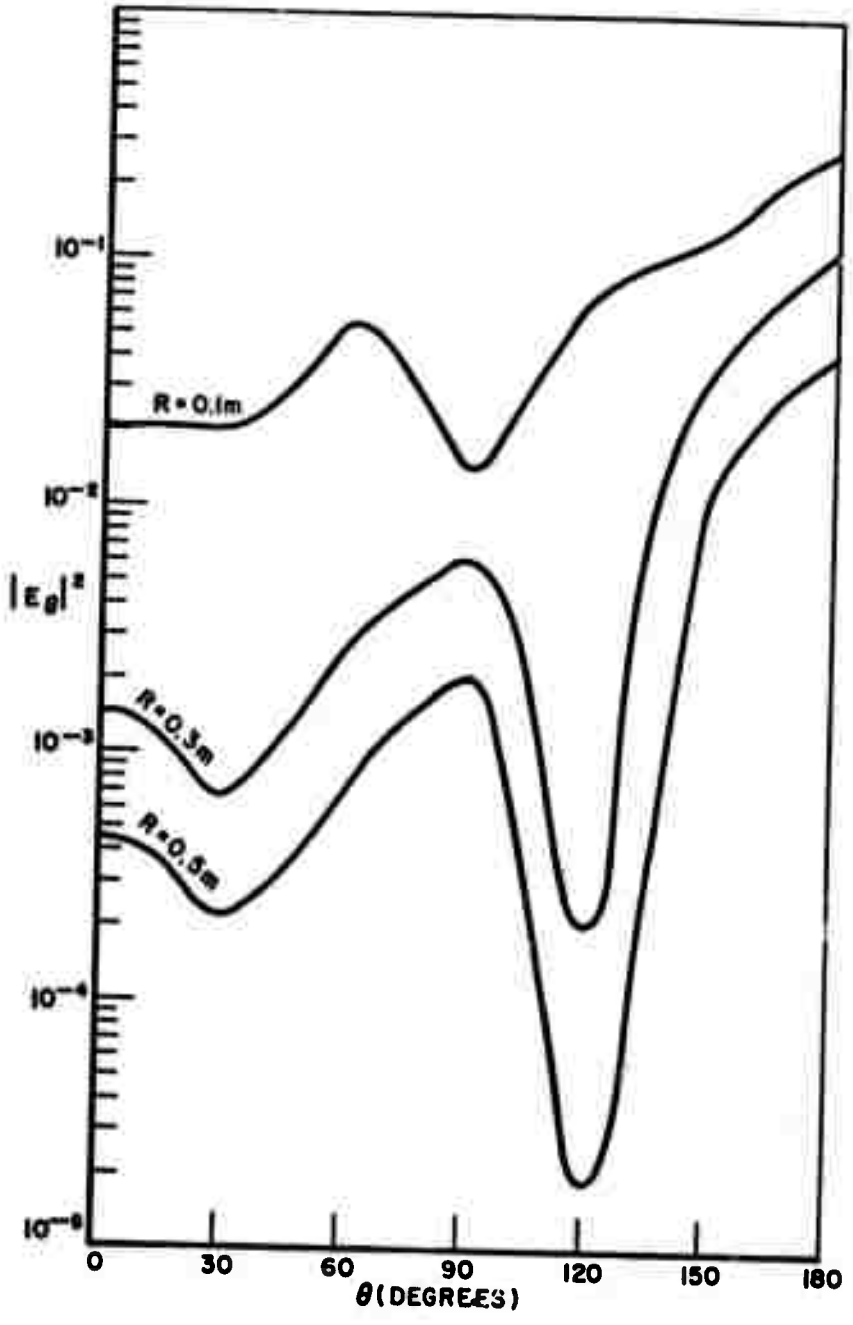

(a)

Fig. 8. Magnitude squared of scattered field vs bistatic angle for a layered lossy sphere in a lossy medium. (a) E-plane, (b) H-plane.

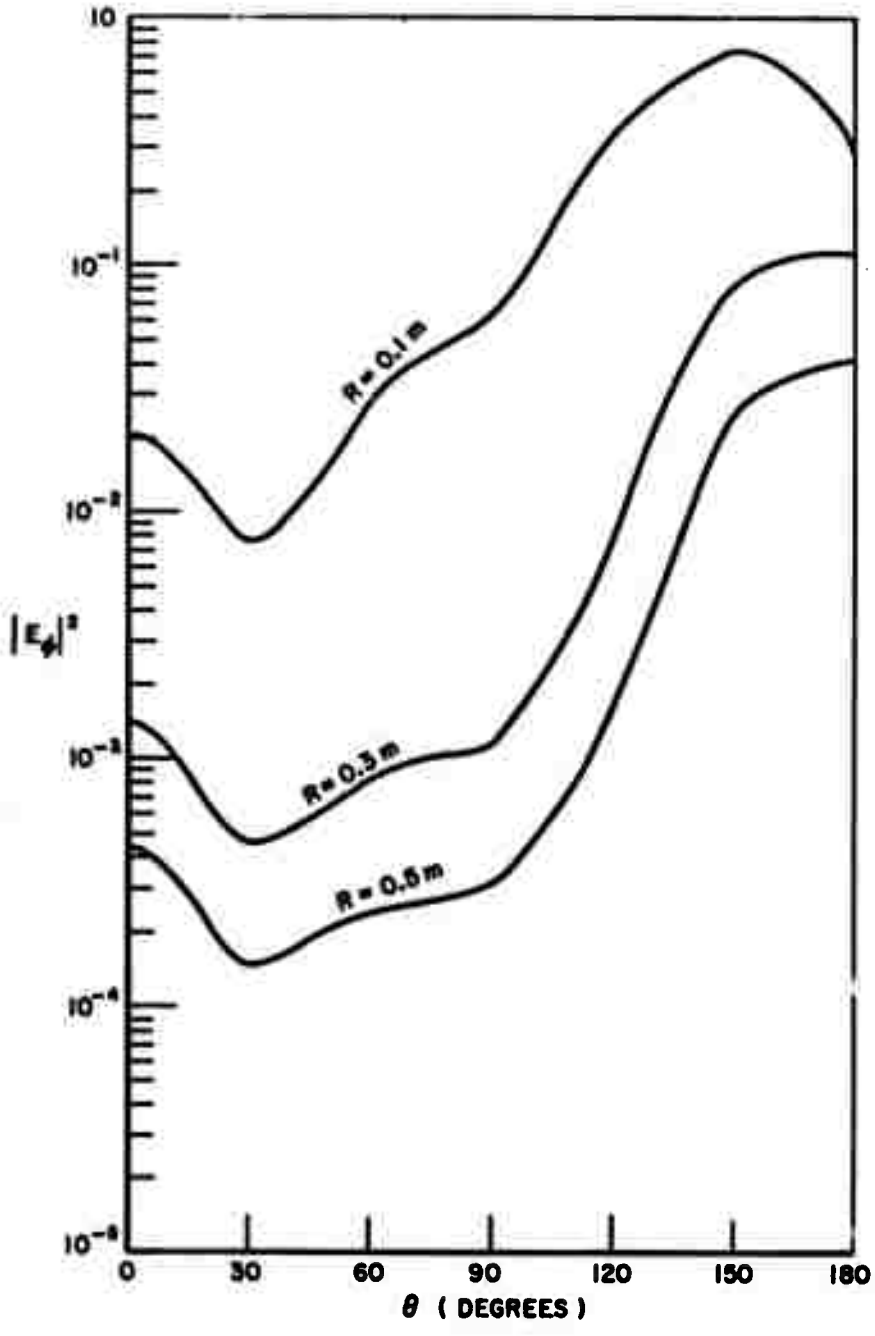
10
10^{-1}
10^{-2}
10^{-3}
10^{-4}
10^{-5}
$|E_\phi|^2$
R = 0.1 m
R = 0.3 m
R = 0.5 m
0
30
60
90
120
150
180
θ (DEGREES)

(b)

Fig. 8. (Cont.)

can be obtained. In each case the fundamental frequency is calculated such that the requirements on electrical size in the medium described in the Introduction are met. This calculation is made under the assumption that the earth is a conductor, i.e.,

$$(4) \qquad \lambda \text{ medium} \simeq \frac{2\pi}{\sqrt{\pi f \mu_o \sigma_m}} \quad .$$

If the required harmonic wavelengths are calculated from Eq. (4) then one response waveform results. This is case of the ramp waveform incident at the target. If one simply takes multiples of the fundamental then a different waveform is obtained. This is the case of a ramp waveform on the transmitting cable. The difference is essentially that of taking the harmonics as $n\omega_o$ or $n^2\omega_o$ (Eq. (4)) where ω_o is the fundamental angular frequency. In practice, either definition could be used provided the period T of the transmitted waveform is sufficiently large that the reflected signal from the target is completely damped out before the onset of the next pulse. This implies a narrowly spaced spectrum over the frequency band of interest and consequently, one could reconstruct via the computer either of the incident ramp waveforms. In Figs. 9, 10 and 11 the free space and underground ramp response waveforms for a conducting sphere, conducting cylinder and conducting disk are shown. The time scale in these figures is in units of the period of the fundamental synthesis frequency. The ground parameters are taken as $\varepsilon_r = 10.0$, $\sigma = 6.11 \times 10^{-4}$ and the targets are at a depth of 30 meters. The interrogating waveform (periodic with ramp discontinuities) is incident at an angle 30° from normal with the electric field parallel to the ground. The targets have a characteristic dimension of 6 meters, i.e., sphere, disk and cylinder have a radius of 3 meters. The cylinder has a 2:1 length to diameter ratio. The axis of the cylinder is parallel to the ground interface and to the incident electric field, the disk is perpendicular to the ground interface with the plane of the disk parallel to the incident electric field. 10 harmonic frequencies were used to produce the waveforms shown. For each target it is seen that the interface and ground propagation has distorted the free space waveform, yet the distortion is not such as to preclude a signature assignment. The known relationships[4] between the physical properties of the target and its free space ramp response waveform have been distorted and clearly, as was anticipated, development of such relationships for subsurface targets will be more difficult than for the free space case. There is, however, no evidence to indicate that the effects of the interface and overburden will negate a time domain signature approach.

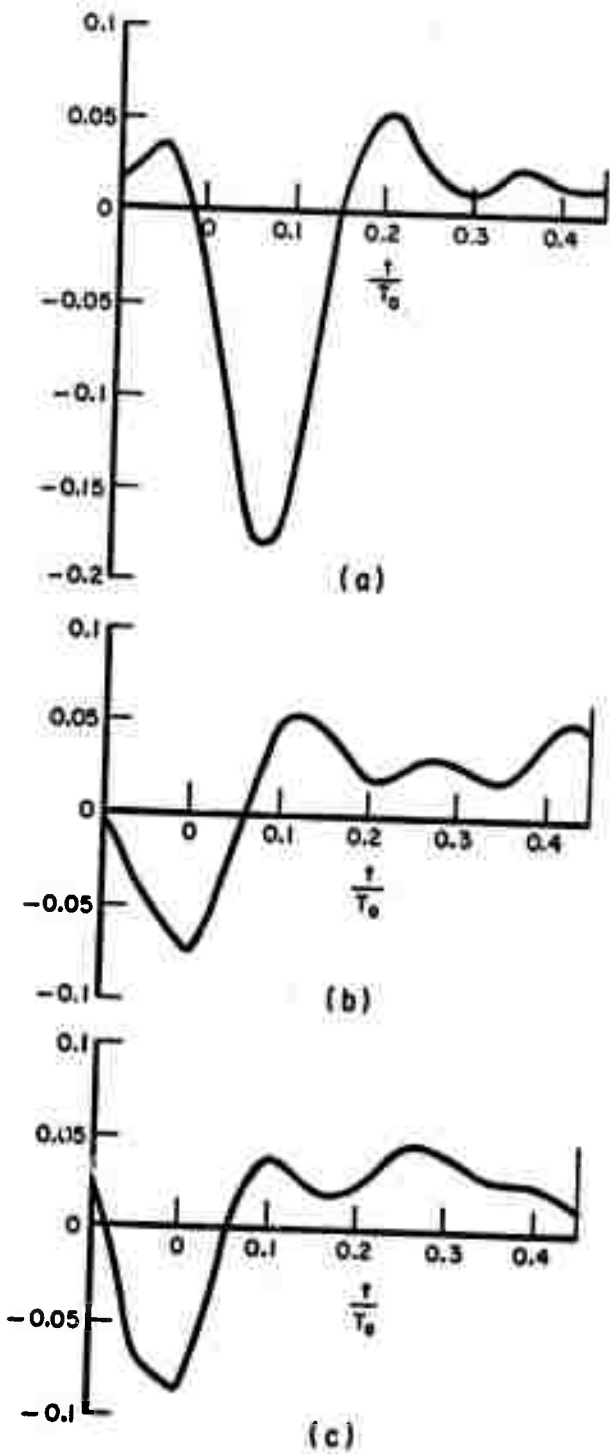

Fig. 9. Ramp response waveforms of a conducting sphere:
(a) free space,
(b) underground - $n\omega_0$ harmonics,
(c) underground - $n^2\omega_0$ harmonics.

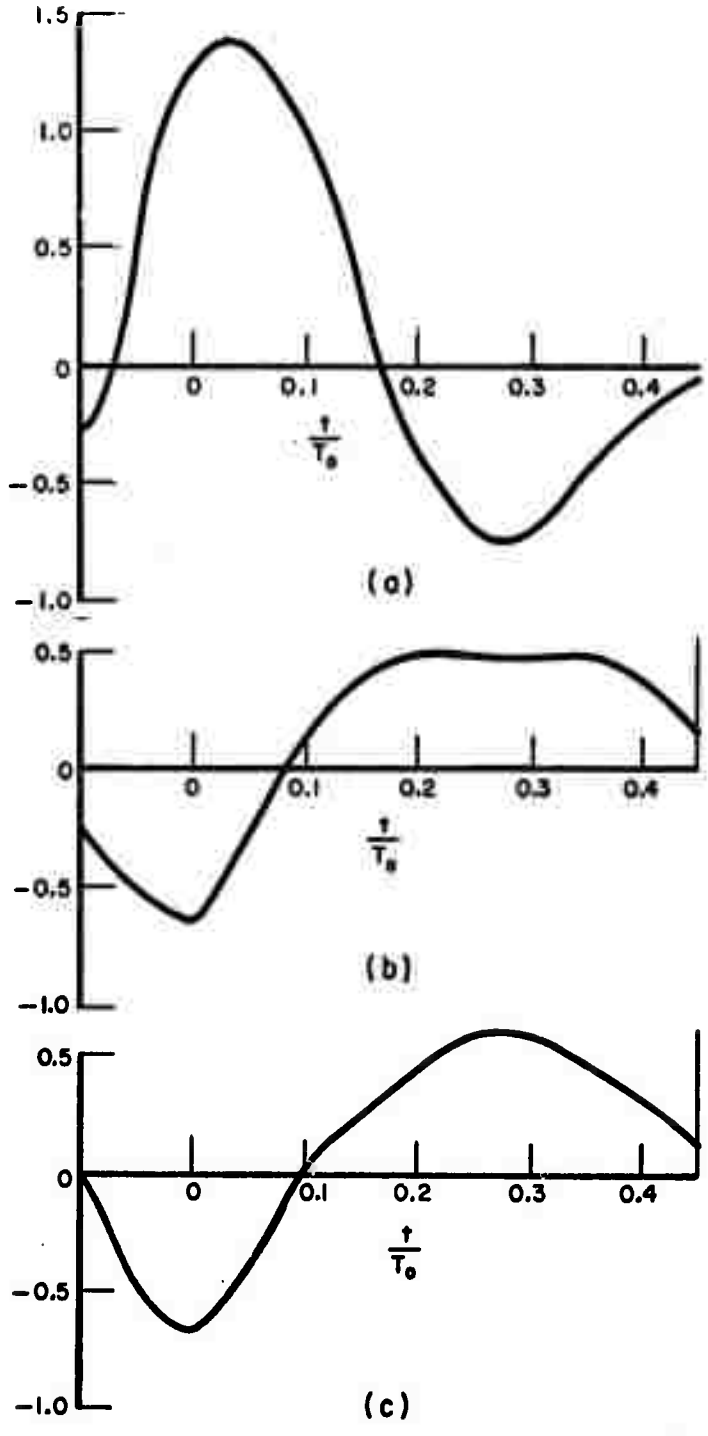

Fig. 10. Ramp response waveforms of a conducting circular cylinder:
(a) free space,
(b) underground - $n\omega_0$ harmonics,
(c) underground - $n^2\omega_0$ harmonics.

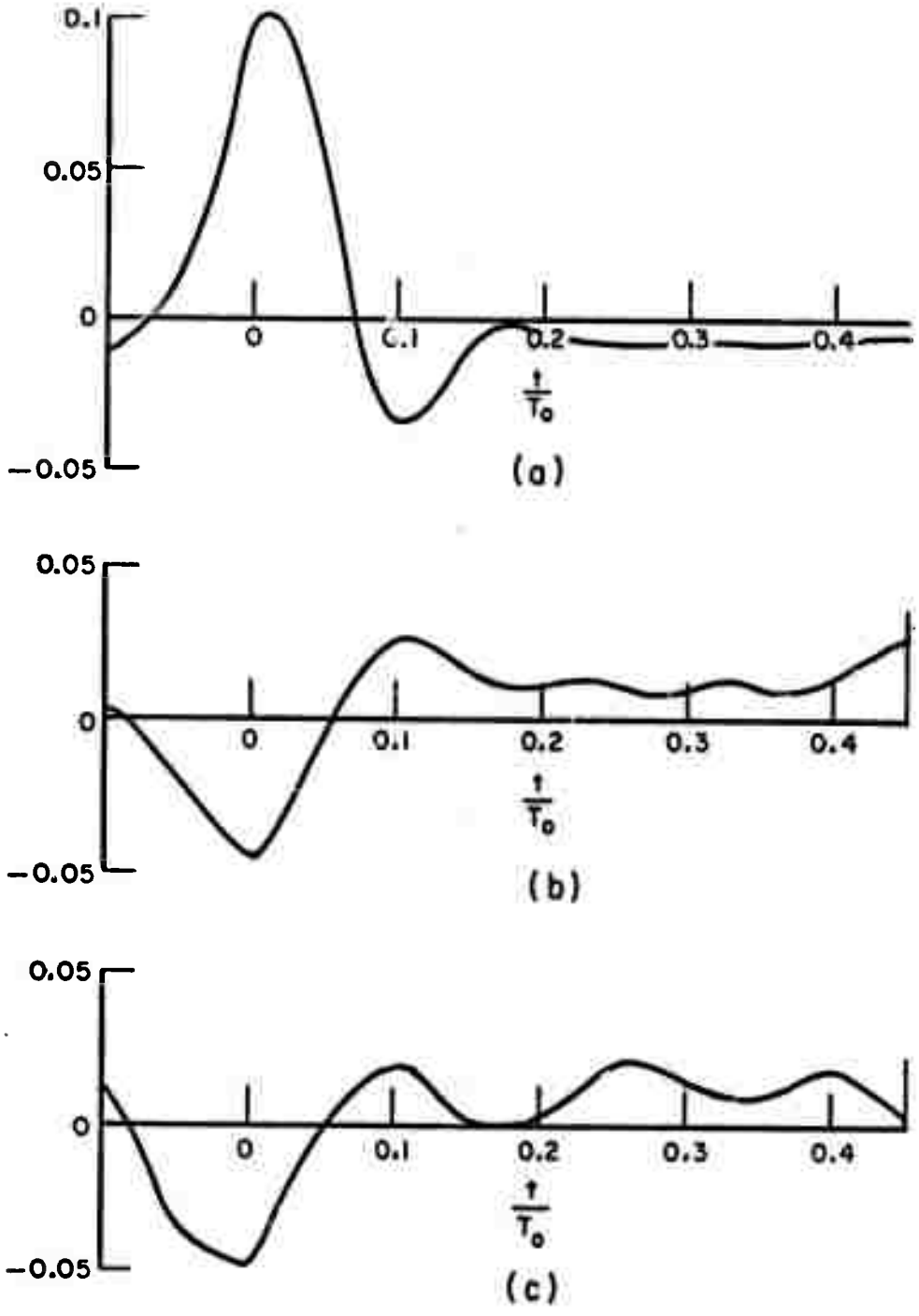

Fig. 11. Ramp response waveforms of a conducting disk:
(a) free space,
(b) underground - $n\omega_0$ harmonics,
(c) underground - $n^2\omega_0$ harmonics.

B. Probe Analysis and Design

We have developed a comprehensive analysis and computer program for wire antennas in a homogeneous dissipative medium. The program handles all types of wire antennas including linear dipoles, V dipoles, rectangular loops, circular loops and arrays. The output provides a complete analysis of the system, including self impedance, mutual impedance, current distribution, near-zone fields, and far-field patterns.

The finite conductivity of the wire antenna is taken into account via the surface-impedance formulation. If some portions of the antenna are insulated from the conducting medium by a thin dielectric sleeve, this is taken into account via the equivalent polarization currents.

A piecewise-sinusoidal expansion is employed for the unknown current distribution on the antenna, and Galerkin's method is used to reduce the integral equation to a system of simultaneous linear equations. The analysis takes place in the frequency domain. The speed, accuracy and generality are sufficient, however, to permit a Fourier transform to the time domain.

Figure 12 illustrates typical data obtained with this computer program. This figure shows the near-zone electric field distribution E_x of a U-shaped wire antenna at 100 KHz. The observation point is on the z axis where E_y vanishes and E_z is much smaller than E_x. The solid curve shows the field distribution of the uninsulated antenna, and the dashed curve shows the effect of insulating the horizontal portion of the antenna. The input power was one watt in both cases. The polystyrene insulation has an inner diameter of 3/8 inch and an outer diameter of 3/4 inch.

The data in Fig. 12 indicate that the uninsulated antenna may be advantageous for detection of targets at close range. Of greater importance is the fact that the computer program can be employed to optimize the antenna design for a given target position, frequency range, and soil conditions.

The expansions published by Banos will be programed to account for the effects of the air-earth interface. When this is completed, the computer program will be applied to the analysis and design of probes for the electromagnetic pulse-sounding system.

C. Transient Fields of a Line Source

Thus far we have considered plane wave incidence for the geometries of interest. It is important to obtain incident fields for different sources since it is not desirable to illuminate the target with a plane wave. While the technique just discussed gives the

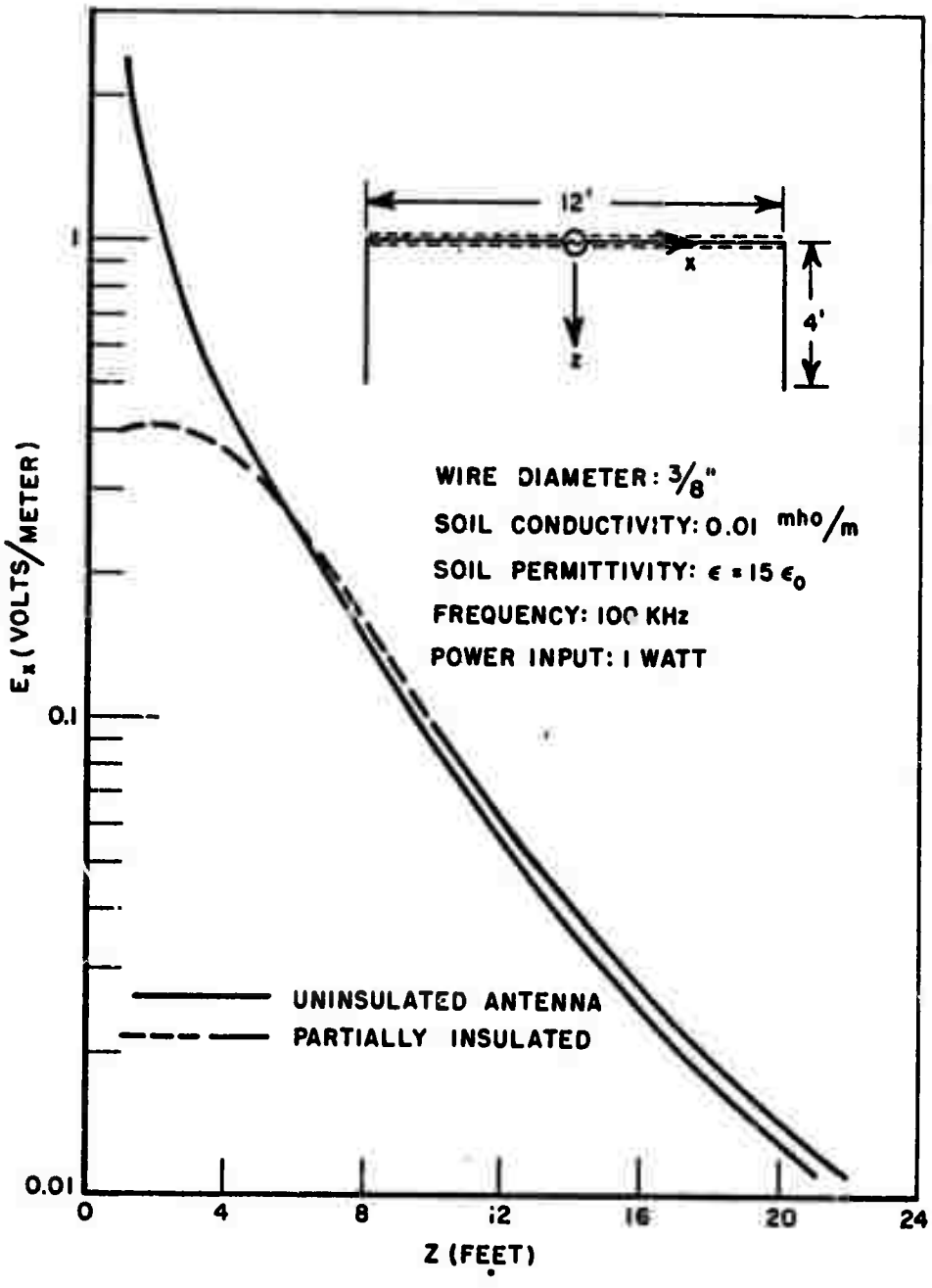

Fig. 12. Calculated electric field distribution of a wire antenna in a homogeneous conducting medium. The observer is on the z axis.

fields for the actual sources of interest, it does this in a quantitative way. It is equally important to evaluate the fields of various sources in functional form so that a more thorough understanding of the physical mechanisms involved can be obtained. The line source above an interface is most important since simple exact closed form expressions can be obtained.

Let a rectangular coordinate frame be oriented with the xy plane on the surface of a half-space with the z axis perpendicular to the half-space and positive into the half-space. A harmonic line source is oriented parallel to the y axis at a height -h above the half-space. The half-space is assumed to be homogeneous and isotropic with constitutive parameters ε_1, μ_0, σ_1. If the observation point is confined to the z axis (x=0) and the half-space is lossless (σ_1=0) then it can be shown that a change of variable and Laplace transformation of the well known semi-infinite integral solutions for the fields[5] yields exact, closed form expressions for the real time-dependent transient fields corresponding to a step current ($I = I_0 u(t)$) excitation of the line source. The y component of the electric field above the half-space ($z \leq 0$) is given by

$$(5) \qquad F^U_{yo}(z,t) = \frac{-\mu_o I}{2\pi}\left[\frac{1}{\sqrt{t^2 - \left(\frac{z+h}{c}\right)^2}}\, u\left[t - \left(\frac{z+h}{c}\right)\right] + \right.$$

$$\left. \frac{1}{\sqrt{t^2 - \left(\frac{z-h}{c}\right)^2}} \left\{ \frac{t - \sqrt{t^2 + \left(\frac{z-h}{c}\right)^2(\varepsilon_{1r} - 1)}}{t + \sqrt{t^2 + \left(\frac{z-h}{c}\right)^2(\varepsilon_{1r} - 1)}} \right\} u\left[t - \left(\frac{z-h}{c}\right)\right] \right] .$$

The y component of the electric field within the half-space ($z \geq 0$) is given by

$$(6) \qquad F^U_{y1}(z,t) =$$

$$\frac{-\mu_o I}{\pi} \frac{1}{\sqrt{(t + h/c)^2 - \varepsilon_{1r}(z/c)^2}} \left\{ \frac{1}{1 + \sqrt{1 - \left(\frac{z}{c(t+h/c)}\right)^2(\varepsilon_{1r} - 1)}} \right\}$$

$$u\left[t + \frac{h}{c} - \sqrt{\varepsilon_{1r}}\, z/c\right]$$

For the same excitation and a lossless half-space an exact closed form solution can also be obtained when both the observation point and line source lie on the half-space (z=h=0).

$$(7) \qquad F_y^U(x,t) =$$

$$\frac{-\mu_o I}{\frac{\pi x^2}{c}(\varepsilon_{1r}-1)} \left[\sqrt{t^2 - (x/c)^2}\, u[t - x/c] - \sqrt{t^2 - \varepsilon_{1r}(x/c)^2}\, u[t - \sqrt{\varepsilon_{1r}}\, x/c] \right] .$$

It is suggested that for short times, i.e., times in the vicinity of the waveform origin, these results also hold for a lossy half-space ($\sigma_1 \neq 0$) since setting $\sigma_1=0$ can be interpreted as a high frequency approximation which neglects the conduction currents. Results similar to Eqs. (5) and (6) can also be obtained for the case where the line source lies within the half-space via reciprocity.

If a low frequency or quasi-static approximation where the displacement currents are neglected is made then on the vertical axis (x=0)

$$(8) \qquad F_{yo}^U(z,t) = \frac{2\, I\, u(t)}{\pi (h-z)^2 \sigma_1} - \frac{2\, I\, e^{\mu_o \sigma_1 \frac{(h-z)^2}{4t}}}{\pi^{3/2} \sigma_1 (h-z)^2} \Gamma\left(3/2, \frac{\mu_o \sigma_1 (h-z)^2}{4t}\right) u(t),$$

and

$$(9) \qquad F_{y1}^U(z,t) =$$

$$\frac{I\, e^{-\mu_o \sigma_1 z^2}}{4\pi \sigma_1 t} u(t) + \frac{\mu_o I}{2\pi t} e^{-\mu_o \sigma_1 z^2} u(t) - \frac{2\, I\, e^{-\mu_o \sigma_1 z^2 (1 - \frac{1}{4t})}}{\pi^{3/2} \sigma_1 z^2} \Gamma\left(3/2, \frac{\mu_o \sigma_1 z^2}{4t}\right) u(t),$$

where $\Gamma(\nu,x)$ is the incomplete gamma function

$$(10) \qquad \Gamma(3/2,x) = \frac{\sqrt{\pi}}{2} - \sum_{n=0}^{\infty} \frac{(-1)^n \, x^{n+3/2}}{n!\,(n+3/2)} \quad .$$

The results in Eqs. (8) and (9) constitute long time estimates of the transient fields for a step current excitation of the line source.

If the half-space is homogeneous with frequency independent parameters then the response waveforms can at best smoothly decay from the short time estimates in Eqs. (5) and (6) to the long time estimates in Eqs. (8) and (9). This suggests that these results might be combined to yield a simple composite waveform which could then be transformed back to the frequency domain. In our studies of the scattering by objects in free space, such time domain combinations of low and high frequency estimates have been shown to yield surprisingly good approximations in mid-frequency ranges. It is not intended to further pursue this topic during this contract period, but such an approach would appear to merit reasonable consideration in a longer range program.

IV. EXPERIMENTAL STUDIES

Near the beginning of the contract period, preparations for experimental measurements at a remote site (a nearby quarry) which offered hazard-type anomalies were initiated. A pulse generator (H.P. 214A) appropriate for such measurements was ordered. This pulser has a peak pulse amplitude of 50 volts into 50 ohms or 100 volts in 1200 ohms, a 15 ns rise time, pulse widths variable from 45 ns to the μs range and repetition rates from 10 kc to 1000 kc. The major preparations involved replacing a direct interfacing of the antenna system with an instrumentation computer, which had been used on earlier studies, with a recording arrangement such that a non-real time use of the computer was feasible. It should be understood that in an ultimate system the computer functions will be replaced by circuitry. At this stage, however, the computer offers an irreplacable flexibility in processing changes and experimentation. The above mentioned preparations are now nearly completed - certain components have not yet been delivered. The system for remote recording of data resamples the oscilloscope output waveforms at a very low speed with computer control of the sampling point relative to a trigger synched with the scope sweep. As shown in Fig. 13 the trigger and sampling point offset voltage are fed into a phase locked loop. The voltage controlled oscillator (VCO) output drives a one shot which provides the proper pulse shape for triggering the sample and hold amplifier. The offset voltage varies the phase of the VCO output relative to

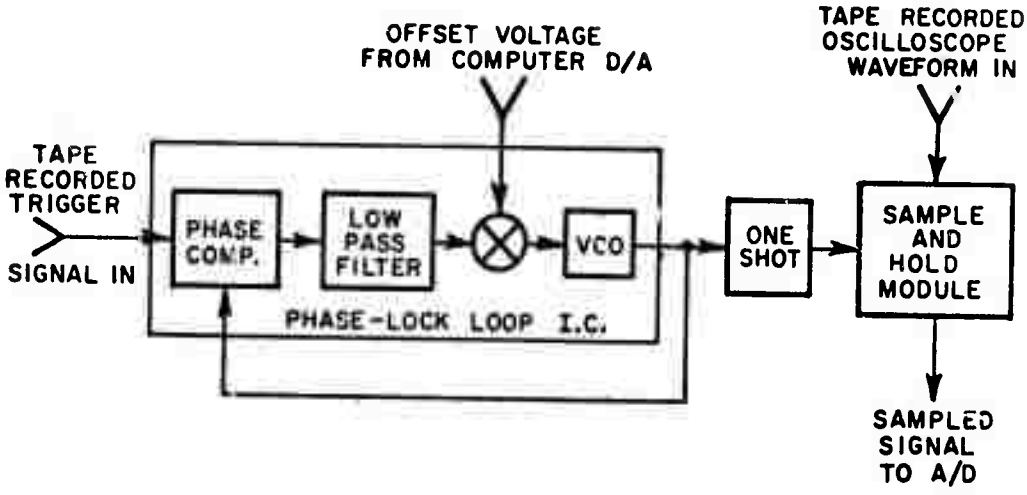

Fig. 13. Data conversion circuit for tape recorded remote site measurements.

the trigger, thus effectively moving the sampling point across the signal waveform. The sampled signal is fed to the computer analog/digital input for conversion to digital form.

A breadboard version of the device is currently being built. A single linear integrated circuit performs the entire function of the phase-locked loop. A miniature hybrid module performs the sample and hold.

The oscilloscope waveforms will be recorded on magnetic tape in the field and the tapes later played back into this device in the laboratory. Since this device does not have to go to the remote site, the breadboard version can be used for actual data conversion as soon as it is operational.

The pulse generator was delivered during the fifth month of the contract; since that date tests of various antenna configurations and preliminary interrogation of certain subsurface targets in the vicinity of the laboratory have been underway using the direct interfacing to the instrumentation computer.

A. First Generation Probe

The basic electromagnetic probe being studied is an insulated, center fed dipole lying on the ground with the ends of the dipole either directly grounded by rods driven into the earth or capacitivly coupled using plates on the ground. The arms of the dipole may be

single wires with ground rods or two wires in a U or V arrangement to two separate ground rods. Alternatively, the dipole arm may be a V-shaped conductor eliminating the need for a ground rod. The system presently envisioned consists of two such dipoles arrayed orthogonally. Two modes of operation are possible; either direct reflection using one or the other of the dipoles as transmitter and receiver or orthogonally using one dipole as a transmitter and the other as a receiver. Both modes are important since the direct mode is sensitive to symmetrical planar stratifications whereas the orthogonal mode is blind to such targets.

A sketch of one version of the probe and a block diagram of the instrumentation is shown in Fig. 14. In Fig. 15, the time domain reflection of one of the dipoles shown in Fig. 14 is shown in the direct reflection mode. The incident pulse for the results shown in Fig. 15 was very long, essentially a step with a 15 ns rise time. Shown in Fig. 15 are the differences when the arms of the dipole are a single wire or two wires in a U or V arrangement. Also shown are the reflected waveforms when the feed cable is terminated in an open circuit, short circuit and a matched load. By adjusting the ground rod depth, the latter portion of the waveform can be reasonably matched to the matched load waveform indicating that at low frequencies at least the antenna is well matched. The effects of tuning by varying the ground rod depths is shown in Fig. 16, these results also indicate that energy is being coupled into the ground.

The waveforms in Figs. 15 and 16 correspond to an incident pulse with approximately a 2 volt peak amplitude. Attempts to operate the probe in either the direct or orthogonal mode using the peak output of the pulse generator revealed that the balun (transformer) used to go from 50 ohms unbalanced to 200 ohms balanced was saturating at a level well below the peak output of the pulser. This is not a basic difficulty since baluns with a higher power handling capability are available and have been ordered. In the interim before their delivery however, the pulser cannot be used at output levels appropriate for interrogation of subsurface targets. Tests did establish however that the probe was insensitive to surface structures (an automobile driven into various quadrants of the probe had no effect for a low level incident pulse) and that a synthetic target in the form of two conducting plates connected electrically could be detected.

The temporary balun difficulty was circumvented by going to essentially a smaller version of the probe (the dipole arms became solid conductors in a V shape) and the use of a different pulse generator. The pulser is not appropriate for deep penetration but can be used to interrogate relatively shallow targets. Using this system, a clay drain tile buried at a depth of 3 feet has been detected. The equipment consisted of an pulse generator, a "four-leaf clover" probe lying on the ground surface, and a computer-controlled sampling oscilloscope. The pulse was approximately

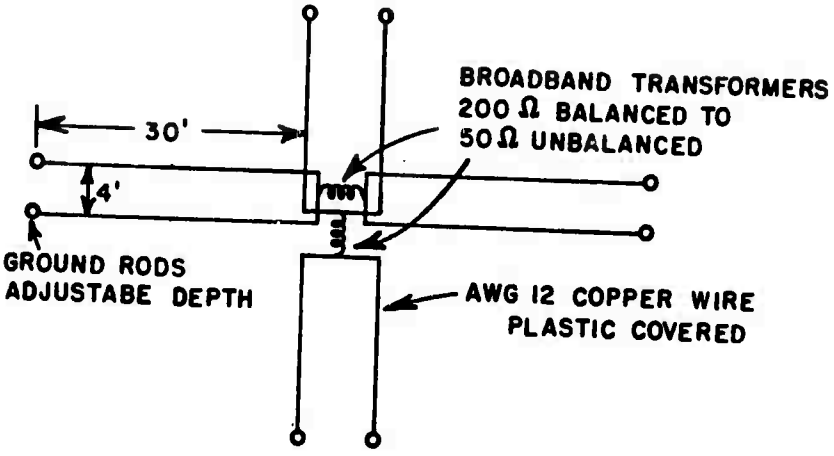

(a) ELECTROMAGNETIC PROBE

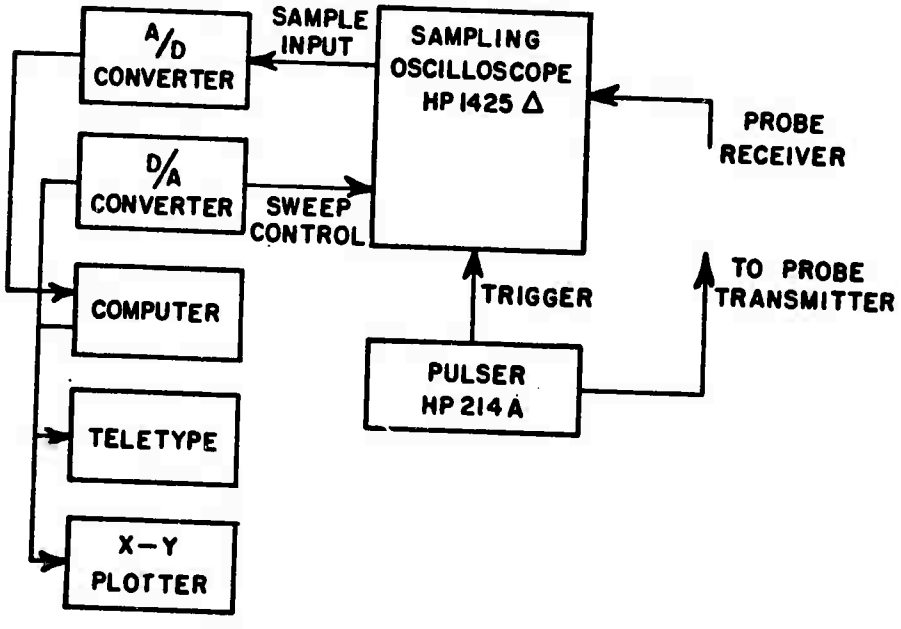

(b) BLOCK DIAGRAM — ORTHOGONAL MODE

Fig. 14. (a) Electromagnetic probe.
(b) Block diagram of pulse sounding system.

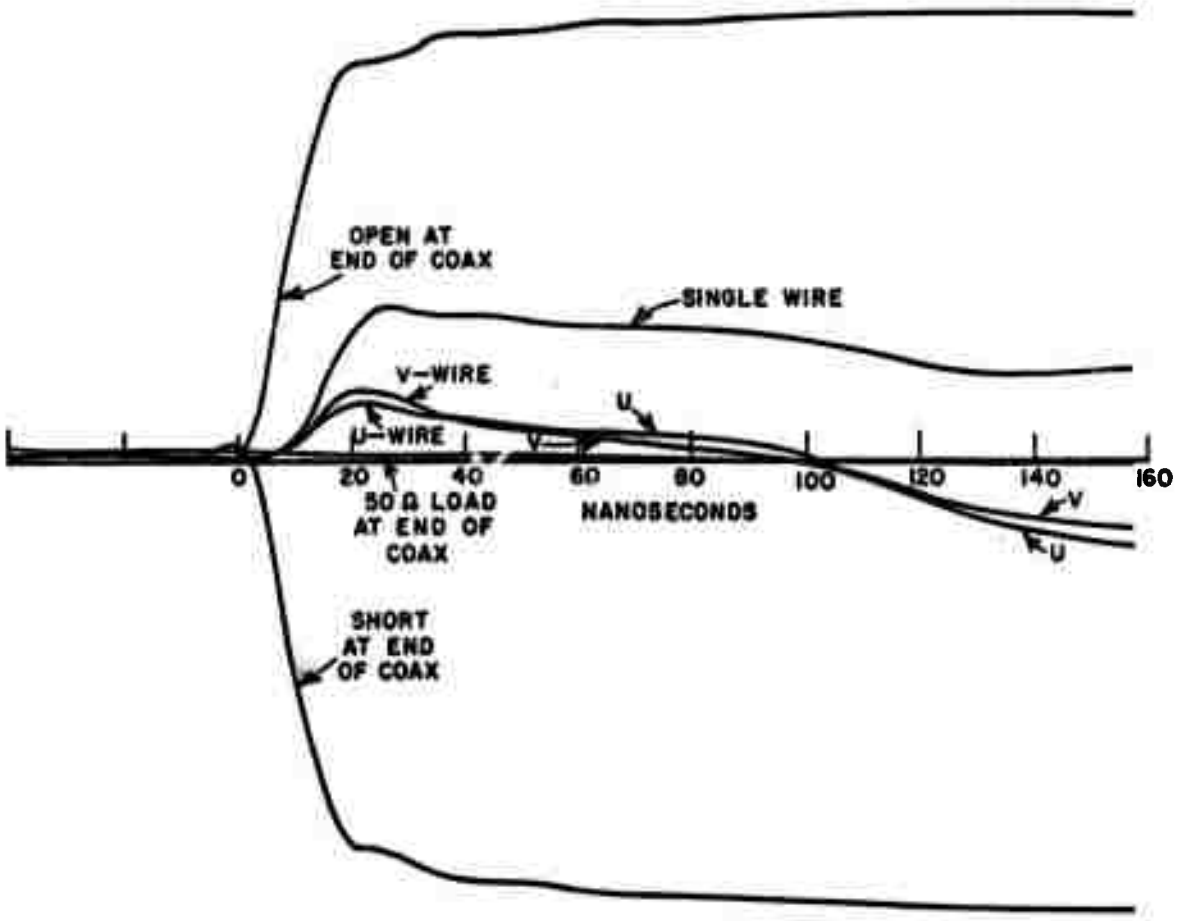

Fig. 15. Direct reflection mode of one probe, various terminations.

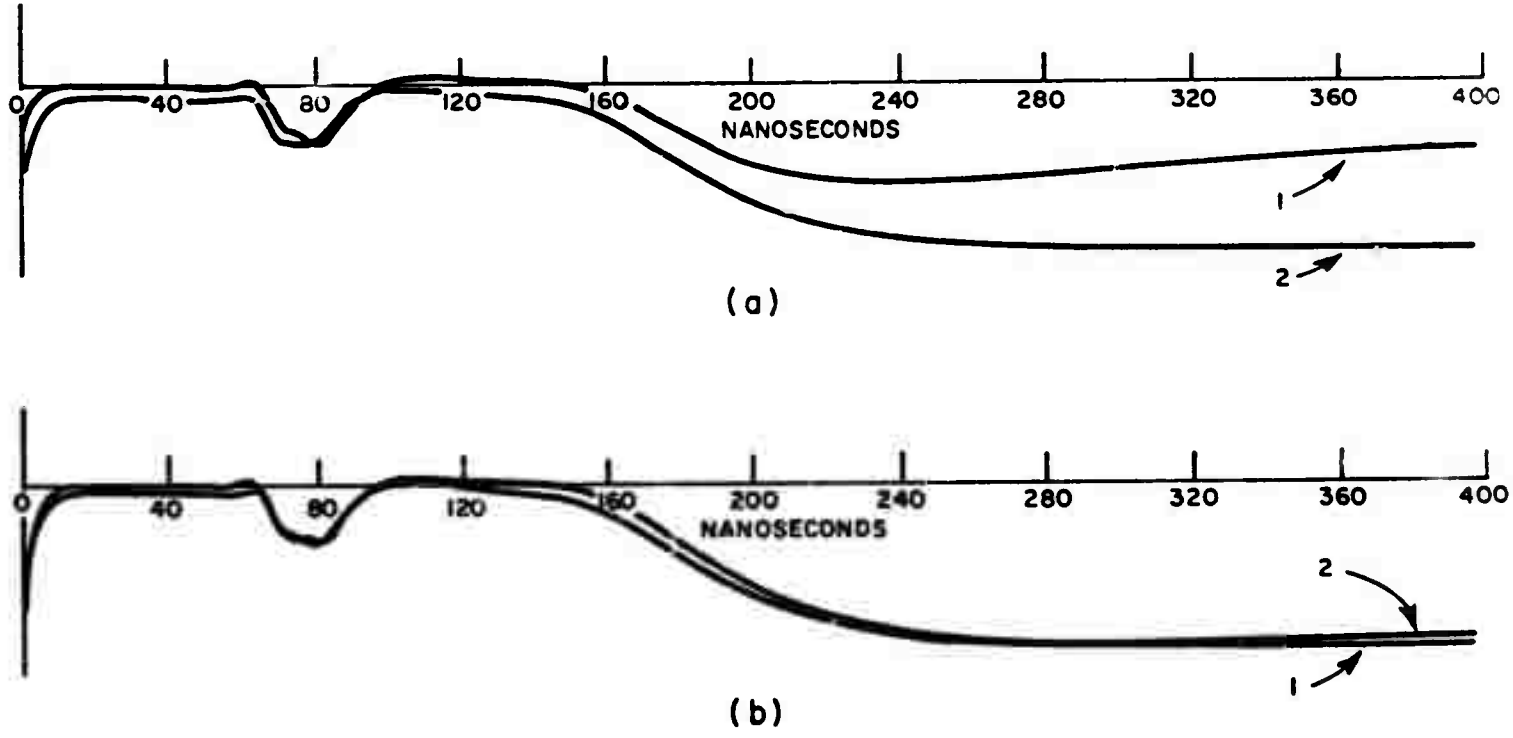

Fig. 16. Direct reflection mode of one probe - effect of ground rod depth.

2 nsec long with a peak amplitude of 10 volts, and a pulse repetition rate of approximately 1 MHz. A sketch of the antenna is shown in Fig. 17.

The antenna was located in several positions in the vicinity of a storm drain-tile line running behind the laboratory building at about a 3 foot depth. Several locations over the drain tile and several locations of assumed "target-free" ground were measured, and the differences between the "target" and "no-target" waveforms were computed and plotted as shown in Fig. 18. Difference curves for target-free ground are shown in Fig. 19. These can be considered to represent the clutter level. These curves demonstrate that the pipe is visible to the system, and that several features of the return waveforms remain constant from one location over the pipe to the next. Based on the variation of these return waveforms it is estimated that the signal-to-clutter ratio of the pipe signature is about 10 dB.

Several measured difference waveforms of the catch basin at the end of the drain tile are shown in Fig. 20. Comparison of these waveforms with those of Fig. 18 indicates that the nature of the return signal is sensitive to the shape of the underground target. Thus, identification of underground object shape from these signature waveforms seems feasible.

B. Propagation Test

While it is not presently possible to use the probe in Fig. 14 with high power because of the balun saturation, the dipoles can be used as receivers. For the transmitter, the balun requirement can be eliminated by going to an unbalanced antenna. To this end a monopole antenna consisting of a 2 foot rod on a circular (1-1/2 foot diameter) ground plane was constructed. In operation, the ground plane rests on the ground with the rod driven into the ground. This antenna can be fed directly by coaxial cable. Results of transmission tests using the monopole as a transmitter and the probe of Fig. 14 as a receiver are shown in Fig. 21. The monopole was near broadside to one dipole and near endfire to the other and located at a distance of 160 feet from the vertex of the probe. The transmitted pulse had a pulse amplitude of 50 volts, a pulse width of 50 nanoseconds, and a repetitive rate of 10 KHz. It was established that the received waveform shown was not the effects of a surface wave by moving a large conducting screen in the vicinity of the monopole without disturbing the received waveform. It is not yet understood why the received waveforms are identical and further measurements are in progress. It has not been established as yet what penetration depths are being achieved; with the monopole as a transmitter it is possible that energy is being confined close to the surface of the ground. Measurements are presently in progress to establish the penetration achieved as well as the attenuation vs frequency for the local ground.

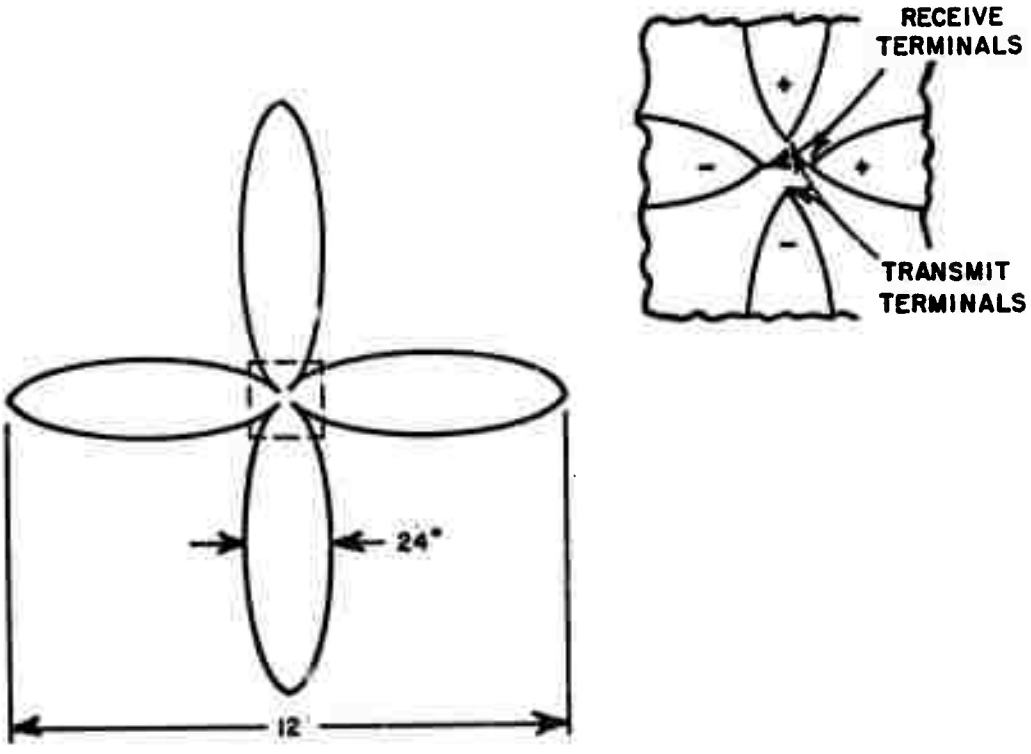

Fig. 17. Sketch of "four-leaf clover" probe.

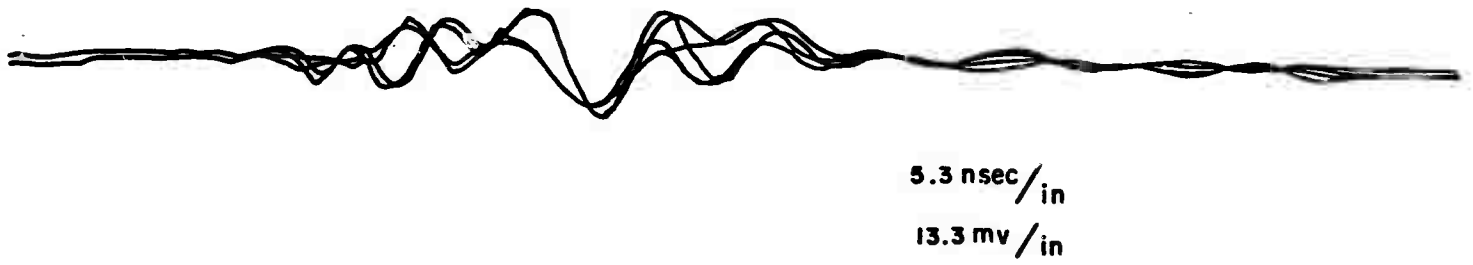

Fig. 18. Drain-tile target difference waveforms.

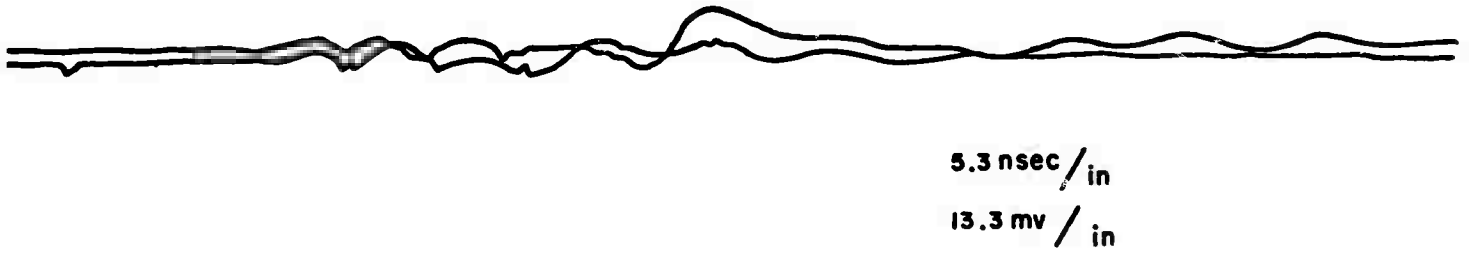

Fig. 19. No-target difference waveforms.

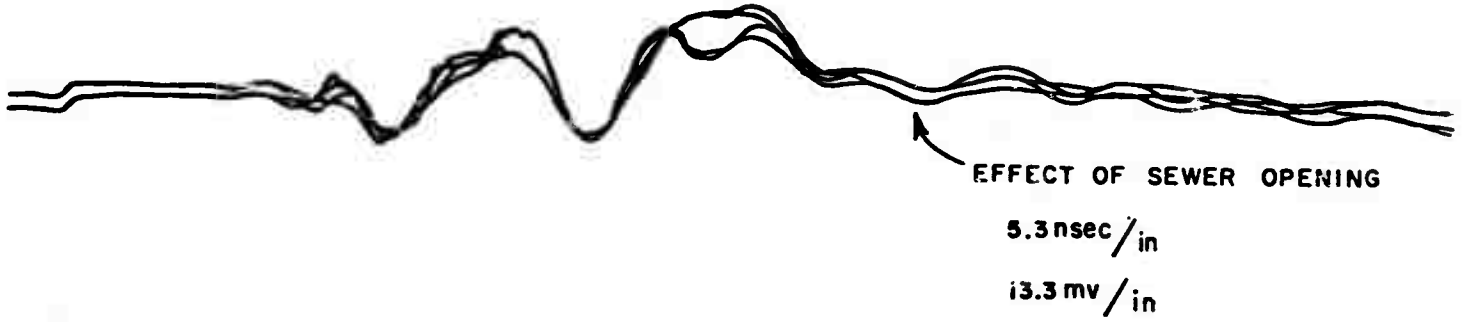

Fig. 20. Catch basin target difference waveforms.

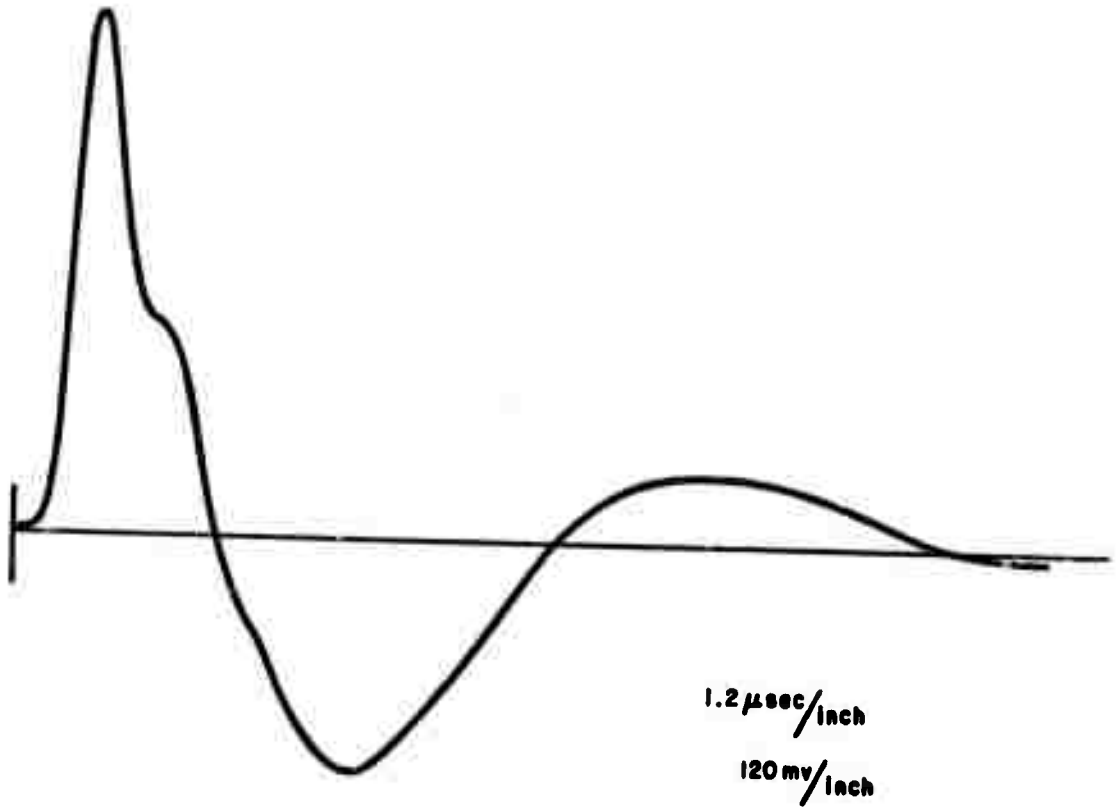

Fig. 21. Received pulse waveform.

VI. CONCLUSIONS

The plane wave scattering by planar conductivity contrasts has been explored via the impulse response waveform for the contrast. A Fourier synthesis technique is utilized to determine the decay rate of the waveform and will be used to explore the effects of frequency-dependent constitutive parameters. The response waveform has a distinctive signature and diagnostic features for both the dielectric constant and conductivity contrasts.

Computer programs for computing the plane wave scattering by arbitrary spherical targets in a dissipative medium have been written and verified, including the case of layered spherical targets. Calculations for realistic spherical-type tunneling hazards and for deducing characteristic response waveforms for such hazards are in progress.

The attenuation and dispersion effects of a lossy overburden have been estimated by assuming plane wave propagation and utilizing the free space scattering characteristics of spherical, cylindrical and disk targets. These results indicate that interface and overburden effects do not preclude unique signatures for the targets.

Exact, closed form expressions for the transient fields of a line source in the presence of a dielectric half-space have been obtained for particular observer locations. Quasi-static estimates of the transient fields for a lossy half-space have also been obtained. From these results, simplified estimates of the fields of a line source in the presence of an arbitrary half-space appear to be feasible.

A comprehensive analysis and computer program for all types of wire probes in a homogeneous dissipative medium have been developed. With these tools, design data for pulse sounding probes to interrogate at various depths are being prepared.

Initial measurements have been made on two versions of the electromagnetic pulse sounding probe. The results indicate that the probe can be well matched, does couple energy into the ground and is insensitive to surface targets. The presence of a clay drain tile at a depth of 3 feet has been detected using a small version of the probe and a pulse generator inappropriate (at least where a lossy overburden exists) for deep penetration. The limited power handling capability of transformers used to match the unbalanced coaxial feed to the balanced probe has temporarily precluded use of the full scale probe with the high power pulse generator. Larger transformers have been ordered and other schemes for eliminating the need for transformers are being studied.

Transmission tests demonstrating that pulsed electromagnetic energy can be propagated through the ground over considerable distances (160 feet) have been made. The energy may be confined to shallow depths, and this possibility is being explored.

VII. FUTURE PLANS

It is intended that major emphasis during the remaining contract period will be concentrated on experimental measurements of subsurface targets, first at this laboratory and then at a remote test site where anomalies characteristic of tunneling hazards are available. This is in accordance with the original research plan.

Analytical studies will be primarily devoted to the wire antenna analysis from which realistic dispersion, attenuation and penetration calculations as well as probe design data are possible. The scattering from spherical contrasts will be calculated for hazard-type parameters and response waveforms obtained via Fourier synthesis. Introduction of frequency-dependent constitutive parameters will be made for both the antenna analysis and spherical scatterer program.

REFERENCES

1. Kennaugh, E.M. and Moffatt, D.L., "Transient and Impulse Response Approximations," Proc. IEEE, Vol. 53, No. 8, August 1965, pp. 893-901.

2. Final Summary Report, 2467-5, 13 March 1970, ElectroScience Laboratory, Department of Electrical Engineering, The Ohio State University Research Foundation; prepared under Contract F44620-67-C-0095 for Air Force Cambridge Research Laboratories, Bedford, Massachusetts. (AD 870 169)

3. Final Report, 2784-2, April 1971, ElectroScience Laboratory, Department of Electrical Engineering, The Ohio State University Research Foundation; prepared under Contract F30602-69-C-0231 for Rome Air Development Center.

4. Final Report, 2971-2, July 1971, ElectroScience Laboratory, Department of Electrical Engineering, The Ohio State University Research Foundation; prepared under Contract F19628-70-C-0125 for Air Force Systems Command, Bedford, Mass.

5. Keller, G.V. and Frischknecht, F.C., Electrical Methods in Geophysical Prospecting, Pergaman Press, 1966.